MAR 7 1968

MASTER

TECHNICAL REPORTS SERIES No. 79

The Plutonium-Oxygen and

Uranium-Plutonium-Oxygen Systems:

A Thermochemical Assessment

INTERNATIONAL ATOMIC ENERGY AGENCY, VIENNA, 1967

DISCLAIMER

This report was prepared as an account of work sponsored by an agency of the United States Government. Neither the United States Government nor any agency Thereof, nor any of their employees, makes any warranty, express or implied, or assumes any legal liability or responsibility for the accuracy, completeness, or usefulness of any information, apparatus, product, or process disclosed, or represents that its use would not infringe privately owned rights. Reference herein to any specific commercial product, process, or service by trade name, trademark, manufacturer, or otherwise does not necessarily constitute or imply its endorsement, recommendation, or favoring by the United States Government or any agency thereof. The views and opinions of authors expressed herein do not necessarily state or reflect those of the United States Government or any agency thereof.

DISCLAIMER

Portions of this document may be illegible in electronic image products. Images are produced from the best available original document.
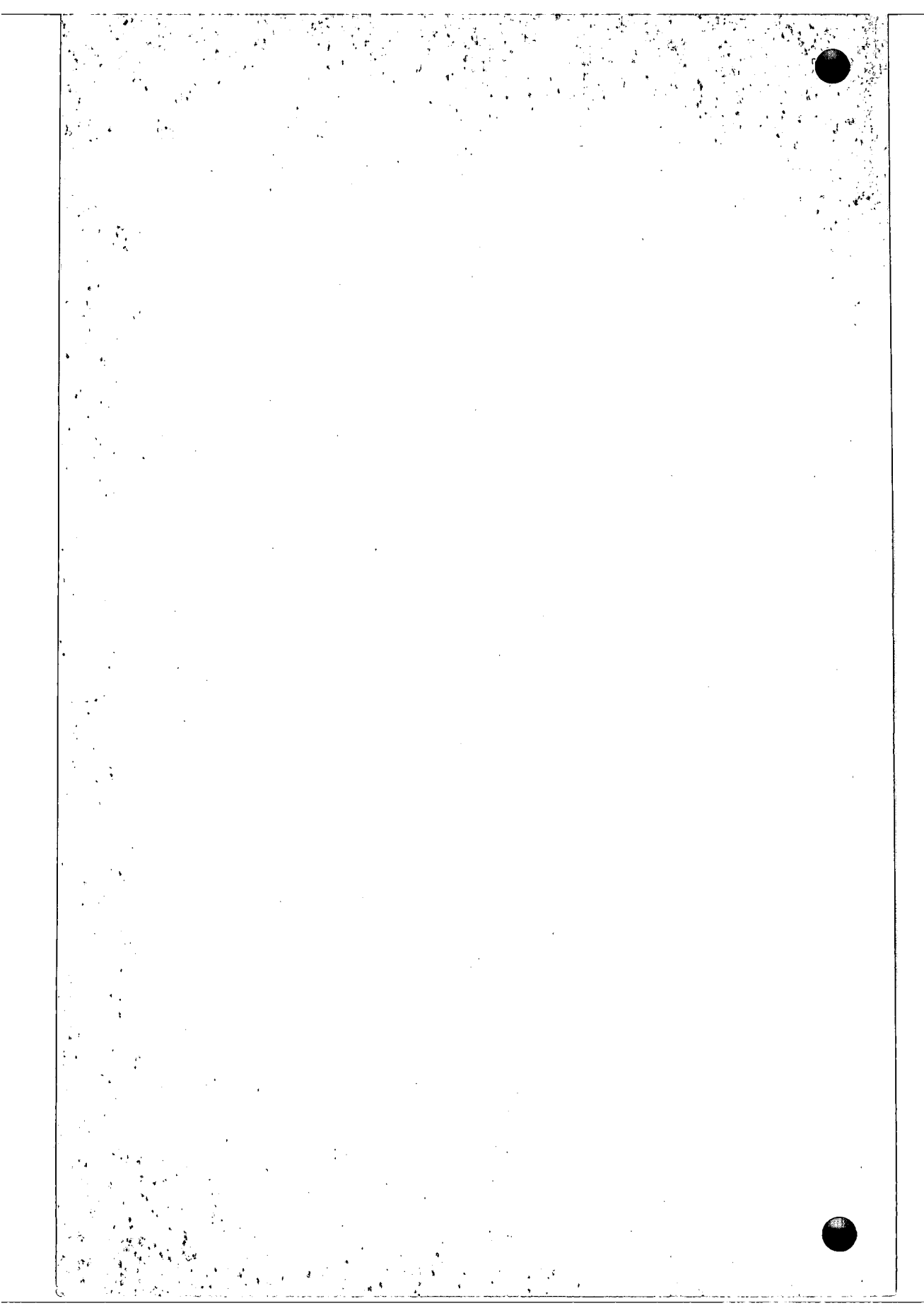
THE PLUTONIUM-OXYGEN

AND URANIUM-PLUTONIUM-OXYGEN SYSTEMS:

A THERMOCHEMICAL ASSESSMENT

The following States are Members of the International Atomic Energy Agency:

AFGHANISTAN
ALBANIA
ALGERIA
ARGENTINA
AUSTRALIA
AUSTRIA
BELGIUM
BOLIVIA
BRAZIL
BULGARIA
BURMA
BYELORUSSIAN SOVIET
   SOCIALIST REPUBLIC
CAMBODIA
CAMEROON
CANADA
CEYLON
CHILE
CHINA
COLOMBIA
CONGO, DEMOCRATIC
   REPUBLIC OF
COSTA RICA
CUBA
CYPRUS
CZECHOSLOVAK SOCIALIST
   REPUBLIC
DENMARK
DOMINICAN REPUBLIC
ECUADOR
EL SALVADOR
ETHIOPIA
FINLAND
FRANCE
GABON

GERMANY, FEDERAL
   REPUBLIC OF
GHANA
GREECE
GUATEMALA
HAITI
HOLY SEE
HUNGARY
ICELAND
INDIA
INDONESIA
IRAN
IRAQ
ISRAEL
ITALY
IVORY COAST
JAMAICA
JAPAN
JORDAN
KENYA
KOREA, REPUBLIC OF
KUWAIT
LEBANON
LIBERIA
LIBYA
LUXEMBOURG
MADAGASCAR
MALI
MEXICO
MONACO
MOROCCO
NETHERLANDS
NEW ZEALAND
NICARAGUA
NIGERIA

NORWAY
PAKISTAN
PANAMA
PARAGUAY
PERU
PHILIPPINES
POLAND
PORTUGAL
ROMANIA
SAUDI ARABIA
SENEGAL
SIERRA LEONE
SINGAPORE
SOUTH AFRICA
SPAIN
SUDAN
SWEDEN
SWITZERLAND
SYRIAN ARAB REPUBLIC
THAILAND
TUNISIA
TURKEY
UGANDA
UKRAINIAN SOVIET SOCIALIST
   REPUBLIC
UNION OF SOVIET SOCIALIST
   REPUBLICS
UNITED ARAB REPUBLIC
UNITED KINGDOM OF GREAT
   BRITAIN AND NORTHERN
   IRELAND
UNITED STATES OF AMERICA
URUGUAY
VENEZUELA
VIET-NAM
YUGOSLAVIA

The Agency's Statute was approved on 23 October 1956 by the Conference on the Statute of the IAEA held at United Nations Headquarters, New York; it entered into force on 29 July 1957. The Headquarters of the Agency are situated in Vienna. Its principal objective is "to accelerate and enlarge the contribution of atomic energy to peace, health and prosperity throughout the world".

THE PLUTONIUM-OXYGEN AND URANIUM-PLUTONIUM-OXYGEN SYSTEMS:

A THERMOCHEMICAL ASSESSMENT

REPORT OF A PANEL ON THERMODYNAMICS
OF PLUTONIUM OXIDES
HELD IN VIENNA, 24-28 OCTOBER 1966

THE PLUTONIUM-OXYGEN AND URANIUM-PLUTONIUM-OXYGEN SYSTEMS: A THERMOCHEMICAL
ASSESSMENT
(Technical Reports Series, No. 79)

ABSTRACT. The report of a panel of experts convened by the IAEA in Vienna in March 1964. It reviews the structural and thermodynamic data for the Pu-O and U-Pu-O systems and presents the conclusions of the panel.

Contents: Introduction; Plutonium oxides; The uranium-plutonium-oxygen system; Other PuO_2-MeO_x oxide systems; References.

Entirely in English.

(86 pp., 16 × 24 cm, paper-bound, 27 figures)
(1967)   Price: US $2.00; 14/2 stg.

THE PLUTONIUM-OXYGEN AND URANIUM-PLUTONIUM-
OXYGEN SYSTEMS: A THERMOCHEMICAL ASSESSMENT,
IAEA, VIENNA, 1967
STI/DOC/10/79

FOREWORD

With the development of advanced types of reactors, plutonium and its compounds have gained importance as nuclear fuels. In view of this growing interest and the need to collect and assess the fundamental data, the International Atomic Energy Agency convened a panel on Thermodynamics of Plutonium Oxides from 24 to 28 October, 1966. The purpose of the panel, which met at the Agency's headquarters in Vienna, was to evaluate critically the thermodynamic data at present available on plutonium oxides and mixed oxides from the viewpoint of nuclear technology.

In the process of this assessment, the work of the panel revealed in what areas more dependable information is needed and more work should be undertaken. The present report, which is the outcome of the panel meeting, presents a set of the most reliable data now available.

CONTENTS

I. INTRODUCTION

The favourable physical properties of uranium dioxide (for example, high melting point, stability under irradiation) have led to its use as a fuel in various types of nuclear reactors. With the increasing installation of thermal reactors for the commercial generation of electricity, large quantities of plutonium will become available, and it will be very attractive to use this in fast breeder reactors. A strong candidate for the fuel of such a reactor is a mixed uranium-plutonium dioxide.

A knowledge of the thermodynamic properties of fuel materials is important in the control of the stoichiometry during fabrication so necessary in a nuclear fuel element, and in predicting the possible behaviour under operating conditions (including compatibility, migration of fuel down a temperature gradient by vaporization, and valency state of fission products).

The thermodynamic properties of the complex uranium dioxide phase were discussed at a panel organized by the International Atomic Energy Agency [1] in March 1964, and it was considered valuable to compile a similar critical assessment of the thermochemical behaviour of plutonium-oxygen and uranium-plutonium-oxygen systems. The present report is a summary of the data available to the panel and the conclusions reached.

The fluorite structure in which the dioxides crystallize has a remarkable capacity for withstanding both the addition and removal of oxygen ions, so that wide homogeneity ranges of general formula $MO_{2\pm x}$ are formed at high temperatures in both the binary systems (except for PuO_{2+x}) and in the ternary U-Pu-O system. These wide deviations from stoichiometry make the measurement of almost all physical properties unusually difficult, and also have wide repercussions on the use of the oxides as fuel materials.

In recent years, a start has been made on the correlation of the various physical properties of UO_{2+x} with a single defect model, and similar calculations on the substoichiometric phases would be most valuable. It is to be hoped that this review of the structural and thermodynamic data for the Pu-O and Pu-U-O systems will stimulate further research in this and other aspects of the behaviour of this fascinating class of compounds.

NOTATION

Symbol	Meaning	Common units
a	Activity	
C_p	Molar heat capacity	cal degK^{-1} mole^{-1}
ΔG	Free energy of reaction	cal
$\Delta \bar{G}_{O_2}$	Partial molar-free energy of solution of 1 mole of O_2	cal mole^{-1}
ΔH	Heat of reaction	cal
ΔH_f^0	Heat of formation at 25°C	cal
$\Delta \bar{H}_{O_2}$	Partial molar heat of solution of 1 mole of O_2	cal mole^{-1}
ln	Log_e	
log	Log_{10}	
p	Pressure	atm
R	Gas constant	1.987 cal degK^{-1} mole^{-1}
S_{298}^0	Standard entropy at 25°C	cal degK^{-1} mole^{-1} (e.u.)
ΔS	Entropy of reaction	cal degK^{-1}
$\Delta \bar{S}_{O_2}$	Partial molar entropy of solution of 1 mole of O_2	cal degK^{-1} mole^{-1}
T	Absolute temperature	°K
< >	Solid state	
{ }	Liquid state	
( )	Gaseous state	
[ ]	Dissolved state (suffix denoting solvent)	

II. PLUTONIUM OXIDES

1. PREPARATION

1.1. Plutonium monoxide

Although plutonium monoxide, PuO, was reported by Mooney and Zachariasen [2] as an impurity phase, and X-ray diffraction patterns attributed to PuO have been described [3], pure bulk samples have not been prepared. PuO is generally seen as a surface film on plutonium metal. The formation of PuO by reduction of pure samples of PuOCl and PuO_2 by barium vapour has been reported by Westrum [4], but chemical evidence for its formation is meagre. Metallographic and X-ray examination [5] of heat-treated and quenched samples of $PuO_2 + Pu$ in the composition range where PuO would be expected to be formed indicated the presence of mixtures only of hexagonal Pu_2O_3 and plutonium.

Akimoto [6] reported the preparation of PuO by direct reaction between molten plutonium and oxygen generated by the thermal decomposition of Ag_2O. Powder patterns of the product indicated a face-centred cubic phase with a lattice parameter that agreed with the value reported by Zachariasen. The preparation of PuO by the reduction of PuO_2 at 1800°C by carbon was reported by Skavdahl [7]. However, more recent experiments of Forbes et al. [8] have indicated that the products always contained carbon. Other attempts to prepare the monoxide [9] have failed and recent work on the Pu-C-O ternary phase diagram [10, 11, 12] has shown conclusively that the oxygen-rich limit of the Pu(O, C) phase lies at approximately $PuC_{0.3}O_{0.7}$.

The reported preparation of the solid monoxide thus apparently refers to a material stabilized by impurity or by surface energy. However, PuO (gas) is almost certainly the major species over plutonium oxides near the sesquioxide composition (see Section II.4).

1.2. Hexagonal Pu_2O_3

Hexagonal plutonium sesquioxide, referred to in the previous literature as β-Pu_2O_3, is a definite phase with the type a rare earth sesquioxide structure. An upper oxygen content corresponding to $PuO_{1.510}$ has been suggested [13]. In general, plutonium dioxide may be reduced to hexagonal Pu_2O_3 by plutonium metal, very dry hydrogen or carbon.

Holley et al. [5] prepared hexagonal Pu_2O_3 by reducing pure PuO_2 with approximately 20% excess of plutonium turnings or chips in a closed tantalum crucible at 1500°C. The mixture was held at that temperature for 3 h, at the end of which the excess plutonium metal was removed by

3

evaporation from the opened crucible. The product was a black sintered mass. At higher reduction temperatures, large flat crystals of hexagonal Pu_2O_3 were produced. Gardner et al. [13] used a similar method of preparation by heating a mixture of pure PuO_2 powder and 20% excess plutonium metal (prepared by the decomposition of plutonium hydride) in a thoria crucible at 1500°C for 3 h in a stream of purified dry hydrogen gas. Excess plutonium volatilized away from the oxide leaving pure hexagonal Pu_2O_3. Dean [9] has shown that the reduction of the PuO_2 by Pu starts at 700°C.

Appreciable reduction of plutonium dioxide to a lower oxide occurs on sintering PuO_2 pellets in "dry" hydrogen gas at temperatures above 1500°C, the precise composition reached being dependent on the sintering temperature and water content in the hydrogen [14, 15]. Gardner et al. [13] reported complete reduction of PuO_2 pellets to hexagonal Pu_2O_3 in dry hydrogen (purified by passage over heated titanium turnings at 600°C) at 1550°C, if further titanium turnings were present in the reduction furnace.

Roberts et al. [16] found that plutonium dioxide is unstable in contact with carbon at low ambient pressures of carbon monoxide and at temperatures above 1000°C. Detailed investigations of Skavdahl [7, 17] and Dean [9] have shown that hexagonal Pu_2O_3 prepared by reduction of PuO_2 with carbon may be contaminated with minor amounts of cubic $PuO_{1.52}$. Essentially pure hexagonal Pu_2O_3 was obtained by heating stoichiometric proportions of PuO_2 and carbon at 1800 ± 50°C for $5\frac{1}{2}$ h in a pure helium atmosphere. Similar preparation [8] with $PuO_2 + C$ blended compacts at 1800°C for 1 h showed essentially single-phase hexagonal Pu_2O_3 with an impurity carbon content of 0.05%.

Skavdahl and Chikalla [18] reported the preparation of hexagonal Pu_2O_3 on a large scale (110 g Pu) by vacuum reduction sintering of PuO_2 - carbon compacts followed by inert gas arc melting. Reaction of PuO_2 with a slight excess of carbon at 1650°C in vacuum produced a mixture of hexagonal Pu_2O_3 and a small amount of Pu (O, C). The Pu (O, C) phase, being much more volatile than hexagonal Pu_2O_3, could be removed by heating in vacuum. Final arc-melting of the product to form a dense product also contributed to further vaporization of any Pu (O, C) impurity giving pure hexagonal Pu_2O_3. The product analysed O/Pu = 1.500 ± 0.015, with 175 ppm carbon impurity and 93% theoretical density.

1.3. Cubic $PuO_{1.52}$

Cubic plutonium sesquioxide, referred to in the previous literature as α-Pu_2O_3, has not been prepared as a single-phase compound, since it is stable only below 300°C, and hexagonal Pu_2O_3 once formed is difficult to transform to cubic $PuO_{1.52}$. Moreover, the exact composition of this phase is not yet known; early reports [5] suggested compositions between $PuO_{1.58}$ and $PuO_{1.62}$, but the recent phase diagram studies [13] indicate a lower oxygen composition limit of $PuO_{1.515}$.

Cubic $PuO_{1.52}$ has been prepared in various two-phase mixtures. Thus heating PuO_2 at 1650 to 1800°C in vacuum or in inert or reducing atmo-

spheres results in partial reduction of the dioxide, and a mixture of cubic $PuO_{1.52}$ and $PuO_{1.98}$ is formed on cooling to room temperature. The proportion of cubic $PuO_{1.52}$ varies from 10 to 40%, depending on the temperature, duration of heating and the nature of the sintering atmosphere [19]. It has been reported [20] that when PuO_2 is heated in helium to 2280°C, dissociation and melting occur to give $PuO_{1.61}$, which would disproportionate to give ~80% $PuO_{1.52}$ at room temperature. However, reduction to this composition could not have occurred unless some strongly reducing constituent such as tantalum or carbon were also present.

Until the exact composition of this phase is known, it will be impossible to obtain single-phase material, but possible methods of preparation are controlled reduction of PuO_2 by carbon or controlled oxidation of hexagonal Pu_2O_3. In any case, very prolonged annealing below 300°C will undoubtedly be necessary to remove the metastable, but enduring, hexagonal phase.

1.4. $PuO_{1.61}$ and non-stoichiometric oxides

Oxides between $PuO_{1.61}$ and PuO_2 are mainly single-phase materials above 650°C; these may be prepared by reduction of PuO_2 with carbon [21] in vacuo, or less conveniently if a specified composition is required, hydrogen [22, 23], or for the higher compositions, by simply heating PuO_2 in vacuo to high temperatures. Oxidation of a lower oxide by oxygen [13] or PuO_2 may also be used. Some annealing may be required, but it should be remembered that prolonged heating in vacuo of any of these compounds will cause a change in composition because of incongruent vaporization (see Section II.4).

1.5. Plutonium dioxide

Plutonium dioxide is the olive-to-brown product of the combustion of plutonium metal or practically any of its compounds (except those with phosphorus) in air or oxygen. The O/Pu ratio of the product is, however, normally greater than 2 [24, 25], being as much as 2.09 for the oxide obtained from $Pu(SO_4)_2$ in air. Since ignition to PuO_2 is often used as a method of analysis for the lower oxides, this is an important effect. As most of the work on this phenomenon was carried out before the lower oxides were well characterized, there have been no detailed studies of the composition of the product from the lower oxides specifically. However, oxidation of the metal in air which probably goes through the lower oxides gives O/Pu ratios varying from 2.00 to 2.03 [24, 25]. Gardner et al. [13] claim that lower oxide pellets do not absorb oxygen above a composition of PuO_2 when heated in air. Jackson and Rand [26] have shown that this excess oxygen in plutonium dioxide is due entirely to surface adsorption rather than to bulk oxidation as in UO_2. They also found that the amount of oxygen adsorbed from air was up to a factor of two greater than that adsorbed from an equivalent pressure of pure oxygen at the same temperature. The preparative routes for PuO_2 are summarized in Table I.

TABLE I: SUMMARY OF METHODS FOR THE PREPARATION OF PuO$_2$: INTERMEDIATE PRECIPITATION AND CONVERSION DETAILS

Intermediate	Process	Scale Pu (g/litre)	Strike solution	Precipitation temperature (°C)	Digestion temperature (°C)	Digestion time (h)	Filtration characteristics	Drying temperature (°C)	Drying time (h)	Calcination temperature (°C)	Calcination time (h)	References
Pu metal	Air oxidation	-	-	160-670[a]	-	1-4[a]	-	-	-	-	-	[27-30]
Pu nitrate	Denitration	-	-	-	-	-	-	300	9	300-1000	9-22	[4, 31, 32]
Pu hydroxide	Ammonium hydroxide precipitation	1-100	NH$_4$OH	25-30	100	0.16-72	Poor	110	26	250-750	0.75	[33-39]
			NH$_4$OH	55-95	55-95	0.5	Good	110	26	250-750	0.75	
			NH$_3$ gas	55	55	0.5	Poor	100	26	840	1.3	
			Urea	95-100	95-100	2-22	Good	100	96	250-850	2.0	
Pu$_2$(C$_2$O$_4$)$_3$	Oxalate precipitation	1-100	H$_2$C$_2$O$_4$	25-30	25-30	0.5	Good	-	-	950	1.0	[33, 35, 38 40-49]
Pu(C$_2$O$_4$)$_2$	Oxalate precipitation	1-250	H$_2$C$_2$O$_4$ + H$_2$O$_2$	35-55	35-55	0.5	Good	100-180	1-24	350-760	0.5	
Pu peroxide	Peroxide precipitation	10-100	H$_2$O$_2$	15-20	5-15	0.5-2.5	Good	55	48	250-760	0.5	[50-53]
PuCl$_3$ in alkali chloride melt	High temperature precipitation	-	O$_2$-Cl$_2$ gas	400-600	-	-	Good	-	-	-	-	[54]

[a] Reaction temperature and time.

The preparative route and process details have a significant influence on the product PuO_2 characteristics, which affect subsequent fabrication and sintering properties of fuel materials containing PuO_2. From the process point of view, precipitation of Pu(IV) oxalate appears particularly attractive. Plutonium losses in the filtrate are nominal, filtration characteristics of $Pu(C_2O_4)_2.6H_2O$ are excellent, and reproducibility of the product PuO_2 powder characteristics is good. The PuO_2 from this route has comparatively low bulk and tap density, its surface area may be controlled by varying the calcination temperature, and a narrow particle size distribution is obtained. The material has good pressing and sintering characteristics, final sintered densities as high as 96% theoretical being attainable. PuO_2 powder obtained through Pu(IV) oxalate is also suitable for mechanical blending with UO_2 and further fabrication.

Precipitation of plutonium peroxide is also a convenient route for the preparation of PuO_2. However, solubility "losses" are high and the process involves handling large volumes of slurry solutions. The powder characteristics of this PuO_2 are, in general, similar to those of PuO_2 derived from Pu(IV) oxalate except that the tap densities are higher from the peroxide.

Ammoniacal precipitation does not appear attractive from a process point of view. Solubility "losses" are low, but the filtration characteristics of the precipitate are particularly bad for precipitations at room temperature, although high-temperature precipitation (95 to 100°C) with ammonium hydroxide or urea facilitates quicker filtration. The PuO_2 characteristics do not correlate well with the precipitation and conversion details. The powder calcined at temperatures over 750°C has a high tap density (about 5 g/cm^3) and is suited for further fabrication by vibration-compaction and sintering (sintered densities vary from 83.5 to 93.5% of the theoretical density).

PuO_2 may be prepared in highly crystalline [54] form from molten alkali chloride solutions by sparging with an O_2-Cl_2 gas stream. The bulk density of the material is approximately 6 g/cm^3 and this might find use as an excellent intermediate for fabrication by vibration-compaction and sintering.

1.6. Higher oxides of plutonium

Brewer [55] has predicted from thermodynamic considerations that any solid anhydrous oxide of plutonium higher than PuO_2 will probably not be stable. In this respect plutonium resembles thorium rather than its immediate analogues, neptunium and uranium.

Attempts were made to prepare a higher oxide by the controlled ignition of plutonyl nitrate, $PuO_2(NO_3)_2.xH_2O$, but the nitrate decomposed to the dioxide at 275°C [4]. Heating PuO_2 in oxygen at 400°C and under 70 atm pressure, in ozone at 600 to 1000°C, and in atomic oxygen failed to produce a higher oxide [4]. Katz and Gruen [56] have reported that PuO_2 was not oxidized by nitrogen dioxide at 500°C. Bagnall and Laidler [57], however, have reported the isolation of a plutonium trioxide hydrate by the action of ozonized oxygen on Pu(IV) hydroxide at 90°C. The reddish-

gold material formed by vacuum drying at 130°C had the composition $PuO_3 \cdot 0.8H_2O$, but its X-ray pattern showed that it was not isostructural with any known uranium trioxide hydrate. Nevertheless, it is probably best to regard it as plutonyl hydroxide.

2. PHASE DIAGRAM

2.1. Crystal structures

2.1.1. Established structures

2.1.1.1. Hexagonal Pu_2O_3. This phase is the lowest oxide in the system and is stable in contact with Pu metal. The structure is hexagonal, La_2O_3 type, with $a = 3.841 \pm 0.006$ and $c = 5.958 \pm 0.005$ Å with one formula unit per unit cell. The space group is $P\bar{3}m1$, the calculated density is 11.47 g/cm^3 [58]. The structure is that of the a-form rare earth sesquioxide and is isotypic with Ac_2O_3 and hex-Am_2O_3.

A variant of hexagonal Pu_2O_3 has been found by Zachariasen in examining data obtained at Los Alamos. Several preparations showed some diffuse diffraction lines, indicating stacking disorder. In a unique preparation made at high temperature the diffuse lines were consistent with the existence of a stacking fault every sixth c-period giving rise to an ordered superstructure with hexagonal axis, $a = 3.842 \pm 0.001$ and $c = 108.41 \pm 0.01$ Å ($= 18 \times 6.023$ Å).

2.1.1.2. Cubic $PuO_{1.52}$. This structure is body-centred cubic, bixbyite type with $a = 11.047 - 11.07$ Å. There are 32 metal atoms and 48 oxygen atoms per unit cell (for the ideal composition $PuO_{1.5}$). The space group is Ia3, the calculated density is 10.2 g/cm^3. The structure of this phase, which appears to exist only below 300°C, is well established from X-ray powder diffraction data as that of the c-form rare-earth sesquioxides and is isotypic with cubic Am_2O_3 and Cm_2O_3. Workers at Harwell [13] have suggested that its composition is $PuO_{1.52}$. Whether or not this phase is a low-temperature modification of hexagonal Pu_2O_3 is at present an open question. The similarity of this structure with those of $PuO_{1.61}$ and PuO_2 is discussed below.

2.1.1.3. Cubic $PuO_{1.61+y}$. The true structure of this phase, which is stable only above 350°C, has not been established; above 650°C it may merely be the lower limit of the substoichiometric plutonia phase. The structure is, however, closely related to that of cubic $PuO_{1.52}$ and hence may be tentatively described as cubic with $a = 11.03$ Å at 350°C; there are 32 metal atoms and an assumed 51 or 52 oxygen atoms per unit cell for the $PuO_{1.61}$ composition. In X-ray films taken at temperatures above 300°C, only the strong pseudo face-centred cubic reflections have been seen. In films of quenched samples at room temperature taken at Los Alamos the weak body-centred cubic reflections are also seen, suggesting that the structure may be body-centred cubic above 300°C. At room temperature the X-ray powder pattern of $PuO_{1.61}$ is distinguished

8

from that of $PuO_{1.52}$ by the smaller lattice parameter and also by the
relative intensities of the reflections for which $h^2 + k^2 + l^2 = 190$ and 192.
For $PuO_{1.52}$, $I_{190} : I_{192} = 10:3$ and for $PuO_{1.6}$, $I_{190}:I_{192} = 7:10$. The shift
in intensity is a consequence of a change in the Pu atom position parameter,
x, from -0.030 for the bixbyite structure to -0.020 for $PuO_{1.61}$ (see
Section II.2.1.3).

2.1.1.4. Plutonium dioxide. This is the highest oxide in the system.
The structure [2], which is isotypic with dioxides of some of the rare-
earth, and all other actinide elements up to at least curium, is face-
centred cubic, fluorite-type, with a = 5.3960 ± 0.0003 Å, space group
Fm3m. With four formula units per unit cell, the calculated density is
11.46 g cm^{-3}. However, in common with all α-active materials, the
lattice parameter increases with time [59, 60] owing to the introduction
of Frenkel defects into the lattice as a result of the α-decay process.
The precise rate of increase depends on the isotopic composition, but for
plutonium containing ~95% ^{239}Pu and ~5% ^{240}Pu, the parameter is
given by

$$a(Å) = 5.3960 + 0.0182 \ (1 - \exp(-9.64 \times 10^{-4} \ t))$$

where t is the time in days that has elapsed since the oxide was prepared
or last annealed. The self-damage anneals out fairly uniformly as the
temperature is heated to 1000°C [60].

At temperatures above about 650°C, PuO_2 can exist with a consider-
able oxygen deficiency, down to at least $PuO_{1.7}$ and perhaps as far as
$PuO_{1.61}$. The effect of removing oxygen is to expand the lattice, and
Atlas et al.[61] have shown from density measurements at 750°C that
this involves oxygen vacancies rather than interstitial plutonium ions.
Although pure PuO_{2-x} can apparently not be quenched to room tempera-
ture, it has been observed at Los Alamos that tantalum or tungsten
impurity will stabilize PuO_{2-x} with an enlarged lattice parameter at
25°C [62].

2.1.2. X-ray powder patterns of the plutonium oxides

The computed powder diffraction patterns of PuO_2, cubic $PuO_{1.52}$
and hexagonal Pu_2O_3 are given in Tables II-IV. The computed intensities
include contributions from the oxygen atoms as well as the plutonium
atoms. For hexagonal Pu_2O_3 (Table II) the atomic positions are 2 Pu in
(d), with z = 0.235, and 1 O in (a) and 2 O in (d), with z = 0.63. The
values for z are those for La_2O_3.

The atomic positions and parameters for the other three cubic
oxides are given in Table V. The positions of the oxygen atoms in $PuO_{1.52}$
and $PuO_{1.61}$ are assumed to be the same as those in bixbyite.

The patterns for cubic $PuO_{1.52}$ and $PuO_{1.6}$ are quite similar to the
pattern for PuO_2, as the strong reflections are those of the face-centred
cubic metal lattice. The additional reflections that occur because of the
body-centred cubic symmetry and larger unit cell are weak, although

TABLE II.   POWDER PATTERN FOR HEXAGONAL Pu_2O_3

$a_0 = 3.840$ Å   Copper radiation $\lambda(K\alpha_1) = 1.54051$ Å
$c_0 = 5.957$ Å

2θ	$\sin^2\theta$	d-spacing	Intensity	h	k	l
26.81	0537	3.326	27	0	1	0
30.00	0670	2.979	24	0	0	2
30.79	0705	2.904	100	0	1	1
40.66	1207	2.219	23	0	1	2
47.35	1612	1.920	26	1	1	0
53.77	2045	1.705	22	0	1	3
55.24	2149	1.663	3	0	2	0
57.07	2282	1.614	22	1	1	2
57.55	2317	1.602	16	0	2	1
62.35	2680	1.489	3	0	0	4
64.14	2819	1.452	5	0	2	2
69.11	3217	1.359	4	0	1	4
74.42	3657	1.275	8	0	2	3
75.66	3762	1.257	3	1	2	0
77.63	3929	1.230	12	1	2	1
81.86	4292	1.177	6	1	1	4
83.47	4431	1.158	4	1	2	2
86.84	4724	1.122	4	0	1	5
88.12	4836	1.109	4	0	3	0
93.08	5269	1.062	8	1	2	3
95.81	5506	1.039	5	0	3	2
105.50	6336	0.969	3	0	2	5

TABLE II. (cont.)

2θ	sin² θ	d-spacing	Intensity	h	k	l
106.75	6441	0.961	3	1	2	4
106.84	6448	0.960	3	2	2	0
115.07	7118	0.914	4	2	2	2
115.51	7153	0.912	7	1	3	1
120.21	7516	0.889	4	0	3	4
121.88	7641	0.882	3	1	1	6
122.08	7656	0.881	3	1	3	2
126.13	7948	0.865	7	1	2	5
134.32	8493	0.837	8	1	3	3
138.48	8743	0.824	3	0	1	7
138.86	8765	0.823	4	0	4	1
145.65	9128	0.807	6	2	2	4
148.60	9268	0.801	3	0	4	2
158.92	9665	0.784	6	1	3	4
163.36	9791	0.779	10	1	2	6
164.50	9818	0.778	6	1	1	7

many are visible in films of well-crystallized material. As noted above, the extra body-centred cubic reflections for $PuO_{1.61}$ have not been observed in the poor quality films obtained at high temperatures.

2.1.3. Comparison of the structures

To provide a clear view of the similarity in structure, Table V describes the detailed structures of the three cubic oxides as based on space group Ia3. This requires doubling of the correct unit cell dimension for PuO_2. In $PuO_{1.61}$ there must be either three or four extra oxygen atoms in the cell, giving ideal formulae of $PuO_{1.594}$ or $PuO_{1.625}$. The latter is more probable, since this allows eight Pu(IV) atoms to occupy the 8-fold b-positions, and 24 Pu(III) atoms to occupy the 24-fold d-

TABLE III.   POWDER PATTERN FOR CUBIC $PuO_{1.52}$ (reflections with an intensity of 2 or less have been omitted)

a_0 = 11.050 Å Copper radiation $\lambda(K\alpha_1)$ = 1.54051 Å

Body-centred cubic

2θ	$\sin^2\theta$	d-spacing	Intensity	h k l
19.66	0292	4.511	5	1 1 2
27.95	0583	3.190	71	2 2 2
32.38	0777	2.763	32	0 0 4
34.40	0875	2.605	5	1 1 4
38.17	1069	2.356	5	2 3 3
41.64	1263	2.167	8	1 3 4
46.45	1555	1.953	51	0 4 4
47.96	1652	1.895	3	3 3 4
50.90	1846	1.793	6	1 1 6, 2 3 5
53.71	2041	1.705	6	1 4 5
55.08	2138	1.666	55	2 2 6
36.43	2235	1.629	9	1 3 6
57.76	2332	1.595	13	4 4 4
59.06	2429	1.563	4	3 4 5
61.63	2624	1.504	5	1 2 7, 3 3 6, 2 5 5
62.88	2721	1.477	3	2 4 6
66.58	3013	1.403	6	1 5 6, 2 3 7
67.79	3110	1.381	10	0 0 8
68.98	3207	1.360	10	1 1 8, 4 5 5, 1 4 7
70.17	3304	1.340	4	4 4 6, 0 2 8
71.35	3401	1.321	5	3 5 6
72.52	3498	1.302	3	0 6 6, 2 2 8

12

TABLE III. (cont.)

2θ	sin² θ	d-spacing	Intensity	h k l
73.69	3596	1.285	9	1 3 8, 3 4 7
74.84	3693	1.268	23	2 6 6
77.14	3887	1.235	19	0 4 8
78.28	3984	1.220	3	3 3 8
79.42	4082	1.206	3	2 4 8
80.55	4179	1.192	7	1 2 9, 1 6 7, 5 5 6
82.80	4373	1.165	6	1 5 8, 4 5 7
85.04	4567	1.140	6	3 6 7, 2 3 9
86.15	4665	1.128	18	4 4 8
87.27	4762	1.116	7	1 4 9, 3 5 8
88.38	4859	1.105	4	0 6 8, 0 0 10
89.50	4956	1.094	3	1 1 10, 2 7 7
90.61	5053	1.084	9	2 6 8, 0 2 10
92.84	5248	1.063	19	6 6 6, 2 2 10
93.96	5345	1.054	9	2 5 9, 5 6 7, 1 3 10
96.19	5539	1.035	8	1 7 8, 5 5 8, 4 7 7
97.31	5636	1.026	8	0 4 10, 4 6 8
98.44	5734	1.017	6	1 6 9, 3 3 10
99.56	5831	1.009	7	2 4 10
100.70	5928	1.000	6	4 5 9, 3 7 8
102.97	6122	0.984	9	3 6 9, 1 5 10, 1 2 11
104.12	6219	0.977	6	0 8 8
106.43	6414	0.962	4	2 8 8, 4 4 10
107.59	6511	0.955	9	6 7 7, 2 7 9, 3 5 10, 2 3 11
108.76	6608	0.948	3	0 6 10, 6 6 8

TABLE III. (cont.)

2θ	$\sin^2\theta$	d-spacing	Intensity	h	k	l								
109.94	6705	0.941	7	1	4	11,	5	7	8					
111.13	6803	0.934	20	2	6	10								
112.33	6900	0.927	4	5	6	9								
113.54	6997	0.921	10	0	0	12,	4	8	8					
114.76	7094	0.915	11	1	1	12,	4	9	7,	3	4	11,		
				1	8	9								
115.99	7191	0.908	7	0	2	12								
117.24	7288	0.902	8	2	5	11,	5	5	10,	1	7	10		
118.50	7386	0.896	10	4	6	10,	2	2	12					
119.77	7483	0.890	8	1	3	12,	3	8	9					
122.37	7677	0.879	10	3	7	10,	1	6	11					
123.70	7774	0.874	15	0	4	12								
125.05	7872	0.868	6	3	3	12,	4	5	11,	7	7	8		
126.42	7969	0.863	20	2	4	12,	6	8	8,	0	8	10		
127.82	8066	0.858	7	3	6	11,	6	7	9,	2	9	9		
129.24	8163	0.853	16	2	8	10								
130.70	8260	0.848	11	1	5	12,	5	8	9					
132.18	8357	0.843	9	6	6	10								
133.70	8455	0.838	8	1	2	13,	2	7	11,	5	7	10		
135.26	8552	0.833	11	4	4	12								
136.87	8649	0.828	6	3	5	12,	4	9	9					
138.52	8746	0.824	30	0	6	12,	4	8	10					
140.23	8843	0.819	14	2	3	13,	1	9	10,	5	6	11		
142.01	8941	0.815	26	2	6	12								
143.86	9038	0.810	19	1	4	13,	1	8	11,	4	7	11		
147.82	9232	0.802	10	3	9	10								

14

TABLE III. (cont.)

2θ	$\sin^2\theta$	d-spacing	Intensity	h k l							
149.98	9329	0.798	3	8	8	8					
152.29	9426	0.793	43	$\left\{\begin{array}{l}3 \\ 3\end{array}\right.$	4 8	13, 11	1	7	12,	7 8 9,	
154.79	9524	0.789	38	4	6	12,	0	0	14		
157.54	9621	0.785	20	$\left\{\begin{array}{l}2 \\ 1\end{array}\right.$	5 1	13, 14,	6 7	9 7	9, 10		
160.66	9718	0.781	60	0	2	14,	6	8	10,	0 10 10	
164.37	9815	0.778	14	3	7	12					
169.25	9912	0.774	100	2	10	10,	2	2	14		

positions. However, since there are no 4-fold positions in this space group, the four additional oxygen atoms are presumably randomly distributed among the 16 vacant c-positions: i.e. $PuO_{1.625}$ (or $PuO_{1.61}$) contains some oxygen disorder.

The discussion, of course, refers to the quenched room temperature structure of $PuO_{1.61}$, which is body-centred cubic. It is not yet known whether the high-temperature structure is body- or face-centred cubic (see below). If it is the latter, the plutonium atoms are all on face-centred cubic positions (i.e. the 24 Pu atoms in d-positions have x = 0) and the 52 (or 51) oxygen atoms are randomly distributed among the 64 (c + e) positions.

It is a further possibility that the poor quality of the diffraction patterns of $PuO_{1.61}$ at high temperatures implies that the structure is slightly distorted from true cubic symmetry.

Because the three structures are all so similar, it appears plausible at first sight that a continuous transition could be achieved from the face-centred cubic PuO_2 to the cubic $PuO_{1.61}$. One can start with PuO_2, produce PuO_{2-x} by a random removal of oxygen to create anion vacancies in random positions until a composition of $PuO_{1.61}$ is reached. Now if $PuO_{1.61}$ has a body-centred cubic structure, the oxygen atoms and hence the anion vacancies are ordered, and a continuous transition from PuO_2 to $PuO_{1.61}$ is not possible because at some point ordering of the vacancies must occur. The disorder-order transition would presumably produce a miscibility gap in the phase diagram.

Some evidence indicating that $PuO_{1.61}$ may be body-centred cubic has been obtained at Los Alamos. X-ray films from quenched samples of $PuO_{1.61}$ show clearly the "extra" body-centred cubic reflections, the lattice parameter being 11.02 Å and the $I_{190}:I_{192}$ ratio that for x = -0.020.

15

TABLE IV.   POWDER PATTERN FOR PuO_2

$a_0 = 5.3960$ Å   Copper radiation $\lambda(K\alpha_1) = 1.54051$ Å

Face-centred cubic

2θ	$\sin^2 \theta$	d-spacing	Intensity	h	k	l			
28.62	0611	3.115	14	1	1	1			
33.18	0815	2.698	7	0	0	2			
47.62	1630	1.908	12	0	2	2			
56.51	2241	1.627	15	1	1	3			
59.22	2445	1.558	4	2	2	2			
69.64	3260	1.349	3	0	0	4			
76.96	3872	1.238	8	1	3	3			
79.34	4075	1.207	7	0	2	4			
88.74	4891	1.101	8	2	2	4			
95.76	5502	1.038	9	3	3	3,	1	1	5
107.70	6520	0.954	4	0	4	4			
115.24	7132	0.912	14	1	3	5			
117.86	7336	0.899	8	0	0	6,	2	4	4
129.04	8150	0.853	9	0	2	6			
138.78	8761	0.823	10	3	3	5			
142.52	8966	0.813	10	2	2	6			
162.96	9780	0.779	6	4	4	4			

Upon heat treatment at temperatures below 300°C, a change to the
pattern for $PuO_{1.52}$ is observed, and the PuO_{2-x} pattern becomes stronger,
indicating that the disproportionation

$$PuO_{1.61} \rightarrow 0.805\ PuO_{1.52} + 0.195\ PuO_{1.98}$$
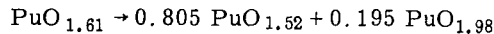
has occurred.   The implication is strong that the high-temperature form,
$PuO_{1.61}$, has been retained by the quench and that it is body-centred cubic

16

TABLE V.   RELATION BETWEEN OXIDE STRUCTURES BASED
ON SPACE GROUP Ia3

	$PuO_{1.52}$	$PuO_{1.61}$	PuO_2
Lattice parameter − Å	11.05	11.02	10.792 ($= 2 \times 5.396$)
Pu atoms			
Type of position			
8 b	8	8	8
24 d	24	24	24
	$x = -0.030 \pm 0.003$	$x = -0.020 \pm 0.003$	
O atoms			
Type of position			
16 c	0	4 $x = 1/8$[a]	16 $x = 1/8$
48 e	48	48	48
	$x = 0.385$[a]	$x = 0.385$[a]	$x = 3/8$
	$y = 0.145$[a]	$y = 0.145$[a]	$y = 1/8$
	$z = 0.380$[a]	$z = 0.380$[a]	$z = 1/8$

[a] Assumed values.

at high temperatures. The evidence is not conclusive, however, and the
final decision can only be made from knowledge of the detailed structure
of $PuO_{1.61}$ at temperatures above 300°C. Definite evidence showing
whether or not the weak "extra" body-centred cubic lines are present in
the high-temperature powder patterns of $PuO_{1.61}$ is most desirable.

2.2. Condensed phase diagram

2.2.1. General

The complete phase diagram of the plutonium-oxygen system is not
well established. The evidence is not as detailed as might be desired,
and it is possible that future work will considerably modify any
diagram chosen at this time.
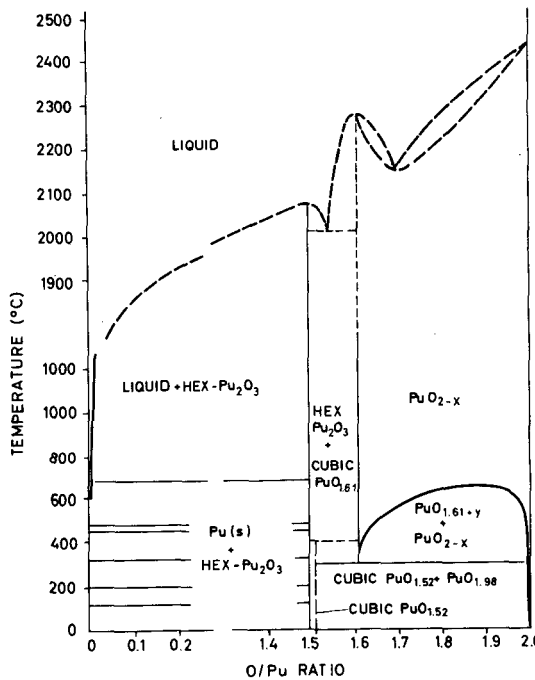
FIG. 1. Tentative plutonium-oxygen phase diagram.

Three aspects may be considered separately: the phases known to exist, the melting behaviour, and the region between $PuO_{1.5}$ and PuO_2 below 1000°C.

2.2.2. Phases.

The four known oxide structures, hexagonal Pu_2O_3, cubic $PuO_{1.52}$, cubic $PuO_{1.61}$ and PuO_2 have been discussed in Section II.2.1.1.

Plutonium monoxide, which has been shown in one proposed phase diagram [20], is now generally believed not to occur as an equilibrium phase (see Section II.1.1.), although a thin PuO film stabilized by surface energy may possibly exist. However, it is noteworthy that positive evidence that such a film is really an oxide is lacking.

2.2.3. Melting behaviour

The melting points of the three high-temperature phases are approximately as shown in Fig. 1 but the liquid-solid relationships sketched must be regarded as hypothetical. The problem in determining the melting behaviour of the Pu oxides is that the temperatures are high enough for vaporization to become a dominant factor. Both hexagonal Pu_2O_3 and $PuO_{1.61}$ vaporize incongruently as does stoichiometric PuO_2. The congruently vaporizing composition near the melting point is, according

18

to Ackermann et al. [63], about $PuO_{1.8}$. Thus, in principle, the melting point of this composition only can be observed in vacuum. The only certain statement that can be made is that the liquidus curve for the range between $PuO_{1.5}$ and PuO_2 lies between 2000° and 2300°C over most of the range and rises to a maximum of about 2400°C or higher near stoichiometric PuO_2. It is not possible to make a firm decision on details of melting behaviour from evidence at present available, nor does it appear possible to select reliable melting points from the literature.

The high temperature part of Fig. 1 follows that of Livey and Feschotte [64], which is based largely on the work of Riley [65], and is also like that suggested by Chikalla et al. [20].

2.2.4. The $PuO_{1.5}$ -PuO_2 region

The existing situation is that there are two major pieces of experimental evidence upon which to base construction of the phase diagram in this region: the high-temperature X-ray study of Gardner et al. [13] (Fig. 2), and the EMF study reported by Markin and Rand [66]. In addition some less detailed high-temperature X-ray studies by Chikalla et al. [20], electrical resistivity measurements by McNeilly [67] and three sets of thermal expansion measurements [20, 68, 69] give useful evidence on the position of the phase boundaries.

Several pieces of work have been derived from these primary data. Following the work of Gardner et al. [13], who constructed a phase diagram, and Markin and Rand [66], who derived free energy data from the EMF work, Rand [70] has made a thermodynamic assessment which co-ordinates all the independent but inter-related raw data. In this assessment, a phase diagram (Fig. 1), very similar to but not identical with that proposed by Gardner et al. [13], was adopted as being the simplest consistent with all the known data. It is now clear, however, that the finer details of the phase diagram cannot be settled from the data at present available. For consistency, therefore, the phase diagram of Fig. 1 and the co-related thermodynamic assessment are adopted here. Other possibilities for the phase diagram are discussed in detail in the subsequent paragraphs, and it must be emphasized that at present it is impossible to endorse a single final version of the phase diagram in the $PuO_{1.5}$ -PuO_2 region.

When all the evidence is considered critically, at least two possibilities for the phase diagram appear likely. One is the diagram presented in Fig. 1, showing that $PuO_{1.61}$ is continuous with PuO_{2-x} above 650°C. This diagram implies either that $PuO_{1.61}$ is face-centred cubic, or that an ordering of the oxygen sub-lattice occurs that does not give rise to any feature in the phase diagram.

Another possibility, equally likely, is that a narrow two-phase miscibility gap exists somewhere between $PuO_{1.61}$ and PuO_{2-x} above 650°C. This alternative diagram would be required if $PuO_{1.61}$ were body-centred cubic, as is quite likely, since a continuous transition between face-centred cubic PuO_{2-x} and body-centred cubic $PuO_{1.61}$ is almost impossible to accept for structural reasons. It should be noted that detailed

19
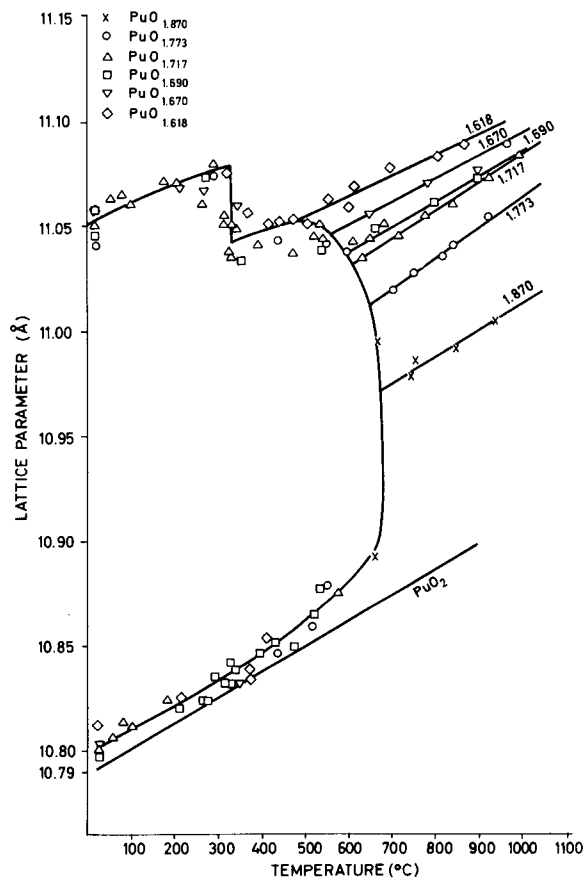
FIG. 2. High-temperature lattice parameters.

work on the Pr-O and Ce-O systems, which exhibit wide ranges of homo-
geneity analogous to those in the Pu-O system, has shown that a con-
tinuous transition from face-centred cubic MO_{2-x} to body-centred cubic
$MO_{1.5+y}$ does not occur [71-74]. The two phases are separated by one
or more intermediate phases (at low temperatures) or by a miscibility gap
(at high temperatures). It seems fairly well established that no ordered
intermediate phases exist in the Pu-O system, but a miscibility gap
appears to be quite possible.

The existence of such a diphasic region is entirely consistent with all
the data mentioned above, although these do, of course, impose some
restrictions on its possible position. Several possibilities remain, how-
ever, and these are discussed in Section II.3.4, together with the changes
required in the free energy diagram. To accommodate a miscibility gap
no adjustment is necessary in the X-ray data.

In addition to the above possibilities, it is evident that the region
below 300°C also can have alternative constructions. Evidence from which

the horizontal at 300°C, corresponding to the eutectoid reaction $\langle PuO_{1.61} \rangle = 0.805 \langle PuO_{1.52} \rangle + 0.195 \langle PuO_{1.98} \rangle$, is deduced might equally well be explained by postulating that $PuO_{1.52}$ and $PuO_{1.61}$ are the same phase with a continuous change in oxygen content occurring over a small temperature range around 300°C.

Evidence for the nature of the diagram around $PuO_{1.5}$ is lacking. The present diagram has been drawn to obey the phase rule and to conform to the suggestion that $\langle PuO_{1.52} \rangle$ contains slightly more oxygen than $\langle Pu_2O_3 \rangle$ hex. An alternative possibility, suggested by the close resemblance of the plutonium oxide structures to those of the rare-earth oxides, is that $\langle PuO_{1.52} \rangle$ is a low-temperature form of $\langle Pu_2O_3 \rangle$ hex. Although this is attractive, it seems unlikely that experimental evidence on which to decide the point will be obtained, as the low temperature at which the transition must occur will not permit equilibrium to be achieved; even in the lanthanide oxides the expected reversion of hexagonal to cubic M_2O_3 at ~800°C has never been observed [75].

To summarize, the phase diagram of Fig. 1 in the $PuO_{1.5}$ -PuO_2 region below 1000°C fits all the evidence available at present, and is consistent with the thermochemical calculations of Section II.3.4. However, alternative constructions to Fig. 1, which seem equally likely, can be postulated. Chief among these is a diagram showing a narrow miscibility gap between $PuO_{1.61+y}$ and PuO_{2-x}.

Definite evidence for the structure of $PuO_{1.61}$ is needed. If $PuO_{1.61}$ is body-centred cubic, it is difficult to see how the diagram can be drawn without a miscibility gap. The position of such a gap will be difficult to locate exactly, since it is likely to be rather narrow. More detailed electrical resistance measurements might be helpful.

3. THERMOCHEMICAL DATA FOR SOLID PHASES

3.1. Heat capacities and entropies

3.1.1. Low-temperature heat capacities and entropies: problems with cryogenic heat capacity measurements

3.1.1.1. General. A discussion of the problems associated with radioactive materials at low temperatures is necessarily somewhat speculative as few data are available. However, the problems encountered are important as they bear directly upon the feasibility of the determination of absolute entropies for plutonium compounds from low-temperature heat capacity measurements. Two difficulties unique to radioactive species, namely self-heat and self-irradiation damage, are discussed below. We may first mention, however, that since the entropies of (PuF_6) and (Pu) are known accurately from spectroscopic data, absolute entropies of other plutonium compounds (including the oxides) can in principle be obtained from accurate equilibrium measurements. Rand [76] has discussed this aspect of the problem. It is also true, of course, that since practical calculations deal only with entropy and free energy differences, absolute entropy values are not essential for this purpose.

3.1.1.2. Self heat. Heat is generated in a radioactive material as a consequence of self-absorption of the radiated particles. For the plutonium most commonly available, which is principally ^{239}Pu, the heat generation rate is about 7 cal/min g-a [77], but a complete precise calculation would need to take into account the fraction of radiation leaving the sample and heating the heat sink. Applying this value to mixtures containing other isotopes of Pu requires correction for the mean half life. Normally, low-temperature heat capacities are measured in an adiabatic calorimeter with the electrical energy input controlled by the experimenter.

It is usually desirable for the temperature to rise at a rate of 1 deg min^{-1} or less to permit attainment of thermal equilibrium between the sample and the calorimeter proper. With plutonium or its compounds the internal energy generation rate is constant, and at low temperatures where the system heat capacity is small, the temperature rise rate is too fast to allow accurate data to be obtained. The problem is principally one of thermal equilibration and will be worse with materials of low thermal conductivity such as PuO_2 than with better conductors such as Pu metal. It is therefore suggested that PuO_2 be diluted with a good heat conductor to minimize the effect of temperature gradients both within the sample and to the container, or plutonium isotopes with much longer half-life times (^{242}Pu or preferably ^{244}Pu) be used. Approximate figures for the centre temperature of a pure PuO_2 sample can be obtained by applying the differential equation for heat flow. Uncertainty in this approximation comes mainly from insufficient knowledge of the thermal conductivity of the sample in the low-temperature range. The effect of the self-heat is thus to set a temperature limit below which heat capacity data are difficult to obtain. Up to now, with ordinary plutonium, this limit appears to be about 10-15°K. With many materials magnetic and other ordering effects are found in the heat capacity below 10°K, and they contribute substantially to the absolute entropy. Such so-called anomalies in plutonium compounds are very likely to be difficult to measure precisely.

3.1.1.3. Radiation self-damage. As a consequence of the production of highly energetic alpha particles and nuclear interactions created therefrom (e.g. α-n), a large number of defects is induced in the PuO_2 lattice. These defects may be present either as single point defects or as clusters of defects. An illustrative example of the effect of this phenomenon is given below.

The volume fraction affected by the passage of alpha particles can be calculated in a simple way by using the following formula:

$$f_{vol} = 1 - e^{-Nv}$$

where N is the number of alpha particles and v is the volume of an alpha-particle track. Reasonable values for the track dimensions of an alpha particle in PuO_2 are 100 Å diam. and 1000 Å length ($v \approx 8 \times 10^{-17}$ cm^3). Introducing these values in the above expression one finds that ∼50% of the volume will be affected by the tracks after 9×10^{15} disintegrations

TABLE VI.   LOW-TEMPERATURE HEAT CAPACITY OF PuO_2

T(°K)	C_p (cal/mole deg K)	T(°K)	C_p (cal/mole deg K)	T(°K)	C_p (cal/mole deg K)
13	0.24	100	6.4	210	12.4
15	0.29	110	7.0	220	12.9
20	0.48	120	7.6	230	13.4
25	0.80	130	8.1	240	13.9
30	1.13	140	8.7	250	14.4
35	1.42	150	9.3	260	14.9
40	1.80	160	9.8	270	15.3
45	2.22	170	10.4	280	15.7
50	2.62	180	10.9	290	16.1
60	3.42	190	11.4	300	16.5
70	4.20	200	12.0	298.15	16.4
90	5.67				

(4 d) and 90% after 3×10^{16} decays (14 d).   Calculation following the formula of Kinchin and Pease [78] gives 40 defects per alpha particle and about 1700 defects per uranium recoil atom.   The presence of a high number of lattice defects will affect to a certain extent the vibrational spectrum of the lattice and hence influence the heat capacity.

In metals such as Pu the lattice defects produced by the alpha particles and recoiling atom can be annealed at relatively low temperatures [79]. In most metal oxides, however, the defects are more permanent and less easily removed by annealing processes.   Radiation self-damage also causes the lattice parameter of plutonium compounds to increase, even at room temperature, and measurements on damaged samples [60] indicate that this damage does not anneal out until about 1000°C.   It is obviously important to make heat capacity measurements on radioactive samples as soon as possible after preparation or annealing.

Nevertheless, some damage will always be present at very low temperatures, and this will affect the measured heat capacities in two ways.   Firstly, the heat capacity itself will be changed by the modification of the lattice vibrational spectrum arising from the defect concentration; quantitatively this effect is likely to be fairly small in samples that are not too heavily damaged.   Secondly, the energy stored in the defects will be evolved as they anneal on warming; this will give measured C_p values which are lower than the true values.   In addition, of course, the self-damage may interfere with any ordering processes that would normally occur (see below).

3.1.1.4. Heat capacity measurements.   Measurements of the heat capacity of PuO_2 below 325°K have been reported by Sandenaw [80].   The
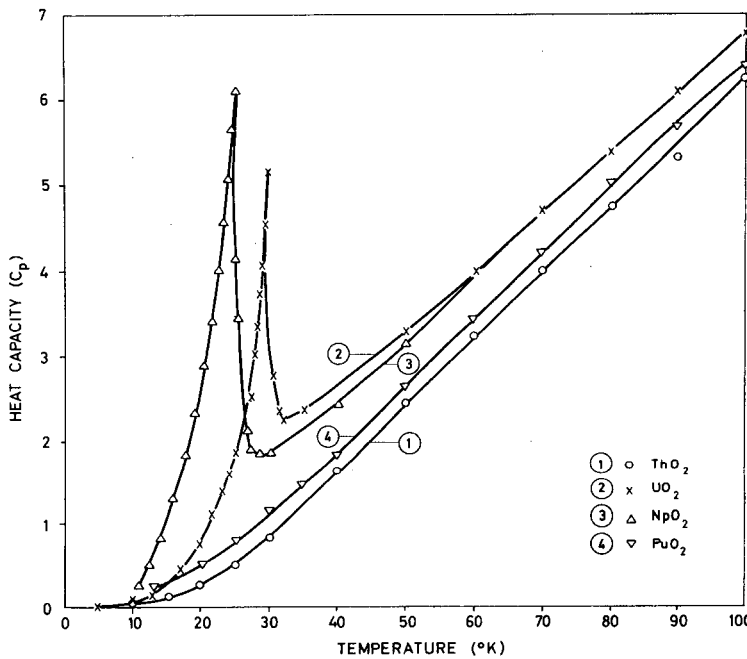
FIG. 3.   Experimental low-temperature heat capacities of ThO_2, UO_2, NpO_2 and PuO_2.

results showed some anomalous and irreproducible effects.   In the first temperature cycle two peaks appeared around 34 and 69°K in the heat capacity curve.   These humps gradually disappeared on further cycling and after the seventh cycle a heat capacity curve free from any peak was obtained.   These data are tabulated in Table VI and represented in Fig. 3 where the values for ThO_2 [81], UO_2 [1, 82] and NpO_2 [83] are included for comparison.   Sandenaw assumed this curve to be the correct one for very slightly substoichiometric PuO_2, but it is now clear that the increased lattice parameter (5.403 Å) of the material was a consequence of self-damage, which causes the lattice parameter of stoichiometric PuO_2 to increase from 5.396 to 5.414 Å at saturation [60].   The above values therefore refer to a substantially damaged PuO_2.   The effect of such damage on the heat capacities in general will first be discussed, followed by a consideration of a possible magnetic ordering phenomenon.

TABLE VII.   DEBYE TEMPERATURE (°K)

| Substance	Elastic moduli	Intensity measurements	Mean	Reference
ThO_2	417	393	405	[84, 85]
UO_2	388	377	382	[84, 85]
PuO_2	-	415	415	[86]

24

Debye temperatures measured from X-ray or neutron diffraction intensity measurements, or calculated from elastic constants, can be used to estimate values of the heat capacity. Table VII shows that the calculated values for the Debye temperatures of ThO_2 and UO_2 are reasonably consistent, although a value of 870°K for UO_2 has been deduced from thermal conductivity measurements.

Comparison of the C_v values calculated from these mean Debye temperatures with experimental C_p values for UO_2 and ThO_2 (the fact that C_p and C_v have different values is unimportant) shows the same behaviour. The calculated values are slightly lower than the experimental at 50°K, but are considerably higher (by up to 2.5 cal deg K^{-1} $mole^{-1}$) above 50°K. Since exactly the same behaviour is found for PuO_2 (see Fig. 4), we may have confidence that Sandenaw's values in general are not greatly in error. The discussion in Section II. 1. 3. implies, however, that they are likely to be slightly low, as Sandenaw recognized.

In a more recent interpretation of the UO_2 neutron diffraction data [1], Willis has analysed the lattice heat capacity in terms of a Debye acoustical branch associated with the vibrations of the uranium sub-lattice (Debye temperature = 182°K) and an Einstein optical branch associated with the oxygen sub-lattice (Einstein temperature = 542°K). This representation leads to excellent agreement with the experimental heat capacity values, and with the lattice entropy at 25°C (calculated = 17.3, experimental = 17.5 e. u.). A similar neutron diffraction study of PuO_2 is thus a possible method of deriving heat capacities and entropies for PuO_2. The heat capacity curves for UO_2 and NpO_2 contain a lambda-type peak near 30°K, which has been shown, for UO_2 at least [1], to be caused by an antiferromagnetic ordering of the electron spins. Since the plutonium atom in PuO_2 has four 5f electrons, a similar, indeed more pronounced, peak could be expected in PuO_2.

It is impossible to infer from Sandenaw's data whether such a peak occurs in the undamaged PuO_2, since the several "spikes" seen in the first runs were also found in his heat capacity curve for plutonium metal, where the latest data [87, 88] indicate a smooth curve free from anomalies. It is thus possible that they were experimental artefacts, although it is tempting to attribute the peak near 34°K to a magnetic ordering. Conversely, there are a number of possible explanations for the absence of the peak in the self-damaged sample. In addition to the possibility of destruction of the long-range order by the self-damage, the lambda peak may have been below 12°K, the lowest temperature measured, which again may not have been the true temperature because of self-heat.

A brief progress report [89] claims that no magnetic ordering could be found by neutron diffraction in $^{242}PuO_2$. It is obviously essential to confirm this somewhat surprising behaviour, and a convenient and relatively simple measurement would be the magnetic susceptibility of PuO_2 down to these temperatures, since dXm/dT changes extremely rapidly near an antiferromagnetic transition. Dawson [90] has measured the magnetic susceptibility of PuO_2, but down to 90°K only. At room
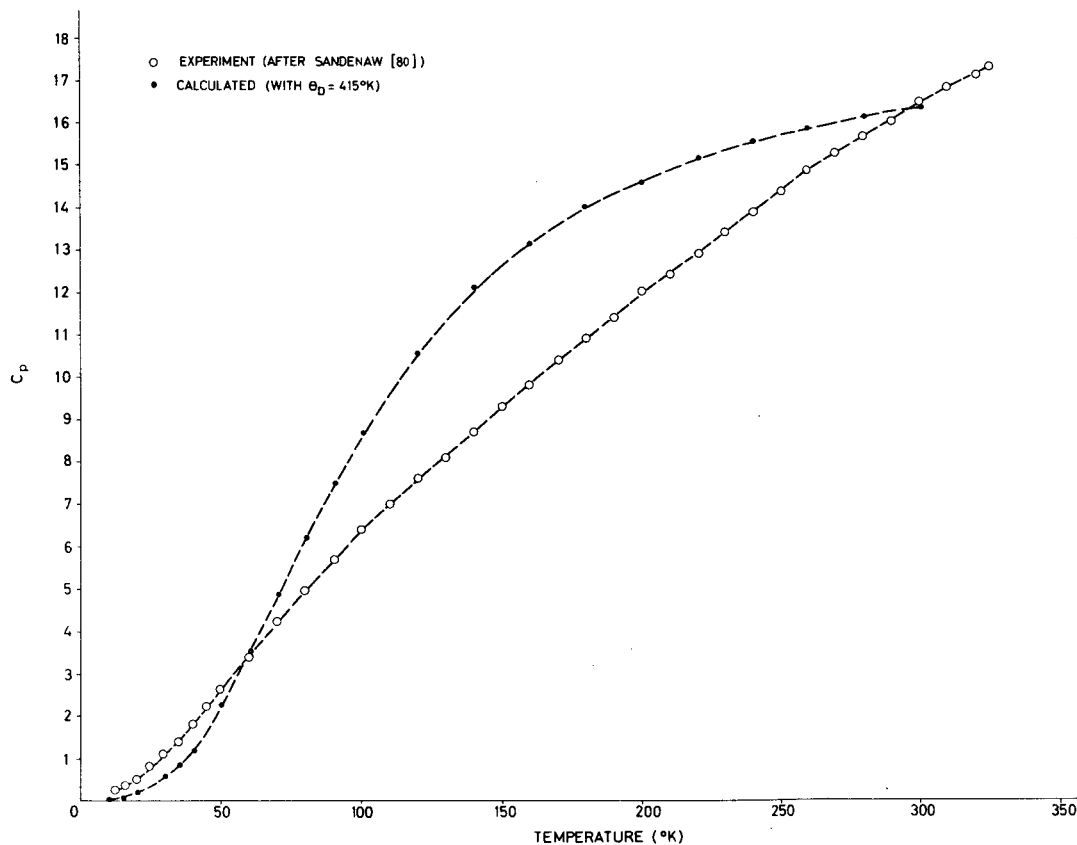
FIG. 4. Experimental and calculated heat capacities of PuO_2.

temperature χ_M for PuO_2 is much smaller than the value expected for a $5f^4$ ion; this may be due to magnetic interactions, however, since the value extrapolated from dilute PuO_2-ThO_2 solid solutions is much higher, and is close to the expected $5f^4$ value.

3.1.1.5. Entropies. The lattice contribution to standard entropies at 25°C can be estimated from the Debye temperatures discussed in the previous section; like the heat capacity values, it is too high for ThO_2 and UO_2 by 4.0 and 2.7 e.u. respectively. Since the value for PuO_2 calculated from a Debye temperature of 415°K is 18.8 e.u., the correct value is probably around 16.0 e.u., in good agreement with Sandenaw's measured value of 16.3 e.u. If it is assumed that magnetic ordering must exist, one can add $R \ln 5 = 3.2$ e.u. to Sandenaw's value to give S°_{298} = 19.5 e.u. This may be a little low because of the effects of stored energy release on the measured heat capacities.

Two other estimates are available from the literature for the entropy of PuO_2 at 298°K. The first by Osborne and Westrum [81] is based on the measured entropies of ThO_2, UO_2 and NpO_2. Osborne and Westrum argue that the magnetic contribution to the entropy can be approximated by the spin-only contribution as computed from the number of unpaired $5f$ electrons in Np^{+4} and U^{+4}. Th^{+4} has no unpaired electrons and hence is diamagnetic and shows no magnetic ordering. The entropy of ThO_2 is thus purely lattice entropy. They then observe that the excess entropy of UO_2 and NpO_2 over the lattice entropy (assumed to be the same as ThO_2) is equal to $R \ln (2S+1) + 0.85$ where S is the spin quantum number for the appropriate number of $5f$ electrons, and 0.85 is a constant presumed to include any electronic entropy. For PuO_2 the estimated entropy is: S°_{298} = 19.7 e.u.

In a later paper Westrum and Grønvold [91] provide another estimate based upon a study of the systematics of the transition metal chalcogenides. Here, following Latimer, they assume a constant contribution of 15.0 e.u. for any actinide cation, plus a contribution of 2.0 e.u. from the two oxygen atoms, plus the $R \ln (2S+1)$ magnetic contribution as above. The result for PuO_2 is S°_{298} = 20.2 cal/degK gfw. Also in this paper Westrum and Grønvold offer a useful procedure for estimating the entropies of oxides other than the dioxide.

The close agreement between Osborne and Westrum's estimate (19.7. e.u.) and Sandenaw's modified value (19.5 e.u.), which is expected to be slightly low, leads us to adopt a value of 19.7 ± 1.0 e.u. for the standard entropy of $\langle PuO_2 \rangle$, and to modify Westrum and Grønvold's calculations for the other oxides as shown in Table VIII.

The oxygen contributions are taken from Westrum and Grønvold's table [91], which was derived from a consideration of many transition metal oxides. The magnetic contributions are the spin-only term, $R \ln (2S+1)$, assuming that Pu^{+3} has five $5f$ electrons and Pu^{+4} has four. In $PuO_{1.61}$ it is assumed that the unit cell contains 24 Pu^{+3} and 8 Pu^{+4} ions.

Despite the plausibility of this estimation scheme the results are probably only accurate to $\pm 10\%$.

TABLE VIII.   ESTIMATION OF ENTROPIES OF PLUTONIUM OXIDES

| Phase | S lattice | | S magnetic | S°_{298} |
	Pu contribution	O contribution		cal/deg K gfw
hex-Pu_2O_3	29.0	0	2 × 3.6	36.2
cubic-$PuO_{1.52}$	14.5	0	3.6	18.1
$PuO_{1.61}$	14.5	0.9	3.5	18.9
PuO_2	14.5	2	3.2	19.7

3.1.2.   High-temperature heat capacities

3.1.2.1.   Plutonium dioxide, PuO_2.   Sandenaw [80] finds C_p = 16.5 cal degK^{-1} mole^{-1} at 300°K, as already discussed.   Rand [70], on the basis of work done at Brussels [92], suggests the equation

$$C_p = 19.34 + 1.56 \times 10^{-3}\ T - 2.8 \times 10^5\ T^{-2}\ cal\ degK^{-1}\ mole^{-1}$$

for the temperature range 300 to 1000°K, which also agrees quite well with Sandenaw's value at 300°K.   Here we shall use Rand's equation with an estimated uncertainty of 5% which is assumed to be in the first term, amounting to 1.0 cal deg K^{-1} mole^{-1}.

3.1.2.2.   Hexagonal Pu_2O_3.   To estimate the heat capacity of this compound we assume that

$$2\ C_p \langle PuO_2 \rangle - C_p \langle Pu_2O_3 \rangle\ hex = 2\ C_p \langle CeO_2 \rangle - C_p \langle Ce_2O_3 \rangle\ hex$$

The values for $\langle CeO_2 \rangle$ are taken from King and Christiansen [93], and those for $\langle Ce_2O_3 \rangle$ are from Pankratz and Kelley [94].   It is noticed that between 300 and 1000°K the difference $2\ C_p \langle CeO_2 \rangle - C_p \langle Ce_2O_3 \rangle_{hex}$ is constant within a few tenths of a unit at approximately 2.1.   Therefore, the value for $\langle Pu_2O_3 \rangle$ hex is taken to be

$$C_p \langle Pu_2O_3 \rangle_{hex} = 2\ C_p \langle PuO_2 \rangle - (2.1 \pm 1.0)\ cal\ degK^{-1}\ mole^{-1}$$

where the rather large uncertainty is assumed because of the somewhat different results obtained by Kuznetsov and Rezukhina [95].   Thus we have

$$C_p \langle Pu_2O_3 \rangle_{hex} = (36.6 \pm 2.3) + 3.12 \times 10^{-3}\ T - 5.6 \times 10^5\ T^{-2}\ cal\ degK^{-1}\ mole^{-1}$$

3.1.2.3.   Cubic $\langle PuO_{1.52} \rangle$.   The heat capacity of cubic $\langle PuO_{1.52} \rangle$ is estimated by ignoring the deviation from stoichiometry and examining

TABLE IX. HEAT CAPACITIES OF RARE-EARTH OXIDES
(cal deg K^{-1} mole^{-1})

T(°K)	a-hex			c-cubic			Reference
	300	500	1000	300	500	1000	
La_2O_3	25.8	29.0	31.7				[96]
Ce_2O_3	27.5	32.2	35.3				[94]
Pr_2O_3	28.2	31.2	35.0				[97]
Nd_2O_3	26.8	30.2	34.6				[98]
Sm_2O_3				27.8	31.6	35.3	[98]
Eu_2O_3				29.8	32.9	36.0	[98]
Gd_2O_3				25.2	28.5	31.1	[98]
Tb_2O_3				27.7	30.5	33.9	[97]
Dy_2O_3				28.1	30.1	32.3	[96]
Ho_2O_3				27.1	29.3	31.3	[99]
Er_2O_3				25.3	28.9	31.2	[99]
Tm_2O_3				27.4	30.0	31.5	[99]
Yb_2O_3				27.3	30.4	31.8	[99]
Lu_2O_3				23.4	27.9	30.5	[94]
Mean	27.1	30.7	34.2	26.9	30.0	32.5	
$TbO_{1.500}$	13.9	15.3	17.0				
$TbO_{1.719}$	14.1	16.1	18.5				
$TbO_{1.812}$	13.9	16.5	19.0				
$PrO_{1.500}$	14.1	15.6	17.5				
$PrO_{1.833}$	15.1	18.2	22.6				

the differences in the hexagonal and cubic rare-earth oxides as shown in Table IX. Unfortunately there are no measurements on the two forms of oxide for the same metal. From the table it is seen that the two oxides have nearly the same heat capacity at room temperature, differ by about 0.7 degK at 500°K, and by about 2 degK at 1000°K, with the hexagonal form having the higher heat capacity. Accordingly, for the reaction

$$2 \langle \text{PuO}_{1.5} \rangle_{\text{cubic}} = \langle \text{Pu}_2\text{O}_3 \rangle_{\text{hex}}$$
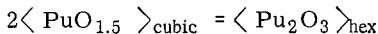
the equation

$$\Delta C_p = -0.8 + 3.0 \times 10^{-3} T \text{ cal degK}^{-1}$$

is used. The uncertainty is estimated to be about 1 cal degK^{-1} mole^{-1}. This gives

$$C_p \langle \text{PuO}_{1.5} \rangle_{\text{cubic}} = (18.7 \pm 1.2) - 2.8 \times 10^5 T^{-2} \text{ cal degK}^{-1} \text{ mole}^{-1}$$

3.1.2.4. PuO$_{1.61}$ -cubic. An examination of C_p for $\langle \text{TbO}_{1.500} \rangle$, $\langle \text{TbO}_{1.719} \rangle$ and $\langle \text{TbO}_{1.812} \rangle$ as well as $\langle \text{PrO}_{1.500} \rangle$ and $\langle \text{PrO}_{1.833} \rangle$ shows that the higher oxides have the higher heat capacities. It is noticed that the difference between $\langle \text{TbO}_{1.500} \rangle$ and $\langle \text{TbO}_{1.719} \rangle$ is about twice the difference between $\langle \text{TbO}_{1.719} \rangle$ and $\langle \text{TbO}_{1.812} \rangle$, which is thus assumed to be the difference between $\langle \text{PuO}_{1.52} \rangle$ and $\langle \text{PuO}_{1.61} \rangle$. It can be represented, with an uncertainty of about 0.3 cal degK^{-1} mole^{-1}, by $\Delta C_p = 8.0 \times 10^{-4} T$ cal degK^{-1} mole^{-1}. From this

$$C_p \langle \text{PuO}_{1.61} \rangle_{\text{cubic}} = (18.7 \pm 1.3) + 8.0 \times 10^{-4} T - 2.8 \times 10^5 T^{-2} \text{ cal degK}^{-1} \text{ mole}^{-1}$$

3.2. Heat of fusion

No direct experimental data are available for the heat of fusion of PuO$_2$, but liquidus-solidus measurements in the UO$_2$ - PuO$_2$ system are consistent with a value of 16.8 ± 1.3 kcal mole^{-1} (see Section III.2.2).

3.3. Calorimetric heats of formation

The only plutonium oxide for which there are experimental heat of formation data is plutonium dioxide. This was measured by oxygen bomb calorimetry by Popov and Ivanov [100], who obtained -252.1 ± 1.1 kcal/mole, and by Holley et al. [101], who obtained -252.87 ± 0.38 kcal/mole. The results are thus in agreement and the weighted average is taken: $\Delta H^0_{f\,298} \langle \text{PuO}_2 \rangle = -252.8 \pm 0.8$ kcal/mole.
Experimental data for the other oxides are very desirable.

3.4. High-temperature equilibria

This section deals with the oxygen pressure measurements over the Pu$_2$O$_3$-PuO$_2$ region at high temperatures. The main treatment is in

30
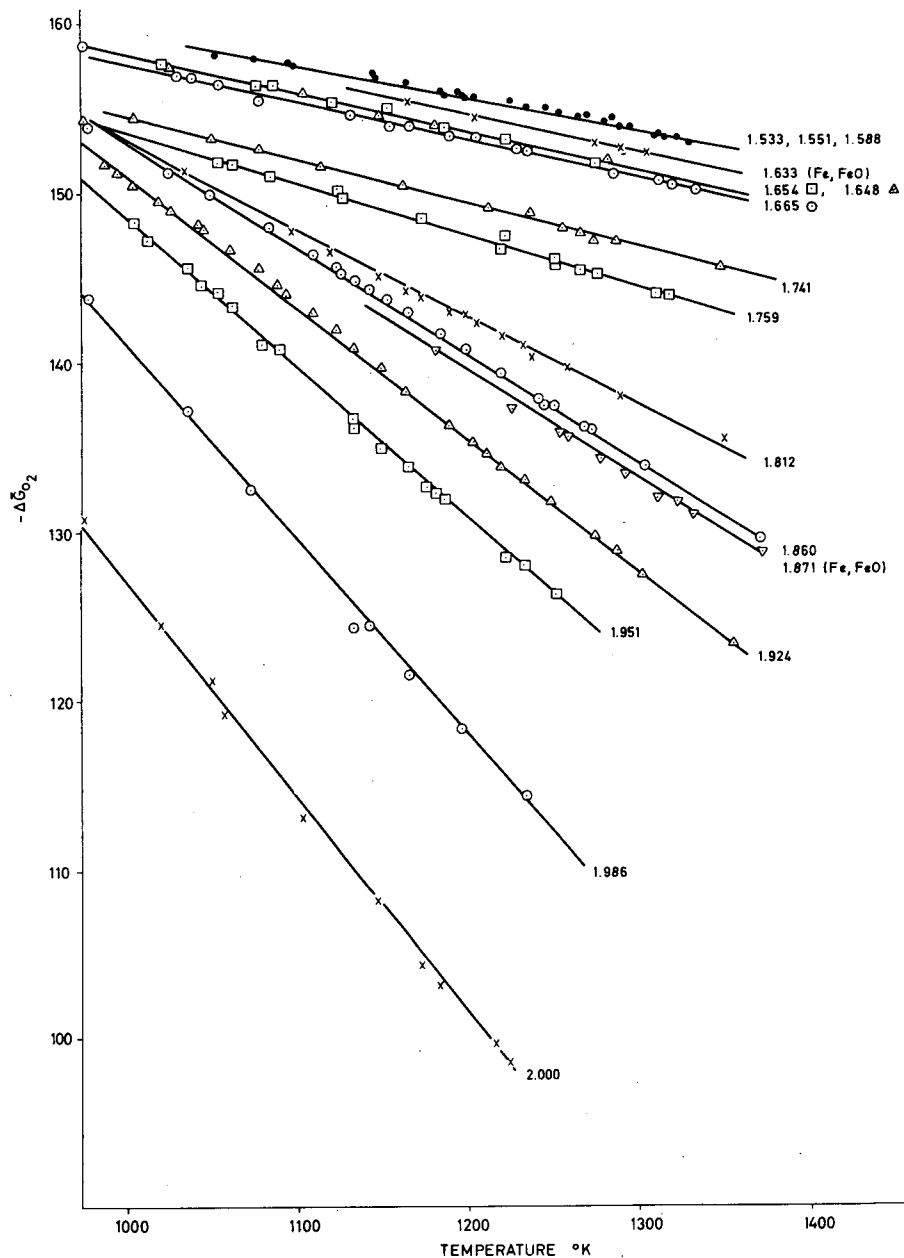
FIG. 5. Partial molar free energy of single-phase PuO_{2-x}.

31

terms of the phase diagram given in Fig. 1, but other possible phase diagrams consistent with the data are also discussed.

3.4.1. $\langle PuO_{1.61} \rangle$ to $\langle PuO_2 \rangle$ region

Above 945°K this region is single phase with a fluorite-type structure. Below approximately 945°K, this phase disproportionates to $\langle PuO_{1.61+y} \rangle$ and $\langle PuO_{2-x} \rangle$ at a temperature depending on the O/Pu ratio.

Markin et al. [102] have measured the oxygen potentials over the single phase oxides between $PuO_{1.61}$ and $PuO_{2.0}$(950 to 1350°K), using an EMF method (Fig. 5). The extremely reducing conditions required the use of a ThO_2-Y_2O_3 solid electrolyte which does not conduct oxygen below 950°K. Therefore it was not possible to measure the oxidation potentials in the $\langle PuO_{1.61+y} \rangle$ and $\langle PuO_{2-x} \rangle$ region. The free energy values from the corrected results of Atlas and Schleman [103](H_2/H_2O equilibration, 1375 to 1575°K) agree well with the EMF data where the temperature ranges overlap but the $\Delta\overline{H}_{O_2}$ and $\Delta\overline{S}_{O_2}$ values are markedly different. Bairiot and Vanhellemont [104] have made measurements on the PuO_{2-x}-C-CO system at 1670 to 1870°K; the derived $\Delta\overline{G}_{O_2}$ values for $PuO_{1.75}$ to $PuO_{1.85}$ agree very well with the extrapolations of the EMF data, rather than the gas equilibration data. The compositional variations of $\Delta\overline{H}_{O_2}$ and $\Delta\overline{S}_{O_2}$ for the AmO_{2-x} system, recently measured by gas equilibration by Chikalla et al. [105] and for the CeO_{2-x} system by Bevan and Kordis [73], both again at temperatures below 1100°C, are very similar to those found by Markin et al. for PuO_{2-x}. This difference in $\Delta\overline{H}_{O_2}$ and $\Delta\overline{S}_{O_2}$ for the two rather different temperature ranges may be real, since different defect types may predominate in the two cases. More free energy data for temperatures above 1100°C are clearly required. For the moment, however, the EMF values are preferred, note being taken that their extrapolation to higher temperatures may be subjected to some uncertainty.

The values obtained by interpolation of smoothed curves from Fig. 5 are given in Table X.

Figure 6 is a partial molar free energy diagram derived from this data. It can be seen that the values of $\Delta\overline{G}_{O_2}$ for $PuO_{1.75}$ to $PuO_{1.90}$ converge at ~ 945°K, which is therefore the point at which the two-phase region begins. This is in agreement with the phase diagram (Fig. 1). The course of the $PuO_{1.61+y}$-PuO_{2-x} two-phase curve down to 800°K can be plotted by combining the isopleths for $PuO_{1.65}$ to $PuO_{1.75}$ with the phase diagram. A more accurate extrapolation to room temperature can be obtained by considering the integral values $\Delta\overline{H}_{O_2}$ and $\Delta\overline{S}_{O_2}$ given in Section II.3.5.

The data are insufficient to determine whether a miscibility gap is present, but do not conflict with the possibility of such a gap. The data presented in Fig. 5 show that in the range 1.648 < O/Pu < 1.665 the partial molar free energy is constant to within 400 cal, the estimated experimental error, so that a two-phase region may be present in this oxygen composition range. Consideration of the X-ray data of Gardner et al. [13] gives the upper and lower limits of this region as 1.665 < O/Pu < 1.675 and 1.633 < O/Pu < 1.648 respectively. If this two-phase region exists then the free energy curve representing the two-phase region, $\langle PuO_{1.61+y} \rangle$

TABLE X.   PARTIAL MOLAR ENTROPIES AND ENTHALPIES OF
SOLUTION OF OXYGEN IN $\langle PuO_{2-x} \rangle$
$((O_2) = 2[O] PuO_{2-x})$

2-x in PuO_{2-x}	$-\Delta \overline{S}_{O_2}$ (e.u.)	$-\Delta \overline{H}_{O_2}$ (kcal mole^{-1})	Temperature range (°K)
1.63	20.8	179.5	750 to 1500
1.65	20.0	178.0	800 to 1500
1.70	20.8	176.0	885 to 1500
1.75	26.8	180.5	900 to 1500
1.80	40.0	192.5	925 to 1500
1.85	54.7	206.0	945 to 1500
1.90	69.3	219.8	945 to 1500
1.95	85.8	233.5	900 to 1500
1.98	96.4	241.0	900 to 1500

$+ \langle PuO_{2-x} \rangle$ in Fig. 6, must be modified so that the intersection with
the postulated two-phase miscibility gap is at a higher temperature than
the intersections with the single-phase lines for O/Pu > 1.670.

It is also possible that a miscibility gap could occur in the region
1.665 < O/Pu < 1.740 but its precise location would have to be consistent
with the X-ray data (Section II. 2. 2. 4).

3. 4. 2. $\langle PuO_{1.61+y} \rangle + \langle PuO_{2-x} \rangle$ two-phase region

The integrated data (Section II. 3. 5) give the following values:

T°K	Phase limits Lower	Upper	$-\Delta \overline{G}_{O_2}$ kcal mole^{-1}
615	1.61	1.98	170.4
700	1.62	1.98	166.5
800	1.65	1.97	161.7
900	1.75	1.95	156.7

3. 4. 3. $\langle Pu_2O_3 \rangle$ hex to $\langle PuO_{1.61} \rangle$ region

The oxygen potential measurements by Markin et al. [102] for the
over-all compositions $PuO_{1.533}$, $PuO_{1.551}$ and $PuO_{1.588}$ with both Ni/NiO
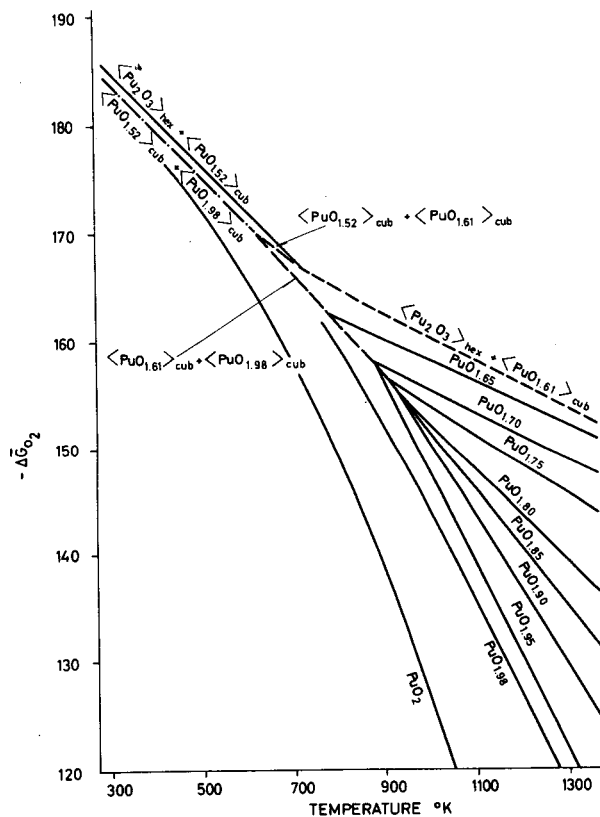
FIG. 6. Partial molar free energy diagram derived from thermodynamic data and Pu-O phase diagram [102].

and Fe/FeO reference electrodes give consistent results (Fig. 5). As discussed in the next section a positive $\Delta \overline{C}_p$ factor must be included and the final values obtained are:

	$\Delta \overline{S}_{O_2}$ e.u.	$\Delta \overline{H}_{O_2}$ kcal mole^{-1}	Temperature range (°K)
$\langle Pu_2O_3 \rangle_{hex} + \langle PuO_{1.61} \rangle$	70.8-16.1 log T	189 500-7.0 T	725 to 1500
$\langle PuO_{1.52} \rangle_{cub} + \langle PuO_{2-x} \rangle$	46.0	198 700	298 to 610

3.5. Integration of partial molar quantities

The partial molar heats and entropies for the entire region from $\langle Pu_2O_3 \rangle_{hex}$ to $\langle PuO_2 \rangle$ can now be integrated according to the equation

$$\Delta Z = 2 \int_{1.5}^{2} \Delta \overline{Z}_{O_2} dx$$

34

where x = O/Pu and Z = H or S. The values obtained are

$$2\langle Pu_2O_3 \rangle + (O_2) \rightarrow 4\langle PuO_2 \rangle$$
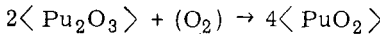
$$\Delta H_{1150} = -196.9 \text{ kcal}; \quad \Delta S_{1150} = -43.0 \text{ e.u.}$$

In order to extrapolate these values to other temperatures, the heat capacities of $\langle Pu_2O_3 \rangle_{hex}$ and $\langle PuO_2 \rangle$ must be used. No experimental data are yet available but estimated values have been given in Section II.3.1.2. The present assessment (taken from [70]) was based on earlier heat capacity data for the cerium oxides, and assumed ΔC_p for the above reaction to be zero, rather than -3.6 e.u. as estimated in Section II.3.1.2. However, since much calorimetric data (including entropies, heats of formation and high-temperatures heat capacities) are likely to appear in the near future, it seemed appropriate to the Panel to leave a re-integration of this region of the phase diagram until all these data are available and until the presence or absence of a miscibility gap in the phase diagram has been established. The assessment presented in this section is therefore not quite consistent with other data used, but the uncertainty introduced in the free energies is less than the precision with which they are known.

A preliminary extrapolation of the partial molar free energies to lower temperatures shows that the lines for $PuO_{2.00}$ and $PuO_{1.98}$ must bend over considerably between 1000°K and room temperature, in order not to intersect with the $\langle Pu_2O_3 \rangle_{hex} + \langle PuO_{1.61} \rangle$ two-phase line above 500°K. (There is evidence from both X-ray [13] and conductivity [67] measurements that the phase in equilibrium with $\langle PuO_{1.61} \rangle$ and $\langle PuO_{1.52} \rangle_{cub}$ has less oxygen than PuO_2.) This curvature may be associated with the fact that PuO_2 can adsorb relatively large amounts of oxygen on its surface below 600°C [26]. This absorption process would thus provide low-energy sites on oxides close to PuO_2 at room temperature but not at high temperatures. Whatever the cause of this curvature, however, it corresponds to a rapid increase (numerical decrease) in $\Delta \overline{H}_{O_2}$ and $\Delta \overline{S}_{O_2}$ for compositions between O/Pu = 1.98 and 2.00.

A similar phenomenon has been found for the partial heats and entropies of the UO_{2+x} phase near the stoichiometric composition, and its origin is fully discussed in [1]. Briefly, this type of curve, having approximately the shape of an oblique S near stoichiometric composition, is due to the approach of atomic order within a disordered solution. Until more detailed thermochemical data in the region near $PuO_{2.0}$ are available, the curvature may provisionally be taken into account by introducing a corresponding $\Delta \overline{C}_p$ term, but it must be borne in mind that such a procedure is purely formal.

Since we have taken

$$\Delta C_p = 2 \int_{1.5}^{2} \Delta \overline{C}_p \, dx \text{ for } 2\langle Pu_2O_3 \rangle_{hex} + (O_2) = 4\langle PuO_2 \rangle \text{ as zero}$$

at 750°K, a positive value of $\Delta \overline{C}_p$ in some other part of the region must be incorporated in order to compensate for the negative value near

35

O/Pu = 2.0. The following values are suggested:

O/Pu	1.50 to 1.61	1.61 to 1.98	1.98 to 2.00
$\Delta \overline{C}_p$ (e. u.)	+7	0	-38.5

We can calculate $\Delta \overline{S}_{O_2}$ and $\Delta \overline{H}_{O_2}$ for (i) the $\langle Pu_2O_3 \rangle_{hex} + \langle PuO_{1.61} \rangle$ two-phase region; (ii) the $\langle PuO_{1.61+y} \rangle$ single-phase region; and (iii) the $\langle PuO_{1.98-z} \rangle$ to $\langle PuO_2 \rangle$ single-phase region, at 900°K, and these values can be combined with the integral values of ΔS_{900} and ΔH_{900} for $2\langle Pu_2O_3 \rangle_{hex} + O_2 \rightarrow 4\langle PuO_2 \rangle_{cub}$, which, with $\Delta C_p = O$, are independent of temperature, to give $\Delta \overline{S}_{O_2}$ and $\Delta \overline{H}_{O_2}$ at 900°K for the two-phase region $\langle PuO_{1.61+y} \rangle + \langle PuO_{1.98-z} \rangle$. Similar calculations were made for temperatures of 800, 700, 615 and 500°K, the latter giving $\Delta \overline{S}_{O_2}$ and $\Delta \overline{H}_{O_2}$ for the $\langle PuO_{1.52} \rangle_{cub} + \langle PuO_{1.98-z} \rangle$ two-phase region. The entire partial molar free energy diagram can now be completed. It is very satisfactory to find that the intersections of the isopleths for $PuO_{1.65}$ to $PuO_{1.80}$ with the $\langle PuO_{1.61+y} \rangle + \langle PuO_{2-x} \rangle$ region reproduce with considerable accuracy the phase diagram obtained independently by Gardner et al [13].

3.5.1. Heat of formation and standard entropy of $\langle Pu_2O_3 \rangle_{hex}$, $\langle PuO_{1.52} \rangle_{cub}$ and $\langle PuO_{1.61} \rangle$

3.5.1.1. $\langle Pu_2O_3 \rangle_{hex}$. The integrated partial molar heats and entropies give

$$2\langle Pu_2O_3 \rangle_{hex} + (O_2) \rightarrow 4 \langle PuO_2 \rangle$$
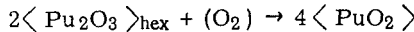
$$\Delta H_{1150} = -196.9 \text{ kcal}, \quad \Delta S_{1150} = 43.0 \text{ e. u.}$$

With the heat capacity values for the oxides estimated in Section II.3.1.2 (or more conveniently, the thermal data in Table XI) and the thermal data for oxygen [106], we find

$$\Delta H_{1150} - \Delta H_{298} = -3.15 \text{ kcal} \quad \Delta S_{1150} - \Delta S_{298} = -4.7 \text{ e. u.}$$

$$\Delta H_{298} = -193.75 \text{ kcal,} \quad \Delta S_{298} = -38.3 \text{ e. u.}$$

and finally, using the discussed values for the heat of formation and standard entropy of PuO_2,

$$\Delta H_f^0, \langle Pu_2O_3 \rangle_{hex} = -408.7 \pm 3.0 \text{ kcal}$$

$$S_{298}^0, \langle Pu_2O_3 \rangle_{hex} = 34.0 \pm 5.0 \text{ e. u.}$$

where the uncertainties include those of the PuO_2 data, the partial molar data and the heat capacity data.

36

3.5.1.2. $\langle PuO_{1.61} \rangle$. The data for the $\langle Pu_2O_3 \rangle_{hex}$ + $\langle PuO_{1.61} \rangle$ region give

$$\langle Pu_2O_3 \rangle + 0.11(O_2) \rightarrow 2 \langle PuO_{1.61} \rangle$$
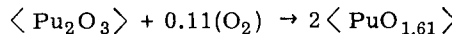
$$\Delta H_{1150} = -20.0 \text{ kcal}, \quad \Delta S_{1150} = -2.4 \text{ e.u.}$$

The thermal data (Table XI) give

$$\Delta H_{298} = -19.0 \text{ kcal}, \quad \Delta S_{298} = -1.0 \text{ e.u.}$$

so that finally,

$$\Delta H_f^0, \langle PuO_{1.61} \rangle = -213.9 \pm 1.5 \text{ kcal}$$

$$S_{298}^0 \langle PuO_{1.61} \rangle = 19.2 \pm 2.5 \text{ e.u.}$$

3.5.1.3. $\langle PuO_{1.52} \rangle_{cub}$. The standard entropy of this phase is assumed to be slightly greater than that of $\frac{1}{2} \langle Pu_2O_3 \rangle_{hex}$:

$$S_{298}^0 = 17.2 \pm 3.0 \text{ e.u.}$$

The fact that the free energy of the reaction

$$\langle PuO_{1.61} \rangle = 0.805 \langle PuO_{1.52} \rangle_{cub} + 0.195 \langle PuO_{1.98} \rangle$$
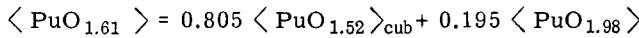
changes sign from negative below 650°K to positive above 650°K may be used to fix the heat of formation of $\langle PuO_{1.52} \rangle_{cub}$. The free energy of formation of $PuO_{1.98}$ is calculated from that of $\langle PuO_2 \rangle$ (Table XI) and $\Delta \bar{G}_{O_2}$ values for the PuO_{2-x} phase. A heat of formation of -206.3 kcal for $\langle PuO_{1.52} \rangle_{cub}$ gives values of -420, -150 and +140 cal for the free energy of the above disproportionation reaction at 400, 600 and 800°K, and a zero free energy at 704°K.

As a check on this value for the heat of formation, we may calculate the free energy of the other disproportionation reaction

$$\langle PuO_{1.52} \rangle_{cub} \rightarrow 0.409 \langle Pu_2O_3 \rangle + 0.182 \langle PuO_{1.61} \rangle$$
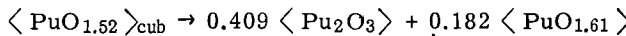
which changes sign from positive to negative as the temperature is increased through 700°K. The data give values of +130, +70 and -30 cal at 400, 600 and 800°K, with a zero free energy at 740°K. Thus with

$$\Delta H_f^0 \langle PuO_{1.52} \rangle_{cub} = -206.3 \pm 2.5 \text{ kcal}$$

the inter-relationships of the three phases near the sesquioxide composition are reproduced very accurately. The small discrepancies in the temperature of the disproportionations are removed by trivial changes in the values for the heats of formation.

37

TABLE XI. THERMOCHEMICAL DATA FOR OXIDES

$\langle Pu \rangle$		$\Delta H_f^0 = 0;$		$S_{298}^0 = 13.2 \pm 0.4\ (\pm 1.0)$ e.u.

T (°K)	C_p (e.u.)	$H_T - H_{298}$ (cal)	$S_T - S_{298}$ (e.u.)	$-(G_T - H_{298})/T$ (e.u.)
298.15	7.67	0	0.	13.20
300	7.68	14	0.05	13.20
395	8.12	764	2.22	13.48
395	8.12	1 569	4.26	13.48
400	8.14	1 610	4.36	13.53
478	8.50	2 259	5.84	14.31
478	8.50	2 399	6.13	14.31
500	8.60	2 587	6.52	14.54
591	9.02	3 388	7.99	15.45
591	9.00	3 518	8.21	15.45
600	9.00	3 599	8.34	15.54
700	9.00	4 499	9.73	16.50
749	9.00	4 940	10.34	16.94
749	8.40	5 403	10.96	16.94
800	8.40	5 831	11.51	17.42
900	8.40	6 671	12.50	18.29
913	8.40	6 780	12.62	18.39
913	8.50	7 450	13.36	18.39
1000	8.50	8 190	14.13	19.14
1100	8.50	9 040	14.94	19.92
1200	8.50	9 890	15.68	20.64
1300	8.50	10 740	16.36	21.30
1400	8.50	11 590	16.99	21.91
1500	8.50	12 440	17.58	22.48
1600	8.50	13 290	18.12	23.02
1700	8.50	14 140	18.64	23.52
1800	8.50	14 990	19.13	24.00
1900	8.50	15 840	19.58	24.45
2000	8.50	16 690	20.02	24.88

$\langle Pu_2O_3 \rangle_{hex}$		$\Delta H_f^0 = -408.7 \pm 3.0$ kcal;		$S_{298}^0 = 34.0 \pm 5.0$ e.u.	

T (°K)	C_p (e.u.)	$H_T - H_{298}$ (cal)	$S_T - S_{298}$ (e.u.)	$-(G_T - H_{298})/T$ (e.u.)	$-\Delta G_f^0$ (kcal)
298.15	31.23	0	0	34.00	389.0
300	31.31	57	0.19	34.00	
400	34.35	3 360	9.67	35.27	382.4
500	35.92	6 880	17.52	37.76	
600	36.92	10 525	24.17	40.62	369.0
700	37.64	14 255	29.91	43.55	
800	38.22	18 049	34.98	46.42	356.0
900	38.72	21 896	39.51	49.18	
1000	39.16	25 790	43.61	51.82	343.1
1100	39.57	29 727	47.36	54.34	
1200	39.96	33 703	50.82	56.74	330.4
1300	40.32	37 717	54.04	59.02	
1400	40.68	41 768	57.04	61.20	318.0
1500	41.03	45 854	59.86	63.29	
1600	41.37	49 974	62.52	65.28	306.0
1700	41.71	54 128	65.03	67.19	
1800	42.04	58 316	67.43	69.03	294.2
1900	42.37	62 537	69.71	70.79	
2000	42.70	66 790	71.89	72.50	282.8

$\Delta G_f^0 = -406\,700 + 62.71\ T$ cal   (298 to 2000°K)

Standard deviation = 955 cal

TABLE XI. (cont.)

⟨PuO$_{1.52}$⟩$_{cub}$ $\Delta H_f^0 = -206.3 \pm 2.5$ kcal; $S_{298}^0 = 17.2 \pm 2.5$ e.u.

T	C_p	$H_T - H_{298}$	$S_T - S_{298}$	$-(G_T - H_{298})/T$	$-\Delta G_f^0$
(°K)	(e.u.)	(cal)	(e.u.)	(e.u.)	(kcal)
298.15	15.57	0	0	17.20	196.4
300	15.61	28	0.10	17.20	
400	16.97	1667	4.80	17.83	193.0
500	17.61	3400	8.67	19.06	
600	17.96	5180	11.91	20.48	186.3
700	18.17	6987	14.70	21.91	
800	18.31	8812	17.13	23.32	179.6
900	18.41	10648	19.29	24.66	
1000	18.48	12492	21.24	25.94	173.0
1100	18.53	14343	23.00	27.16	
1200	18.58	16199	24.62	28.32	166.4
1300	18.61	18058	26.10	29.41	
1400	18.64	19921	27.48	30.45	160.0
1500	18.67	21786	28.77	31.45	
1600	18.69	23654	29.98	32.39	153.7
1700	18.71	25524	31.11	33.30	
1800	18.72	27395	32.18	34.16	147.4
1900	18.74	29268	33.19	34.99	
2000	18.75	31142	34.15	35.78	141.3

$\Delta G_f^0 = -205760 + 32.49$ T cal (298 to 2000° K)

Standard deviation = 300 cal

⟨PuO$_{1.61}$⟩ $\Delta H_f^0 = -213.9 \pm 1.5$ kcal; $S_{298}^0 = 19.2 \pm 2.5$ e.u.

T	C_p	$H_T - H_{298}$	$S_T - S_{298}$	$-(G_T - H_{298})/T$	$-\Delta G_f^0$
(°K)	(e.u.)	(cal)	(e.u.)	(e.u.)	(kcal)
298.15	15.79	0	0	19.20	203.9
300	15.83	29	0.10	19.20	
400	17.27	1693	4.88	19.84	200.5
500	17.98	3459	8.81	21.09	
600	18.40	5280	12.13	22.53	193.7
700	18.69	7135	14.99	24.00	
800	18.90	9015	17.50	25.43	187.0
900	19.07	10915	19.74	26.81	
1000	19.22	12829	21.76	28.13	180.4
1100	19.35	14758	23.59	29.38	
1200	19.47	16699	25.28	30.57	173.8
1300	19.57	18651	26.85	31.70	
1400	19.68	20613	28.30	32.78	167.4
1500	19.78	22586	29.66	33.80	
1600	19.87	24568	30.94	34.78	161.1
1700	19.96	26560	32.15	35.72	
1800	20.05	28561	33.29	36.62	154.9
1900	20.14	30571	34.38	37.49	
2000	20.23	32589	35.41	38.32	148.8

$\Delta G_f^0 = -213240 + 32.51$ T cal (298 to 2000° K)

Standard deviation = 358 cal

TABLE XI. (cont.)

$\langle PuO_2 \rangle$ $\Delta H_f^0 = -252.8 \pm 0.8$ kcal; $S_{298}^0 = 19.7 \pm 1.0$ e.u.

T	C_p	$H_T - H_{298}$	$S_T - S_{298}$	$-(G_T - H_{298})/T$	$-\Delta G_f^0$
(°K)	(e.u.)	(cal)	(e.u.)	(e.u.)	(kcal)
298	16.66	0	0	19.70	240.1
300	16.70	30	0.10	19.70	
400	18.21	1786	5.14	20.38	235.8
500	19.00	3650	9.30	21.70	
600	19.50	5576	12.81	23.22	227.1
700	19.86	7545	15.84	24.76	
800	20.15	9546	18.52	26.28	218.6
900	20.40	11574	20.90	27.74	
1000	20.62	13625	23.06	29.14	210.0
1100	20.82	15697	25.04	30.47	
1200	21.02	17789	26.86	31.73	201.5
1300	21.20	19900	28.55	32.94	
1400	21.38	22030	30.13	34.09	193.2
1500	21.56	24176	31.61	35.19	
1600	21.73	26341	33.00	36.24	185.0
1700	21.90	28522	34.33	37.25	
1800	22.06	30720	35.58	38.22	176.9
1900	22.23	32934	36.78	39.15	
2000	22.39	35165	37.92	40.04	168.8

$\Delta G_f^0 = -252340 + 42.02 \, T$ cal   (298 to 2000° K)

Standard deviation = 334 cal

3.5.2. The instability of plutonium monoxide

It is sometimes useful to have an estimate of the instability of the plutonium monoxide phase. It is known [11, 107] that the oxygen-rich limit of the Pu(O, C) phase is approximately $PuC_{0.3}O_{0.7}$ at about 1500°K. Thus the free energy of the reaction

$$\langle PuO \rangle \rightarrow 1/3 \langle Pu_2O_3 \rangle_{hex} + 1/3 \{Pu\}$$
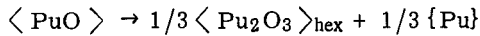
is negative when PuO is in its standard state (pure solid), but is approximately zero when the mole fraction of PuO dissolved in "PuC" is about 0.7. Assuming ideal solution behaviour, $\Delta G^0 = RT \ln 0.7 = -1063$ cal. The monoxide is thus unstable to disproportionation by about a kilocalorie.

3.6. Tabulation of thermochemical data

The thermochemical data for the oxides are presented in Table XI together with an equation for the free energy of formation. The more convenient two-term equations are given, since these always fit the data to within their precision. One more significant digit than is warranted by the precision of the data is retained to avoid rounding errors. At temperatures above 1000°K the error in the values given may increase,

40

since the equations relating C_p to temperature, given in Sections II.3.1.2.1 - II.3.1.2.4, and ensuring precision in the range 300-1000°K, were used in calculating C_p, H_T -H_{298} and S_T - S_{298} up to a temperature of 2000°K.

The data in Table X for condensed plutonium were calculated from the specific heat and transformation data given by Rand [70]; data for oxygen were taken from Stull and Sinke [106].

II.4. VAPORIZATION BEHAVIOUR

4.1. Introduction

The vaporization behaviour of almost all refractory binary materials is significantly influenced by the composition variable. Wide deviations from ideal stoichiometry are frequently encountered at the temperatures necessary to cause measurable vaporization. These systems are bivariant in the sense of the Phase Rule and the vapour pressures are, therefore, a function of both the temperature and composition variables. The previously published measurements of the vapour pressure of plutonium oxide systems are summarized in Table XII. Inspection of these measurements reveals that in the case of Refs [63] and [109] only, the vapour pressure has been correlated with a condensed phase(s) of known composition. The results of the transpiration measurements described in Refs [109] and [110] were obtained in three different atmospheres. In general appearance the values obtained in oxygen are lowest, and those in air and argon are somewhat higher. However, the pronounced lack of precision of the data as indicated by the large random errors associated with the least-squares equations in Table XII, and also the relatively small temperature dependence of the pressure, severely limits the credibility of the accuracy of these measurements. The agreement among the results (cell No. 1) of Mulford and Lamar [62] and Ackermann et al. [63] obtained with tungsten effusion cells is within a factor of 1.5 and, in the case of tantalum cells, the results of Ackermann et al. [63] are virtually identical with the much earlier measurements of Phipps et al. [108]. The vapour pressures obtained with tantalum cells, corresponding to a greater degree of reduction of the dioxide phase, are approximately a factor of ten greater than those corresponding to the less reducing tungsten cells. Ackermann et al. [63] have accounted for this increase in vapour pressure, and have described thermodynamically the vaporization behaviour of the bivariant PuO_{2-x} phase ($\sim 1.6 < 2-x < 2.00$) based on their effusion data given in Table XII and the thermodynamic data for the solid phase(s) reported by Markin and Rand [66]. We shall be concerned primarily with the published results of Ackermann et al. [63] and with the data of Pascard [21] and Ohse [22] submitted to this Panel since they represent the most successful attempts at the present time in correlating the pressure and composition variables.

4.2. Résumé of experimental data and thermodynamic analysis

The pattern of vaporization behaviour for the PuO_{2-x} phase ($\sim 1.6 <O/Pu < 2.0$) observed by Ackermann et al. [63] for tungsten,

TABLE XII.   VAPOUR PRESSURES OF PLUTONIUM OXIDES

Solid phase(s) [a]	$\text{Log } p_e \text{ (atm)} = A + B/T$		Temperature range (°K)	Method of measurement	Reference
	A	B			
$(PuO_{\sim1.6}, Pu_2O_3)$	8.13 [b]	$-27\,910$	1790-2075	Ta-effusion cell	[108]
$(PuO_{\sim1.87})$	7.82 ± 0.23	$-29\,700 \pm 500$	1990-2380	W-effusion cell (No. 1)	[62]
PuO_2	3.70 ± 1.64	$-23\,300 \pm 3100$	1770-2060	Transpiration-1 atm O_2	[109, 110]
$PuO_{\sim2}$	-0.13 ± 1.42	$-15\,000 \pm 2700$	1730-2060	Transpiration-1 atm air	[109, 110]
(PuO_{2-x})	-1.91 ± 1.00	$-11\,800 \pm 1900$	1730-2060	Transpiration-1 atm argon	[109, 110]
$PuO_{1.92 \pm 0.01}$	7.50 ± 0.15	$-29\,260 \pm 280$	1640-2070	W-and R-effusion cells	[63]
$PuO_{\sim1.6}, Pu_2O_3$	8.09 ± 0.27 [b]	$-27\,800 \pm 500$	1645-2105	Ta-effusion cell	[63]

[a] The parentheses indicate uncertainty in the identification and composition of the solid phase(s).

[b] Calculated by assuming that the vapour is entirely PuO(g); in all other cases the vapour is assumed to be $PuO_2(g)$.
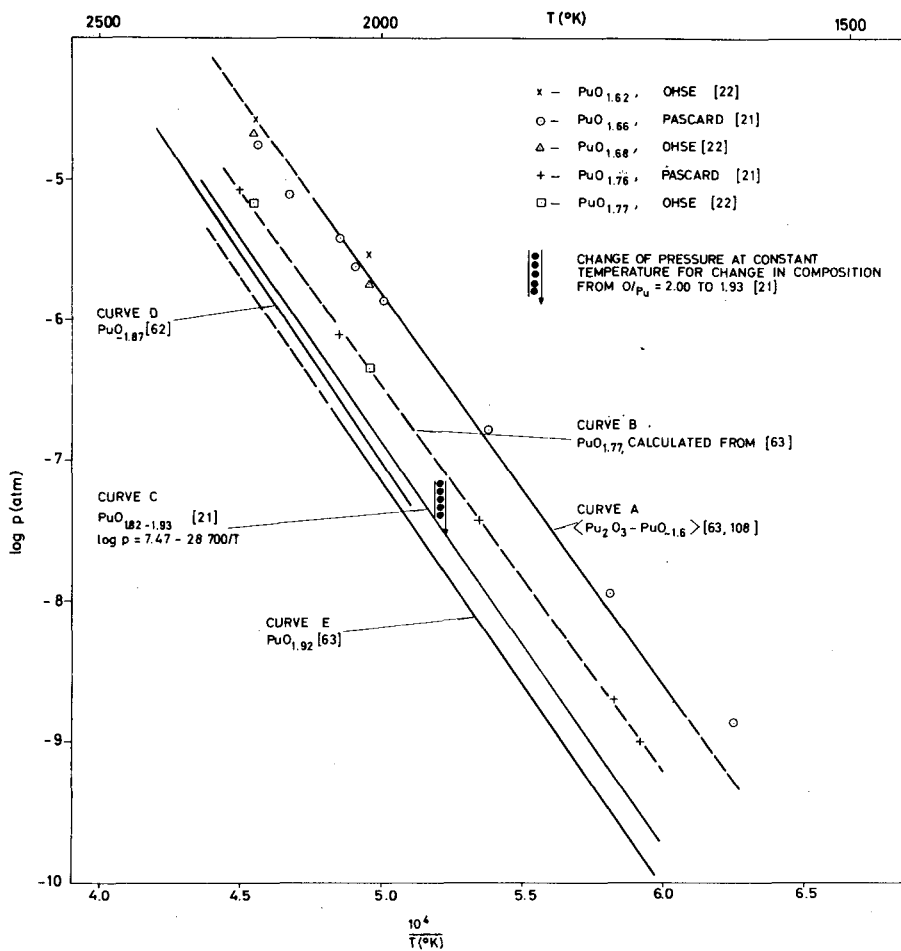
FIG. 7. Vapour pressure of plutonium-bearing species versus composition and temperature for sub-stoichiometric plutonium oxides.

rhenium and tantalum effusion cells, and by Pascard [21] and Ohse [22] for tungsten cells, demonstrates two important aspects: the pressure-composition bivariancy of the dioxide phase and the existence of at least two principal modes of vaporization involving plutonium-bearing species. The effusion rates were measured by the radiochemical analysis of collections corrected for americium content and correspond to systems whose compositions were obtained from chemical and X-ray analysis before and after the measurements. The combined results of the three investigations are shown in Fig. 7. Curve A represents the nearly identical results of Phipps et al. [108] and Ackermann et al. [63] obtained from tantalum effusion cells and given by Eqs 1 and 7 in Table XII. Curve B represents the dependence of log p versus $1/T$ for O/Pu = 1.77 calculated from the thermodynamic data given by Ackermann et al. [63]. Curve C represents a composite least-squares treatment of various

sets of experimental data corresponding to the compositions, O/Pu = 1.82, 1.85 and 1.93. Within the precision of the data the measured pressures appear to be insensitive to the composition variable and, therefore, are represented by a single curve. Curve D gives the plot of Eq. 2 in Table XII obtained by Mulford and Lamar [62] for their principal set of data (tungsten cell No. 1). The composition of $PuO_{1.87}$ has been assigned via the value of the lattice parameter of the quenched residue, 5.44 Å, and the results of Gardner et al. [13] extrapolated to room temperature. Curve E represents the data of Ackermann et al. [63] given by Eq. 6 in Table XII and corresponding to the composition $PuO_{1.92}$. Ackermann et al. [63], Pascard [21] and Ohse [22, 111] have observed a gradual decrease in the pressure of plutonium-bearing species at constant temperature during the incongruent vaporization of initially $PuO_{2.00}$. In the former case the extent of decrease was approximately 30%, whereas in the latter case the decrease was a factor of three as shown by the vertically arrayed solid points in Fig. 7.

The examination by X-ray diffraction of the vaporization residues, having compositions between O/Pu = 1.66-1.93 in the investigations by Ackermann et al. [63], Pascard [21] and Ohse [22] invariably indicated the presence of the two phases $PuO_{1.98}$ (face-centred cubic) and $PuO_{1.52}$ (body-centred cubic) in varying proportions. Quite clearly both phases could not have been present at the temperatures of the effusion measurements since their presence would have defined a univariant system, so that constant rather than varying effusion rates would have been observed. This evidence suggests the disproportionation of the PuO_{2-x} phase upon cooling, and confirms the findings of many previous investigators [66]. Only Mulford and Lamar [62] have succeeded in quenching the PuO_{2-x} phase to room temperature and this singular success is believed to have resulted from the stabilization of the phase by a small tungsten impurity.

Apart from minor discrepancies, as indicated by curves C, D, and E, the data in Fig. 7 clearly show that the effect of changing composition on the total pressure of plutonium-bearing species is relatively small for compositions in the range O/Pu = 1.93 - 1.82, but becomes more important at lower compositions. This behaviour and the decrease in the pressure observed from initially stoichiometric oxide demonstrate the existence of a congruently vaporizing composition in the PuO_{2-x} phase region. When the condensed phase contains more oxygen than this, the vapour is richer in oxygen than the solid, which is thus chemically reduced; conversely, when the condensed phase contains less oxygen than the congruently vaporizing composition, it is oxidized by loss of a vapour richer in plutonium. In both cases, the total effusion rate decreases and the composition of the solid moves towards the congruently vaporizing composition. Ohse [111] has observed this decrease in the pressure of plutonium-bearing species at 2000°K from both sides of the high-temperature single-phase region starting at O/Pu = 1.62 and 2.00 towards a minimum at the congruently vaporizing composition near 1.85. An extrapolation of the vapour pressure towards $PuO_{2.00}$ confirms the results of Pascard [21].

The existence of a congruently vaporizing composition requires at least two modes of vaporization. The atomic and molecular vapour

44

## TABLE XIII. STANDARD FREE ENERGIES OF FORMATION

Species	$\Delta G_f^0 = \Delta H_f^0 - T\Delta S_f^0$		Temperature range (°K)	Reference
	ΔH_f^0 (cal/mole)	ΔS_f^0 (e.u.)		
Pu(g)	80 500	23.0	1500-2500	[112]
PuO(g)	-29 000	12.1	1600-2150	[63]
PuO$_2$(g)	-113 100	-4.35	1600-2150	[63]
O(g)	61 250	16.07	1500-2500	[106]
PuO$_2$(s) [a]	-249 500	40.3	1600-2150	[63]

[a] This equation is derived for the relatively short temperature range indicated, and yields values of ΔG_f^0 that are virtually identical with those given in Table XI.

species in equilibrium with the solid plutonium oxides have not been directly observed in any of the previous measurements. They can be deduced, however, with reasonable certainty from the following consideration [63]. On the basis of the measurements of the partial molar free energy of oxygen for the PuO$_{2-x}$ phase [66], the vapour pressure of liquid plutonium [112], the previous studies of the vaporization behaviour of the thorium-[113], uranium-[114-116] and neptunium-oxygen [117] systems, and the trends in chemical bonding observed in actinide-metal oxides [118], it is concluded that both atomic and molecular oxygen are overwhelmingly predominant near the stoichiometric composition and that the principal plutonium-containing species is PuO$_2$(g). At the lower phase boundary PuO(g) is predominant and the principal mode of vaporization that occurs is

$$\frac{0.61}{0.22}\langle Pu_2O_3\rangle_{hex} = (PuO) + \frac{0.50}{0.11}\langle PuO_{1.61}\rangle$$

From the known free energies of formation of the two solid phases [63,70] and the vapour pressure given by Eq. 7 in Table XII, the standard free energy of formation of PuO(g) is calculated and given in Table XIII. The known contribution of PuO(g) to the measured vapour pressures of PuO$_{1.92}$(Eq. 6 in Table XII) via the mode of vaporization,

$$\langle PuO_{1.92}\rangle \longrightarrow (PuO) + 0.92\,(O)$$
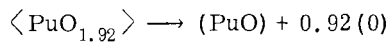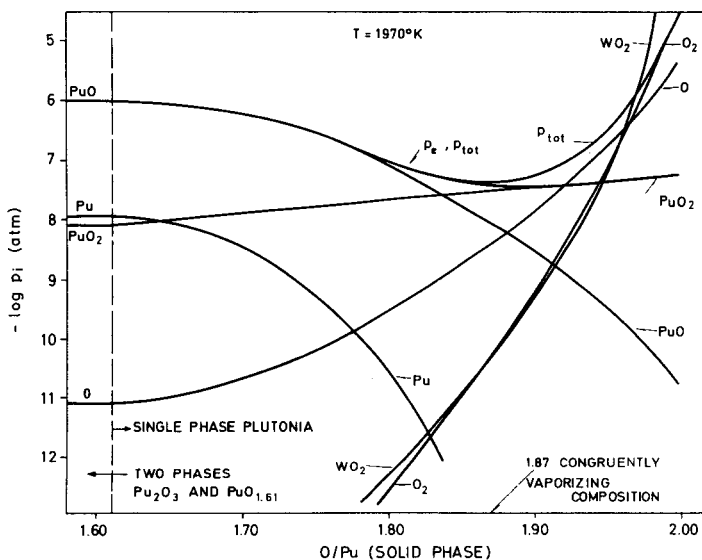
FIG. 8. Partial pressures of vapour species versus composition of substoichiometric plutonium dioxide at 1970°K. (Courtesy of the Journal of Physical Chemistry [63].)

can be calculated from the thermodynamic quantities cited above and subtracted from the measured vapour pressure to yield the partial pressure of $PuO_2(g)$ via the mode of vaporization,

$$\langle PuO_{1.92} \rangle + 0.08\,(0) \longrightarrow (PuO_2)$$
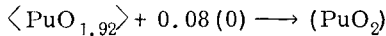
from which the standard free energy of formation of $PuO_2(g)$ given in Table XIII is obtained.

This thermodynamic analysis was carried out using the data from Markin and Rand [66], with slightly different values for the free energies of formation of $\langle Pu_2O_x \rangle_{hex}$ and $\langle PuO_{1.61} \rangle$ from those given in Table XI. The differences, however, are quite trivial (less than 100 cal, except at 2000°K for $\Delta G_f^0 \frac{1}{2} \langle Pu_2O_3 \rangle$ where the difference is 300 cal) and well within experimental error.

There is a small uncertainty in this thermodynamic analysis arising from the lack of knowledge concerning the composition of the $\langle PuO_{1.61} \rangle$ phase at high temperatures. Preliminary experiments by Pascard [21] suggest that the lower boundary of this phase may shift to $\sim PuO_{1.55}$ above 2000°K, which would change ΔG_f^0 of $PuO(g)$ by 1 to 2 kcal [63].

The detailed vaporization behaviour of the PuO_{2-x} phase at a temperature of 1970°K is summarized in Fig. 8 in which the partial pressures of the various vapour species are given as a function of the composition of the solid phase. This isotherm is typical of many which can be calculated from the thermodynamic data given in [63]. The quantity p_{tot} includes the partial pressure of oxygen as well as those of plutonium-bearing species. Quite clearly the partial pressures of

TABLE XIV.   CALCULATED CONGRUENTLY VAPORIZING
COMPOSITION OF THE PuO_{2-x} PHASE AS A FUNCTION OF
TEMPERATURE

T($^\circ$K)	O/Pu
1600	1.92
1800	1.89
2000	1.86
2200	1.85
2400	1.84

PuO(g), Pu(g), O(g) and O_2(g) depend markedly on the composition
variable in sharp contrast to the rather insensitive dependence of the
partial pressure of PuO_2(g). The values of the pressure of plutonium-
bearing species at 1970°K given in Fig. 7 agree within a factor of two
with the calculated values in Fig. 8 over the entire range of composition.
The minimum total pressure in the system occurs for the congruently
vaporizing composition O/Pu = 1.87. The relatively insensitive dependence
of the pressure p_e on the composition is immediately recognized. The
dependence of the congruently vaporizing composition on temperature
has been calculated [63] and is shown in Table XIV. At present, one
value at 2000°K has been confirmed experimentally by Ohse [111] by
extrapolating both parts of the isotherm.
    The agreement of the various sets of data within a consistent
thermodynamic framework is generally encouraging. The nearly
identical agreement shown by Curve B in Fig. 7 between the pressures
measured by Pascard [21] and Ohse [22] for the composition $PuO_{1.76}$
and $PuO_{1.77}$ respectively, and that calculated for the composition $PuO_{1.77}$
from the thermodynamic data of Ackermann et al. [63], is certainly
noteworthy.
    However, there is evidence in Curve A of a small discrepancy
between the least-squares results of the univariant system Pu_2O_3-$PuO_{1.61}$
vapour, and the data of Pascard [21]. Since in the former system the
measured pressure corresponds to the lower phase boundary of the
plutonia phase, the values obtained for more oxidized compositions cannot,
in principle, be larger. It should be noted also that the thermodynamic
description of the plutonia phase does not account for the decrease of
a factor of three in the total plutonium pressure in the composition
range between the stoichiometric and congruently vaporizing compositions
observed by Pascard [21] but rather predicts a decrease of approximately
30% only. In fact the large decrease observed by Pascard may indicate
the existence of another vapour species (at the quite large pressures

of oxygen near the stoichiometric composition), which may be $PuO_3(g)$, or perhaps a ternary species involving tungsten, plutonium and oxygen.

It is difficult to accommodate the transpiration measurements of Pardue and Keller [109] within the framework of the analysis of the effusion studies. The vapour pressures measured under one atmosphere of oxygen, which corresponds to the stoichiometric dioxide, are inconsistent with the present analysis and are nearly an order of magnitude smaller than those calculated by means of the equations given in Table XIII for the process $PuO_2(s) \longrightarrow PuO_2(g)$. An apparent increase in vapour pressure was observed when the transpiring gas was changed to air and argon. This increase is attributed to the vaporization of $PuO(g)$. It is possible, of course, to reduce $PuO_2(s)$ beyond the congruently vaporizing composition in an inert atmosphere such as argon to an extent limited by the value of the partial pressure of oxygen in the argon, and thereby increase the total vapour pressure through the vaporization of $PuO(g)$. But it is difficult to see how this species can make a significant contribution to the vapour pressure via the process $\langle PuO_2 \rangle \longrightarrow PuO(g) + O(g)$ when the oxygen pressure is reduced from one atm to 0.2 atm; both of these high oxygen pressures will overwhelmingly suppress the evaporation of $PuO(g)$.

4.3. Intercomparison of the plutonium- and uranium-oxygen systems

In the intercomparison of the vaporization behaviour of the plutonium and uranium oxides there exists a broad spectrum of similar as well as dissimilar aspects. The vapour pressures of both dioxides for the stoichiometric as well as the congruently vaporizing compositions are nearly equal with respect to the gaseous dioxide, which is the predominant metal-bearing species. It is the relatively insensitive dependence of the gaseous dioxide on the composition of the solid phase that allows the less rigorous identification of its partial pressure with a precisely known composition as has been described in Ref.[117].

In the case of plutonium dioxide, however, the preferential loss of atomic and molecular oxygen (see Fig. 8) is considerably greater than for uranium dioxide, and hence the congruently vaporizing composition of uranium dioxide is much nearer the stoichiometric value. It is the relatively large partial pressure of oxygen that explains the observed reaction between plutonium dioxide and the refractory metals tungsten and rhenium [63,111].

At the lower phase boundary of the MO_{2-x} phase the gaseous monoxide is the major vapour component in both the uranium and plutonium systems. Since there is no stable sesquioxide phase in the uranium system, this is also the case at the oxygen-rich boundary of the metal phase; for plutonium, however, the principal species over the $\{Pu\} + \langle Pu_2O_3 \rangle$ phase region is the gaseous metal and not the monoxide, at least up to $\sim 2750°K$. Whereas uranium dioxide can dissolve oxygen and extend its upper phase boundary to superstoichiometric values thereby causing the predominant vaporization of $UO_3(g)$ at high temperatures, plutonium dioxide does not show any evidence either for dissolving oxygen [26] or for stable higher solid oxides.

48

It is possible to examine the consistency and, to some extent, the reliability of the thermodynamic properties of the gaseous plutonium oxides via the homogeneous equilibrium

$$(M) + (MO_2) \rightarrow 2\,(MO)$$
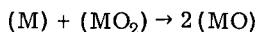
From the values given in Table XIII one calculates

$$\Delta G^0\,(M = Pu) = -25\,400 - 5.6T$$

From the measurements of the equilibrium constant by Ackermann et al. [116] one calculates

$$\Delta G^0\,(M = U) = -9600 - 5.8T$$

Quite evidently the equilibrium is displaced to the right for the case of plutonium, which indicates the relatively greater thermodynamic stability of PuO(g) compared with UO(g). The consistency between the two systems appears to be borne out by the nearly constant entropy change ($\Delta S^0 \simeq 5.7$ e.u.), which is to be expected for such closely related equilibria.

II.5. CONCLUSIONS AND FUTURE WORK

The plutonium oxygen system is known to contain at least four solid phases, some of which have wide homogeneity ranges, and although there is agreement about the general shape of the phase diagram, the finer details are still far from clear. In particular the detailed crystal structure of the $\langle PuO_{1.61} \rangle$ phase is not known, nor is the interrelationship of the cubic $\langle PuO_{1.52} \rangle$ phase with hexagonal $\langle Pu_2O_3 \rangle$; these uncertainties lead to an uncertainty in the phase diagram.

Body-centred cubic symmetry for the $PuO_{1.61}$ phase requires the presence of a miscibility gap between it and the substoichiometric fluorite-type PuO_{2-x} phase, whereas no such gap is required if $PuO_{1.61}$ has face-centred cubic symmetry. The existing lattice parameter and oxygen potential measurements, from which the phase diagram is mainly inferred, are consistent with either representation, and impose only a few restrictions on the possible position of the miscibility gap. The area between 1100°C and the liquidus has received little study and the liquidus lines themselves are not well defined.

A further high-temperature X-ray study, using well-crystalline samples, is most necessary, but detailed knowledge of the position of the oxygen atoms in $PuO_{1.61}$ must await a neutron diffraction study of this phase, which will of course necessitate the use of an oxide containing [240]Pu or [242]Pu isotopes rather than [239]Pu. Useful information on the existence of a miscibility gap in the phase diagram could come from a

more detailed study of the electrical resistivity of oxides between Pu_2O_3 and PuO_2, since there is a suggestion that the face-centred cubic oxides are n-type semiconductors, whereas the body-centred cubic phase is p-type. A valuable contribution to the phase diagram near $PuO_{1.61}$ at temperatures between 1200 and 2200°C could come from a study of the vaporization behaviour, since there is some evidence that the lower phase boundary of $PuO_{1.61}$ moves to lower compositions at temperatures around 1600°C. The lower part of the temperature range would require the use of a [238]Pu doped oxide to obtain sufficient sensitivity.

It must also be remembered that the application of thermobalance techniques to the lanthanide oxide systems has brought out a great deal of the fine structure of these diagrams, and a similar study of the plutonium-oxygen system, though experimentally much more difficult because of the very low oxygen potentials involved, might well be worth undertaking. In addition, such a study might throw some light on the existence of a miscibility gap.

Reliable and accurate heat capacity data for the oxides are lacking, so that absolute values of all the entropies are based on estimates. Some entropy differences, however, are known with fair precision from equilibrium data. However, both low- and high-temperature heat capacity values are likely to be available within the next two years, and it will be interesting to observe whether PuO_2 is found to have a magnetic ordering effect similar to that in UO_2 and NpO_2; there is a little evidence that such an effect is lacking even down to 2°K.

Magnetic susceptibility measurements of all the oxides down to liquid helium temperatures are urgently required to provide supplementary evidence to elucidate their electronic structure at low temperatures. The success of the attempt to reproduce experimental heat capacities up to room temperature from a relatively simple lattice dynamical calculation derived from the intensities of neutron diffraction reflections for UO_2 suggests that a similar calculation should be made for PuO_2, particularly in view of the difficulties associated with accurate heat capacity measurements of radioactive materials at low temperatures.

Calorimetric determinations of the heat of formation of hexagonal Pu_2O_3 and cubic $PuO_{1.52}$ are desirable. Since the latter material is difficult to prepare as a pure single phase material, it may be necessary to burn a number of oxides of varying composition between $PuO_{1.52}$ and $PuO_{1.98}$, which would consist of these two phases at room temperature. Such a method would provide a bonus in the shape of the heat of formation of the $\langle PuO_{1.98} \rangle$ phase.

The oxygen potential measurements at high temperatures agree reasonably well over the temperature range at which they overlap, though the partial molar enthalpies and entropies derived therefrom show a markedly different compositional variation. This may be a real effect, due to different types of defect predominating in the relevant temperature ranges. However, the good agreement of the experimental and calculated vapour pressures for the PuO_{2-x} phase suggests that the free energy values obtained by extrapolation of the EMF data cannot be seriously in error. Further equilibrium data at temperatures above 1100°C are clearly required; in addition to the H_2/H_2O reaction already employed, C-CO

equilibrations may be very useful for certain temperature ranges. However, the good agreement of the experimental and calculated vapour pressures for the PuO_{2-x} phase suggests that the values obtained by extrapolation of the EMF data cannot be seriously in error. Further work by gas equilibration is planned, but the possibility of C-CO equilibration should not be overlooked.

It must also be remembered that the use of the Calvet microcalorimeter now makes possible the direct measurement of the partial molar heat of solution of oxygen in non-stoichiometric phases, and such measurements on PuO_{2-x}, particularly near the stoichiometric composition, would provide a rigorous test for the statistical thermodynamical treatment of this defect structure, which is being developed.

The partial molar enthalpies and entropies derived from the EMF work have been integrated to give enthalpy and entropy differences between hexagonal Pu_2O_3 and PuO_2. Recent work on the cerium oxide heat capacities suggests that the heat capacity values assumed in the original integration may not now be the best values, but since accurate data for the oxides are likely to be available shortly the Panel did not feel justified in attempting the re-integration involved, particularly in view of the uncertainty in the phase diagram. The differences in free energies involved are well within the precision with which the data are known.

There is generally excellent agreement on the vaporization data for the plutonium oxides between five sets of workers, using the effusion technique, and the free energies of formation calculated from the results (and the extrapolated oxygen potential data) can in turn be used to calculate the vapour pressure and composition over any plutonium oxide. The agreement between these calculated and experimental values is most encouraging, and indicates that the free energies of the gaseous species cannot be greatly in error. However, a mass-spectrometric study of the vapour species, particularly near the stoichiometric composition, would be most welcome. In addition, some further experimental verification of the congruently vaporizing composition is required.

III. THE URANIUM-PLUTONIUM-OXYGEN SYSTEM

1. PREPARATION

1.1. Preparation of closely stoichiometric solid solutions with 0 to 30% Pu

Homogeneous solid solutions can be prepared by sintering various co-precipitated materials. Mechanical mixtures of fine grained powders of UO_2 and PuO_2 can be used if prolonged heat treatment at 1500 to 1600°C is used. The degree of homogeneity can be estimated in this case from the line profiles of diffractometer traces, preferably using monochromatic X-rays [119].

In the range from pure UO_2 up to 30% PuO_2, the sintering conditions required to produce near stoichiometric solid solutions are not critical. It is sufficient to sinter in an atmosphere of wet hydrogen with 1 to 10% water or wet hydrogen-inert gas mixtures at temperatures around 1500°C. Non-stoichiometric compositions may be brought to stoichiometry by equilibrating the specimen with a gas mixture of $CO/CO_2 \approx 10$ at 700-850°C or again wet hydrogen. The ease of obtaining the stoichiometric composition is due to the fact that the oxygen potential changes by many orders of magnitude over a very narrow range of composition near $MO_{2.00}$ (see Section III.3). The oxygen partial pressures for this near-stoichiometric region have been collected in Fig.9.

The thermochemical behaviour for oxides containing more than 30% Pu has not yet been studied. Studies in the U-Ce-O system in the high cerium region show that one should be cautious in extrapolating the results at 30% Pu to higher plutonium contents in the U-Pu-O system [120] (see Section III.3).

1.2. Preparation of other compositions

Superstoichiometric and substoichiometric mixed oxides of any plutonium content may be prepared from the near stoichiometric composition MO_2 by equilibration with a gas or gas mixture of determined oxygen partial pressure between 750 and 1600°C. Convenient gases are carefully dried hydrogen at 1600°C for very reduced oxides, H_2O/H_2 or CO_2/CO mixtures for slightly oxidized compositions, and air or pure oxygen at 750°C for complete oxidation.

Another way of preparing mixed oxides of any desired $Pu/(U+Pu)$- and O/M-ratio is the reaction sintering of mechanically mixed powders. In the case of mixtures of PuO_2 or MO_2 with carbon, the blended powder compacts are sintered at 1500 to 1600°C under a vacuum of 3×10^{-6} to 1×10^{-5} Torr. The CO gas evolved during the reaction is pumped off. The reaction products have densities of about 95% for Pu contents in the vicinity of 20%. For compositions higher in Pu the density is lower.

The desired O/M ratio can be adjusted by varying the amount of carbon used [121]. In this way the limiting oxygen deficient O/M ratio can be produced corresponding to the equilibrium of the mixed oxide with the carbon stabilized monoxide $M(O, C)$. The other method of reaching the lower limit in the O/M ratio is reaction sintering of a powder compact of MO_2 and the corresponding alloy, or $U + PuO_2$ or $UO_2 + Pu$ with an excess of metal under hydrogen [9].

Mixed oxides with a desired plutonium content not too far from stoichiometric MO_2 can be produced by blending the appropriate amounts of U_3O_8 and PuO_2, and sintering under inert gas/wet hydrogen mixtures at about 1600°C [9].
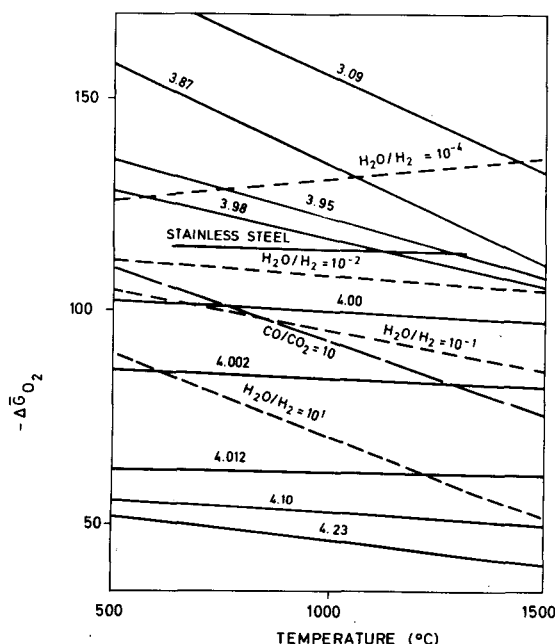
FIG. 9. $\Delta \bar{G}_{O_2}$ for $(U, Pu)O_{2 \pm x}$ solid solutions for various values of U and Pu valence. Oxygen potentials of H_2O/H_2 and CO/CO_2 mixtures and stainless steel are included.

1.3. Analysis

The U/Pu ratio in the mixed oxides is usually taken to be that in the initial mixture; analytical checks, in which the uranium content is measured by fluorescence and the plutonium usually by alpha counting, have shown that this assumption is justified for homogeneous materials for the normal method of preparation.

O/M ratios are obtained by bringing the sample back to the stoichiometric $MO_{2.00}$ compositions by equilibration in CO/CO_2 mixtures as discussed above, with measurement of the weight change or the volume of oxygen taken up by or removed from the gas phase.

2. PHASE DIAGRAM

2.1. Below 1400°C

2.1.1. General

The details of the U-Pu-O phase diagram up to 1000°C have been obtained mainly by lattice parameter measurements, both at temperature (up to 1000°C) and on quenched samples; metallographic examination has provided useful information on samples quenched from rather higher temperatures.

In the following sections percentages of plutonium refer to the percentage of the cations, i.e. $100 \times Pu/(U + Pu)$.

2.1.2. Stoichiometric compositions

It is now well established that the mixed (U, Pu) oxides with the stoichiometric composition form a continuous solid solution from UO_2 to PuO_2, and the lattice parameters of the stoichiometric composition obey Végard's Law as long as the stoichiometry is carefully controlled [122-125].

2.1.3. Oxidation to MO_{2+x}

Oxidation in air at 750-1000°C of (U, Pu) oxides results in the formation of cubic and/or orthorhombic phases when the oxide is allowed to cool to room temperature [9, 123, 124]. Oxides containing more than 39% Pu can be oxidized until the valency of all the uranium has changed from 4 to 5, and a single face-centred cubic phase results. The lattice parameter versus Pu concentration plot for more than 39% Pu is consistent with oxidation of uranium to U(V). For a 1 : 1 ratio of (U, Pu), when all the U is U(V), the over-all composition is M_4O_9. Oxides containing between 5 and at least 30.7% Pu undergo a disproportionation reaction when oxidized in air to form an orthorhombic phase, rich in uranium, and a face-centred cubic phase, rich in plutonium. Oxides containing less than 5% Pu oxidize in air to a single orthorhombic phase.

Oxidation of samples containing 10% Pu at 750-800°C to compositions between $MO_{2.05}$ and $MO_{2.20}$ results in two cubic phases, one MO_{2+x} and the other an M_4O_9-type phase [126], whereas partial oxidation of material containing 11% Pu gives a single face-centred cubic phase up to $MO_{2.11}$, and two phases, $MO_{2.11}$ plus M_4O_9 at higher O/M ratios [127]. The room temperature phase-boundary at $MO_{2.11}$ moves to higher O/M ratios as the temperature is increased. Oxidation of samples with 11% Pu beyond M_4O_9 results in an orthorhombic M_3O_{8-y} phase in equilibrium with M_4O_9. Lattice parameter measurements indicate no appreciable range of homogeneity for the M_4O_9 phase between room temperature and 800°C when the Pu concentration is 11%. The O/M ratio of the face-centred cubic phase in equilibrium with the M_4O_9 phase for oxides with 15% Pu is 2.19, virtually independent of temperature up to 800°C; a small range

54
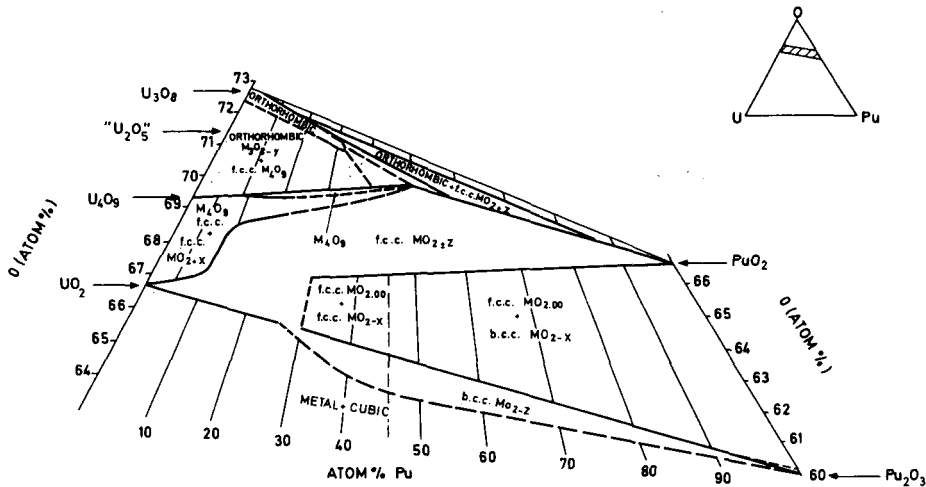
FIG. 10. U-Pu-O ternary section at 20°C.

of homogeneity, increasing slightly with temperature, has been observed
for the M_4O_9 phase at this Pu concentration; further partial oxidation
results in two phases, M_4O_9 plus M_3O_{8-y}[127]. For oxides containing
30% Pu, M_3O_{8-y} is in equilibrium with MO_{2+x}(or M_4O_9) for oxides of
composition $MO_{2.30}$(at most) and above.

Oxides containing 15, 20 and 35% Pu have been oxidized to various
O/M ratios at 600°C and quenched to 20°C [23, 119]. They are two-
phase, face-centred cubic + tetragonal, for $2.00 < O/M \leq 2.2$ and
two-phase, tetragonal + orthorhombic for $O/M \geq 2.39$. The highest
O/M ratios obtained so far are 2.64 with 15% Pu and 2.58 with 35% Pu.
These two values lie sensibly beyond the line connecting U_2O_8 and PuO_2
(Fig. 10).

The composition of the tetragonal phase has been determined
approximately as $2.28 < O/M \leq 2.35$ ($\sim M_3O_7$) by correlating X-ray line
intensities of the two-phase mixtures with the oxygen content of the
specimens. The lattice parameters are a = 5.38_7 and c = 5.54 Å
(c/a = 1.028) and do not vary with plutonium content in the range 15 to
35%. Specimens oxidized at 1200 and 1400°C and annealed for 3 h
at 600°C do not give the tetragonal phase. Thus it is not yet clear
whether this phase is stable only below 600°C or is a metastable product
of low-temperature oxidation of MO_2. The c/a ratio of the ternary
phase, which can clearly contain a considerable proportion of plutonium,
is close to that of the γ_1-$UO_{2.33}$ phase [1], which is not stable above 460°C.

2.1.4. Reduction to MO_{2-x}

In this region oxides containing less than 30% Pu behave rather
differently from those with more than 30%, and it is convenient to treat
these regions separately.
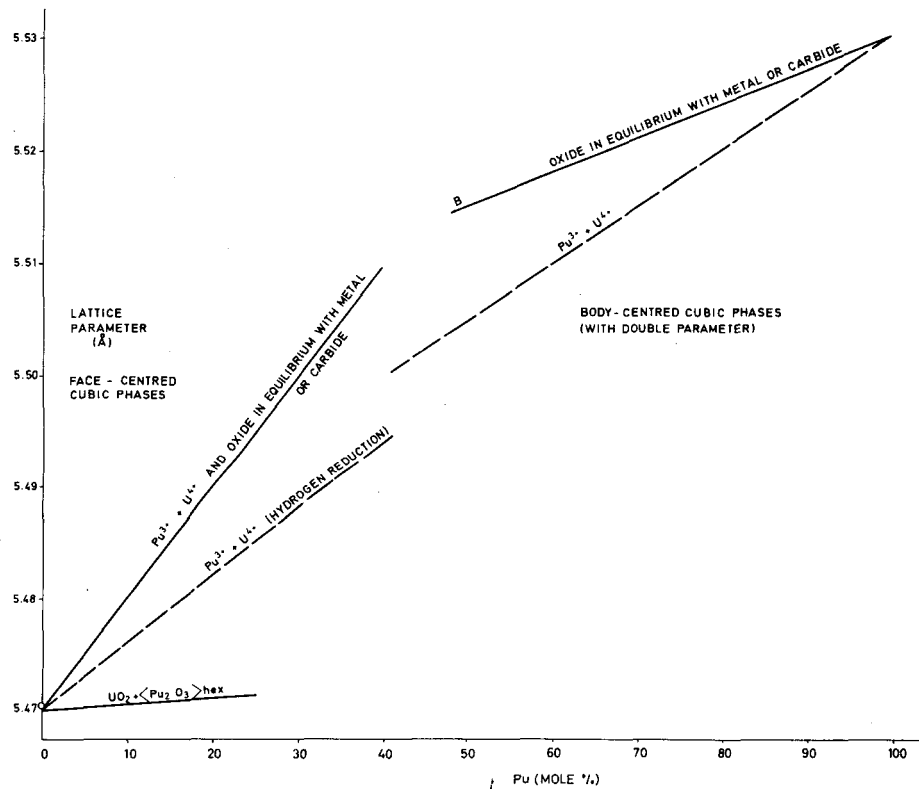
FIG. 11.   Lattice parameters of "fully-reduced" uranium-plutonium oxides.

2.1.4.1. Below 30% Pu. For these oxides the single-phase fluorite
type MO_{2-x} extends down to the alloy in equilibrium with (U, Pu) alloy
[9, 121] ; at this lower phase boundary all the plutonium is reduced to
Pu (III), but the uranium seems to remain at U (IV). Nevertheless, there
are considerable discrepancies in the lattice parameters found for oxides
comparing the pseudo-binary UO_2-$PuO_{1.5}$ oxides in this region. Figure 11
shows that the three methods of preparation (sintering of UO_2 with
hexagonal Pu_2O_3 [9] and reduction of UO_2-PuO_2 by dry hydrogen
[23, 119, 127] and by carbon [121] give oxides with very different
lattice parameters, although chemical analysis shows they are all
on the UO_2-$PuO_{1.5}$ join. The reason for this behaviour is unknown.

2.1.4.2. Above 30% Pu. Partial reduction of oxides containing more
than 30-40% Pu to a substoichiometric composition results in two cubic
phases when the oxide is cooled to room temperature ; one phase is
the $MO_{2.00}$ phase and the other is the MO_{2-x} phase in which all the Pu is
trivalent; this phase is face-centred cubic when the Pu concentration is
less than ~45% but body-centred cubic above this. There is no ex-
perimental evidence for a miscibility gap between these two structures,
although a narrow gap cannot be excluded. At a temperature depending

56
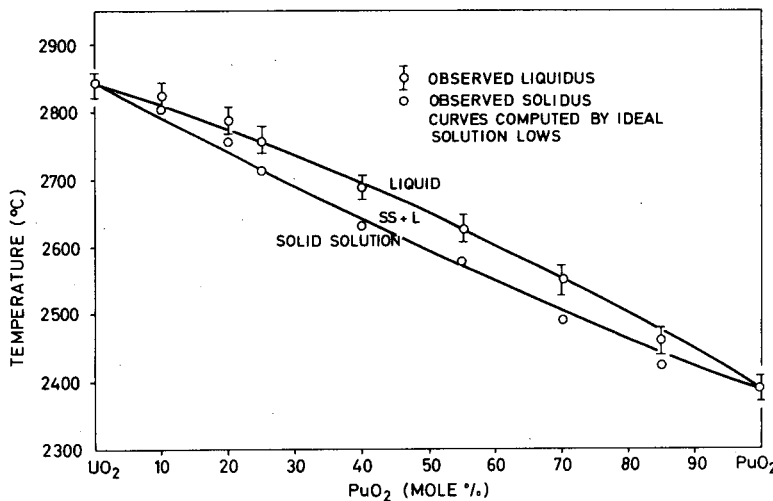
FIG. 12.   Solid-liquid phase diagram for the UO_2-PuO_2 system.

on the Pu concentration, the two cubic phases become a single fluorite-type phase. The limiting concentration for two phases to appear at room temperature is not certain; X-ray [127] and metallographic and X-ray [23] results differ for the 30% Pu composition.

However, in contrast to the region below 30% Pu, the phase in equilibrium with (U, Pu) alloy has a large parameter and presumably less oxygen than the UO_2. $PuO_{1.5}$ pseudo-binary compositions. The obvious inference is that some reduction of U(IV) to U(III) has occurred. Thus the MO_{2-z} phase can exist with a range of O/M ratios; the composition at the lower phase boundary has not been determined, but extrapolation of line B on Fig. 11 to the uranium axis suggests that the uranium valency may be about 3.8 in the oxides in equilibrium with metal; these thus lie on the $UO_{1.9}$ · $PuO_{1.5}$ join.

2.2.   Melting behaviour

The early determinations [128-130] of melting points in the UO_2 . PuO_2 system, which indicated a maximum in the liquidus curve near 5-10% PuO_2, were carried out under conditions which must have resulted in some reduction of the plutonium. Recently, however, Lyon and Baily [131] have studied material encapsulated in tungsten. Some slight reduction (to give the equilibrium pressure of gaseous tungsten oxides, see Section II.4) will have occurred at the plutonium-rich end, but the simple liquidus-solidus curve obtained (see Fig. 12) must be closely representative of the stoichiometric system. These curves are consistent with ideal solution theory if the heats of fusion of UO_2 and PuO_2 are taken to be 21.2 ± 1.3 and 16.8 ± 1.3 kcal mole[-1] respectively [132].
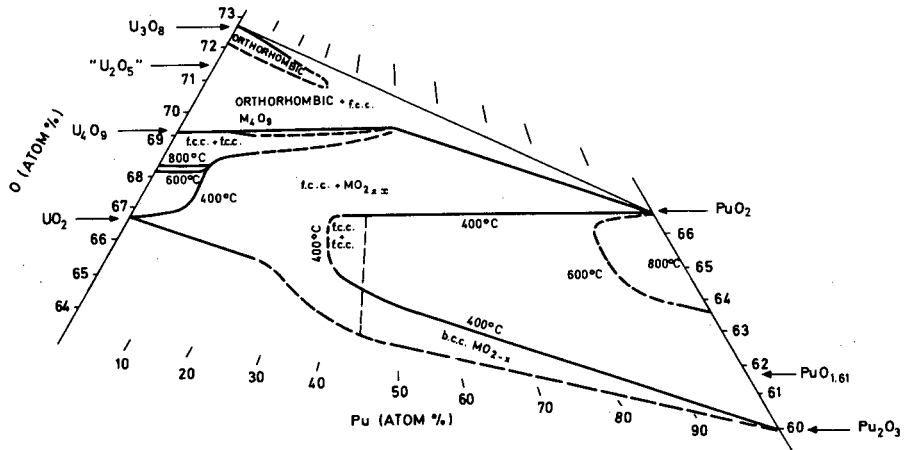
FIG. 13.   U-Pu-O ternary section at 400, 600 and 800°C.

2.3.   The U-Pu-O phase diagram

Isothermal sections of the phase diagram at 25, 400, 600 and 800°C (Figs 10 and 13) for the U-Pu-O system have been constructed between the limits $UO_{1.88}$-U_3O_8 and PuO_2-$PuO_{1.5}$ for all concentrations of Pu from the results reviewed in the preceding paragraphs and the U-O [133] and Pu-O (Section II.2) phase diagrams.

The phase boundary for the MO_{2-z} phase in equilibrium with the metal has been drawn between $PuO_{1.5}$ and $UO_{1.88}$ for oxides containing more than 40% Pu, since extrapolation of the lattice parameter versus Pu/(U + Pu) plot for MO_{2-z} in equilibrium with (U, Pu) metal alloy to Pu = 0 results in a = 5.500 Å. This lattice parameter corresponds to $UO_{1.88}$ by analogy with the change in lattice parameter in going from PuO_2 to $PuO_{1.52}$. The phase boundary for oxides in equilibrium with (U, Pu) metal alloy has been drawn between UO_2 and PuO for oxides containing less than 30% Pu.

The lower phase boundary of the orthorhombic plus MO_{2+x} two-phase region above ∼ 45% Pu must lie slightly above the PuO_2 . $UO_{2.5}$ join, the single-phase compositions attained in air at 850°C. Oxidation of oxides containing 5 to 30% Pu in air results in the formation of some U(VI), and cation disproportionation occurs; the lines have been drawn on the ternary phase diagram from the experimental results. The single orthorhombic phase has been drawn when the Pu content is less than 5%.

At room temperature, the substoichiometric dioxide has been drawn to begin when the Pu content is 30%, from the metallographic and X-ray examinations of Blank et al. [119] ; other X-ray lattice parameter data place this point between 30 and 40% Pu [127].

The high-temperature lattice parameter data of Markin and Street [127] have been used to construct the ternary phase diagram at 400, 600 and 800°C.

No detailed work has been reported for high concentrations of Pu, above 90%, but the ternary phase diagram for the condition that nearly

58

all the Pu has been reduced to Pu(III) must be complex since reduction of pure PuO_2 to $PuO_{1.5}$ results in a structural rearrangement to form hexagonal Pu_2O_3. Dashed lines have been drawn on the ternary phase diagram to be consistent with the Pu-O phase diagram and the suggestion [9] that the hexagonal phase is suppressed when the U content is greater than 5%.

The phase diagram between MO_2 and M_3O_{8-y} has been constructed for Pu concentrations below 30% from the results of Dean [9] and Markin and Street [127]. A narrow single-phase region has been drawn at M_4O_9 for oxides with more than 15% Pu. The phase boundary for the M_4O_9 phase in equilibrium with M_3O_{8-y} has been drawn between U_4O_9 and $(U_{0.5}Pu_{0.5})O_{2.25}$, the M_4O_9 composition when the U valency is five. This composition has been taken to be the limit of the order-disorder transition for M_4O_9-MO_{2+x}. The upper and lower phase boundaries of the M_4O_9 + MO_{2+x} two-phase region have been drawn as dashed lines from 15% Pu to the order-disorder transition at $(U_{0.5}Pu_{0.5})O_{2.25}$.

A narrow single-phase M_3O_{8-y} region has been drawn on the phase diagram to a Pu content of about 35%. Tie lines for 11, 15 and 30% Pu in the two-phase M_4O_9 + M_3O_{8-y} region have been drawn along lines of constant U/Pu ratio because the lattice parameter of the M_4O_9 phase in equilibrium with M_3O_{8-y} is independent of the oxygen content. Lattice parameter measurements have been made for partially oxidized samples of UO_2-ThO_2 [134] and the authors interpreted their data as a cation disproportionation reaction occurring between U_3O_8 and the M_4O_9 phase (referred to as face-centred cubic in their paper) below 50% Th, although the lattice parameter data show that the U_3O_8 contains several per cent of Th. A similar interpretation does not fit the data for the U-Pu-O system below 30% Pu, although the phase diagrams for U-Pu-O and U-Th-O are similar when the uranium content is less than 50%. Oxides with O/M ratios between 2.18 and 2.25 were two phase when the Th content was between 10 and 50% if the oxide was allowed to cool slowly to room temperature after oxidation; this result is in agreement with the postulated U-Pu-O phase diagram for Pu contents between 15 and 50%.

3. THERMODYNAMIC PROPERTIES

Only one group of workers have obtained thermodynamic data for the mixed (U, Pu) oxides. Markin and McIver [122] have used the high temperature EMF cell, reversible to oxygen ions for $U_{0.89}Pu_{0.11}O_{2\pm x}$ and $U_{0.70}Pu_{0.30}O_{2\pm x}$ close to the stoichiometric composition at temperatures between 750 and 1100°C. There are no other data for the (U, Pu) oxides with which to compare these results but the EMF cell used by Markin and McIver has been shown to give meaningful and reproducible results when thermodynamic data for the systems UO_{2+x} [135], CeO_{2-x} and PuO_{2-x} (at 1050°) [135, 136] obtained from cell measurements have been compared with data for these systems employing other methods. The EMF cell used to obtain data for the mixed oxides was identical with the cell used to obtain the PuO_{2-x} and CeO_{2-x} data. Pellets were analysed as for the U-Pu-O ternary phase diagram experiments.
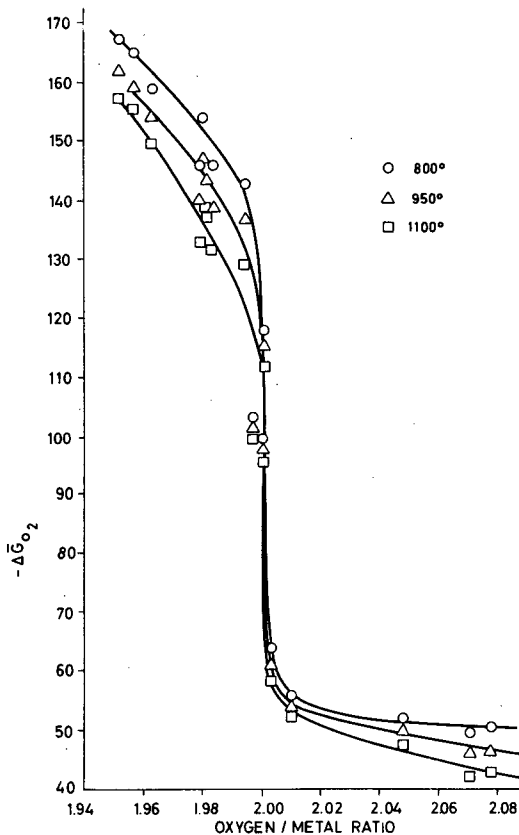
FIG. 14. $\Delta \bar{G}_{O_2}$ versus oxygen/metal ratio for $U_{0.89} Pu_{0.11} O_{2\pm x}$.

Figures 14 and 15 show plots of $\Delta \bar{G}_{O_2}$ isotherms versus O/M ratio for oxides containing 11 and 30% Pu. A very large change in $\Delta \bar{G}_{O_2}$ occurs when $MO_{1.99}$ is oxidized to $MO_{2.01}$ and the obvious inference is that the stoichiometric composition occurs at the steepest part of the curve, close to $\Delta \bar{G}_{O_2} = -100$ kcal, thus justifying the original definition of the stoichiometric composition as the oxide resulting after equilibration with a 10/1, CO/CO_2 gas mixture at 850°C.

Figures 16 and 17 show plots of $\Delta \bar{G}_{O_2}$ isotherms versus Pu valency for substoichiometric oxides and U valency for superstoichiometric oxides respectively. It can be seen that $\Delta \bar{G}_{O_2}$ values for $U_{0.89} Pu_{0.11} O_{2\pm x}$, $U_{0.85} Pu_{0.15} O_{2-x}$, $U_{0.70} Pu_{0.30} O_{2\pm x}$ and UO_{2+x} fall on the same curves when plotted versus valency. This is extremely fortunate because it allows the $\Delta \bar{G}_{O_2}$ values for all single-phase (U, Pu) oxides containing between 10 and 30% Pu to be predicted; presumably Fig. 17 may be extended to solid solutions outside this range, as long as the oxide remains single phase. However, for reasons discussed below, the $\Delta \bar{G}_{O_2}$ values for PuO_{2-x} do not, in general, fall on the curve in Fig. 16

60
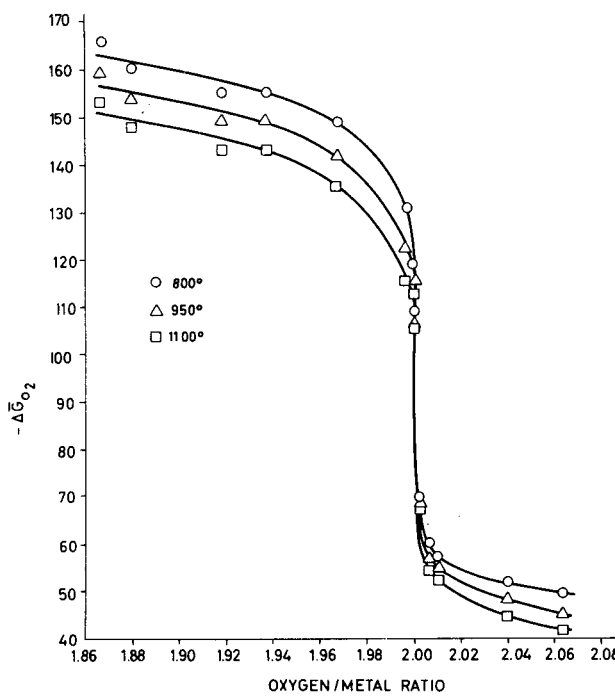
FIG. 15. $\Delta\overline{G}_{O_2}$ versus oxygen/metal ratio for $U_{0.70}$ $Pu_{0.30}$ $O_{2\pm x}$.
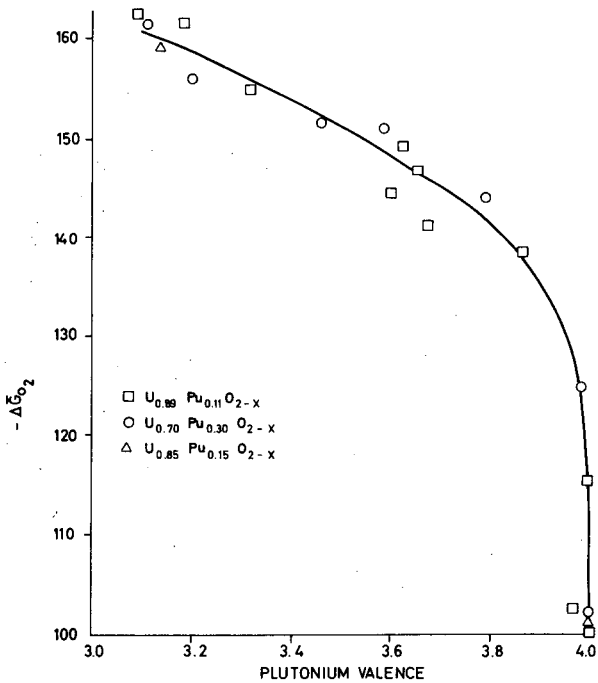
FIG. 16. $\Delta\overline{G}_{O_2}$ at $1173°K$ versus plutonium valence for $(U,Pu)O_{2-x}$.
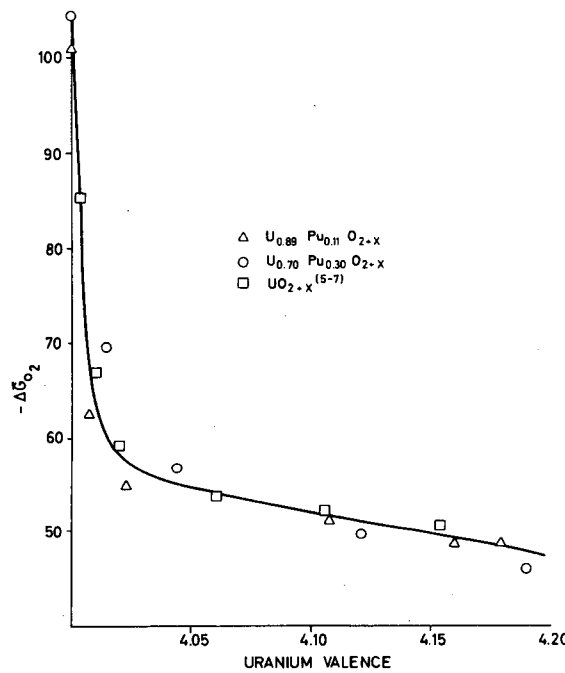
FIG. 17. $\Delta \bar{G}_{O_2}$ at 1173°K versus uranium valence for $(U, Pu) O_{2+x}$ and $UO_{2\mp x}$.
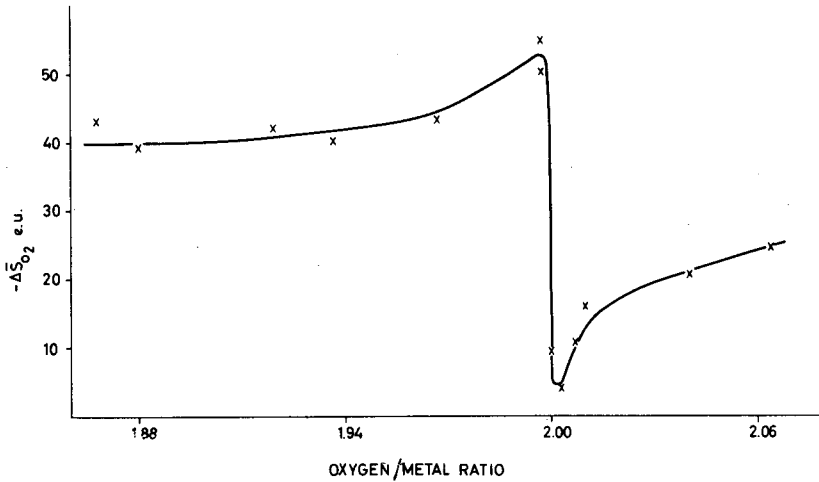
FIG. 18. $\Delta \bar{S}_{O_2}$ versus oxygen/metal ratio for $U_{0.70} Pu_{0.30} O_{2\pm x}$.

(by chance, the values are not far different at 1173°K, the temperature for which Fig. 16 is drawn; this is not so at other temperatures). The figure should therefore not be used much outside the range 10 to 30% Pu without corroboration, particularly as results on the similar U-Ce-O

62
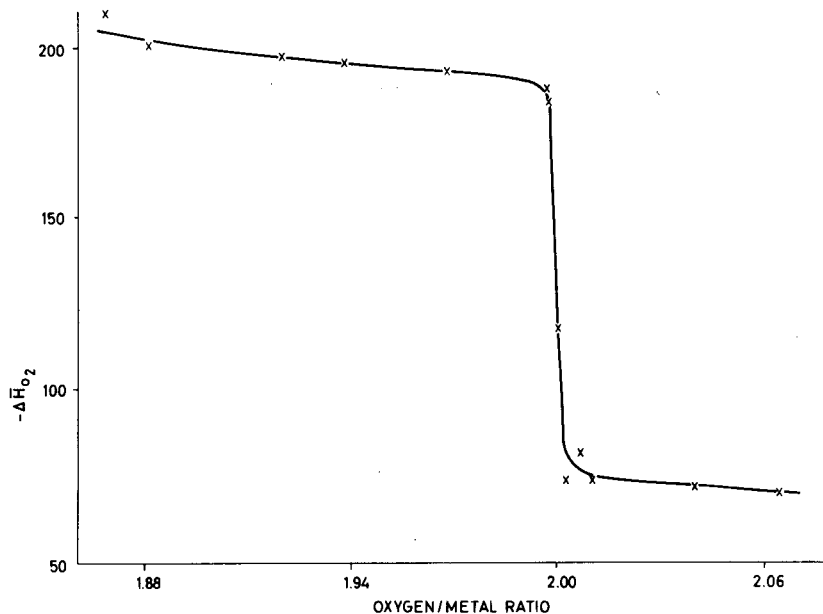
FIG. 19. $\Delta\bar{H}_{O_2}$ versus oxygen/metal ratio for $U_{0.70}\,Pu_{0.30}\,O_{2\pm x}$.

system [137] show that $\Delta\bar{G}_{O_2}$ is not the same function of Ce valency between 35 and 75% Ce as between 10 and 15% Ce.

Figures 18 and 19 show the variation of $\Delta\bar{S}_{O_2}$ and $\Delta\bar{H}_{O_2}$ with O/M ratio for $U_{0.70}\,Pu_{0.30}\,O_{2\pm x}$. Similar plots have been obtained for $U_{0.89}\,Pu_{0.11}O_{2\pm x}$. The values for $x > 0$ are very similar to those for UO_{2+x} but for $x < 0$, $\Delta\bar{H}_{O_2}$ and $\Delta\bar{S}_{O_2}$ show no similarity to the corresponding values for PuO_{2-x}. The variation of $\Delta\bar{H}_{O_2}$ with composition for (U,Pu) oxides was small, no more than 10 kcal as the Pu valency was reduced from 4.0 to 3.1, in sharp contrast to the change of 80 kcal in going from PuO_2 to $PuO_{1.75}$ (i.e. a change of valency from 4.0 to 3.5).

Markin and Roberts [136] have considered the reason for the difference between $(U,Pu)O_{2-x}$ and PuO_{2-x}. The oxygen vacancies in PuO_{2-x} were assumed to agglomerate locally to form regions having the structure of a stable oxide; this can only occur if a large fraction of the cations can take part in this co-operative mechanism leading to local ordering. The U(IV) ions cannot take part in this process unless, of course, they are reduced to U(III). The behaviour of solid solutions of $(U,Pu)O_2$ suggests that oxygen is removed from the same environment at all compositions. This may be oxygen sites between two Pu atoms, with localization of the charge. Even at 11% Pu, 80% of the Pu atoms have a Pu atom as one nearest neighbour. It was pointed out in the same paper that measurements on a wider range of Pu content would be instructive because the Pu concentration at which a significant change in behaviour occurred might indicate the number of Pu atoms involved in co-operative local ordering.

63

4. VAPORIZATION BEHAVIOUR

The partial vapour pressures of UO_2 and PuO_2 in equilibrium with solid $(U, Pu)O_2$ have been measured [21] recently for three compositions: 10, 20 and 25% Pu, in the temperature range of 1800-2500°K. The use of ^{233}U for the composition 20% Pu permitted the direct measurement by alpha counting of U deposited on the target. In the other two cases, where the samples were made with natural uranium, uranium on the target was determined by X-ray fluorescence.
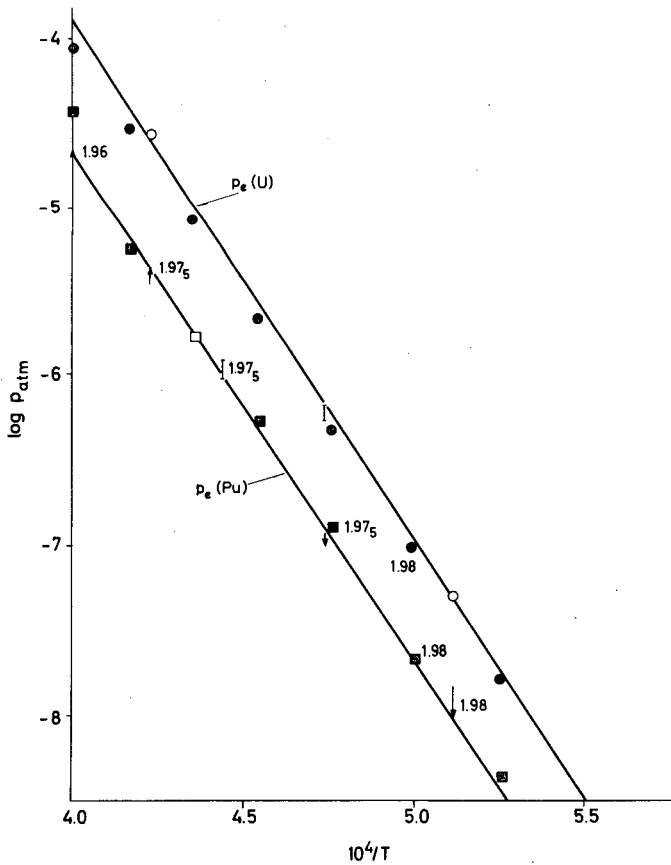
FIG. 20. Total pressures of uranium- $(p_e(U))$ and plutonium- $(p_e(Pu))$ bearing species over $U_{0.9}\ Pu_{0.1}\ O_{2-x}$. Initial oxygen/metal ratio = 1.983.

↓○ $p_e(U)$ experimental	↕□ $p_e(Pu)$ experimental
● $p_e(U)$ calculated	◪ $p_e(Pu)$ calculated

The results are represented on Figs 20 and 21 for two compositions, 10 and 20% Pu. As for pure PuO_2, the partial vapour pressures are time dependent. Consequently, targets were exposed at successive times up to apparent steady-state conditions. The arrows on the figures indicate the extent of this pressure change at fixed temperature. Figures near the experimental points give the final O/M ratio of the solid corresponding

64
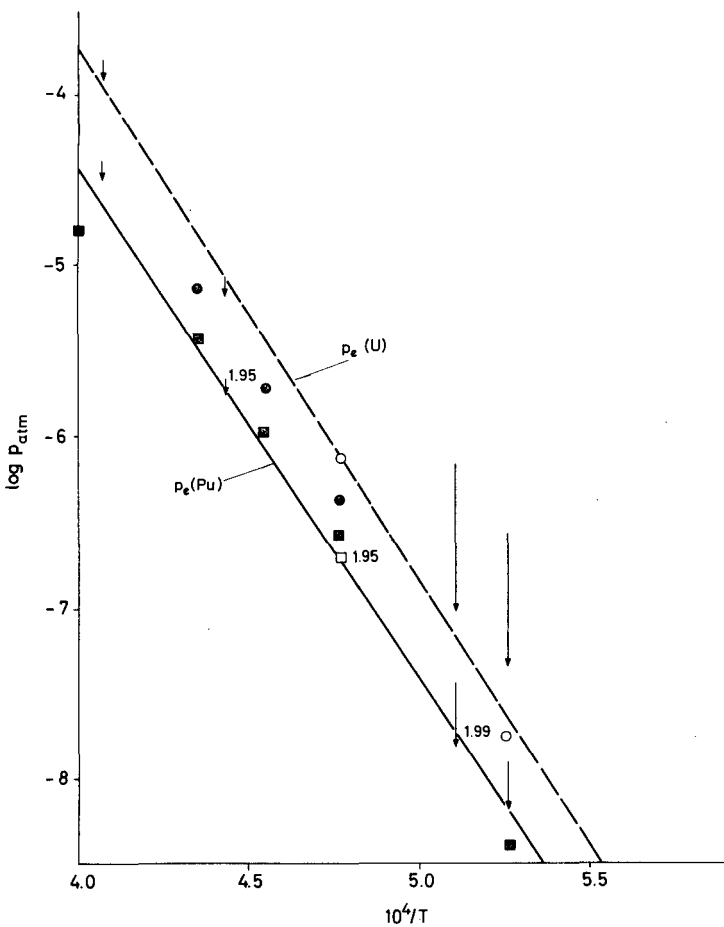
FIG. 21. Total pressures of uranium- (p_e(U)) and plutonium- (p_e(Pu)) bearing species over $U_{0.8}$ $Pu_{0.2}$ O_{2-x}. Initial oxygen/metal ratio = 2.00.

↓ ○ p_e(U) experimental   ↓ □ p_e(Pu) experimental
● p_e(U) calculated   ■ p_e(Pu) calculated

to the apparent equilibrium. These O/M values have been deduced from the increase of the lattice parameter with respect to that of the stoichiometric product. Sufficient thermodynamic data are now available ([63,116] and Section II.4) to calculate the total pressure and composition of the vapour over substoichiometric mixed oxides. With the known free energies of formation of the gaseous species (UO, UO_2, UO_3, PuO and PuO_2) and known oxygen pressures (Section III.3) the only assumption required is that UO_2 and PuO_{2-x} form ideal solid solutions. This assumption is likely to be valid when x is close to zero, since Aitken et al. [138,139] have shown that UO_2 and ThO_2 do form ideal solid solutions, but UO_2 and Y_2O_3 do not. The calculated points [140] for the total uranium- and plutonium-bearing species are shown in Figs 20 and 21. The agreement is indeed excellent.

It will be seen from Fig. 21 that the initial uranium-bearing pressures over stoichiometric $U_{0.8} Pu_{0.2} O_{2.00}$ are remarkably high in the lower

temperature range, around 2000°K. Initially the pressure is about ten times that of pure UO_2 and even at the end of the run, when apparent equilibrium had been reached, it is significantly higher than for UO_2. This phenomenon is due to the relatively high oxygen potentials over the mixed oxides (Section III.3), these being several orders of magnitude higher than that over UO_2. Under these conditions the $(UO_2) + (O) \rightarrow (UO_3)$ equilibrium lies far to the right, and thus (UO_3) is the principal uranium-bearing species over stoichiometric mixed oxides, which in this respect behave as would solutions of UO_{2+x} and PuO_{2-x}. The observed initial pressure would correspond to $UO_{2.04}$. Conversely, of course, the principal plutonium-bearing species over highly substoichiometric mixed oxides is (PuO); calculation shows that over $U_{0.8} Pu_{0.2} O_{1.95}$ the (PuO) partial pressure is ten times that of (PuO_2).

5.   CONCLUSIONS AND FUTURE WORK

    The phase diagram for low concentrations of Pu (below 30%) is fairly well established for both the super- and substoichiometric compositions, since these are the Pu concentrations of interest to the reactor chemist. More work is required to fix the $MO_2 + MO_{2-x}$ phase boundary at a precise Pu composition; at present the boundary can only be placed near 30% Pu. The $M_4O_9 + M_3O_{8-y}$ two-phase region for oxides containing 35 to 50% Pu must be investigated to determine whether cation disproportionation does occur in accordance with the postulated phase diagram. Some very careful work is needed to define the homogeneity range and Pu concentration limit of the single-phase M_3O_{8-y} region. Superstructure lines in the X-ray pattern of the M_4O_9 phase should be looked for. The evidence to date suggests that superstructure lines appear only after the oxide has been heated to 1000 to 1400°C when the cation mobility becomes sufficiently high to allow the cations to order. The phase diagram for oxides containing more than 90% Pu needs very careful examination and this may throw more light on the Pu-O phase diagram for the pure plutonium system.
    The cause of the differences in lattice parameter of the fully reduced oxides containing less than 30% Pu is not known (Fig. 11). Analyses showed that all the Pu had been reduced to Pu(III) in all cases. Measurement of the lattice parameter of the fully reduced oxide, prepared by H_2 reduction of co-precipitated and physically mixed oxide at the same temperature and under the same conditions, may help to explain the large differences in lattice parameter. The Panel did not believe that the differences were due to lack of homogeneity but could offer no alternative explanation.
    It is very gratifying to note that the thermodynamic data for the solid (U, Pu) oxides obtained from the EMF cell, extrapolated to higher temperatures, together with the vaporization data for uranium and plutonium oxides, are consistent with the vaporization data of Pascard. However, vaporization data for only three compositions are available, and although these agree well with the calculated values some more results for different compositions are desirable.

IV. OTHER PuO_2 - MeO_x OXIDE SYSTEMS

Very few thermochemical properties of the binary plutonium oxide-metal oxide systems are described in the literature. Some phase diagrams and relevant basic data (melting points, X-ray analysis, ceramographic studies) are available, but practically no thermochemical data are given. The same situation is found with the ternary plutonium-metal-oxides.

In nearly all the reported systems there is grave doubt about the actual valency of the plutonium. The simple eutectic systems or the systems of continuous solid solutions contain Pu(IV), Pu(III) or usually both, depending on the experimental conditions. The ternary oxides (using the nomenclature of Keller [141], i.e. those in which compound formation is possible, contain the plutonium in various valency states up to six. Unfortunately this problem is very rarely discussed explicitly in the published papers. Most investigators used sintering at 1500 - 1600°C in inert atmospheres, which will usually result in reduction of the plutonium, so that the results are not fully representative of the Pu(IV) system.

1. BINARY SYSTEMS PuO_2 - MeO_x

1.1. Simple eutectic systems

Eutectic composition, temperature and terminal solubility limits have been reported for the systems BeO-PuO_2 (by Hough and Marples [142] and Dayton and Paprocki [143-147]), MgO-PuO_2 (by Carroll [148]), Al_2O_3-PuO_2 (by Hough and Marples [142])and SiO_2-PuO_2 (by Carroll [149]) (see Table XV). Hough and Marples [142] used the most oxidizing conditions (oxygen atmosphere inside a thoria tube) and their data are to be preferred at present.

The phase diagram of MgO-PuO_2 described by Carroll [148] (Fig. 22) must be regarded as preliminary only because of the large impurity content ($PuO_{1.52}$, $MgWO_4$, WO_3 and W) found by X-ray diffraction.

The surprisingly high terminal solubility of MgO in PuO_2 (3.2 ± 1.5 mole%) found by Hough and Marples [142] could be explained by the small counting rate obtained on the microprobe and by a large "atomic number" correction [142].

The perovskite type compound $PuAlO_3$ described by Russell et al. [151] and McEwen [152] was prepared in reducing atmospheres and contains only Pu(III). Runnalls [153] has shown that its structure is [151] orthorhombic and not rhombohedral as first reported [151].

The ternary system BeO-ThO_2-PuO_2 was studied by Pardue et al., reported by Dayton and Paprocki [147] and by Hough and Marples [142], who have drawn part of the ternary phase system (Fig. 23) showing the

TABLE XV.   EUTECTIC AND TERMINAL SOLID SOLUBILITY DATA FOR BeO-PuO_2, MgO-PuO_2, Al_2O_3-PuO_2 SYSTEMS

| System	Terminal solid solubility			Eutectic composition (mole % PuO_2)	Eutectic temperature (°C)	References
	of	in	value (mole %)			
BeO-PuO_2	PuO_2	BeO	0.016 ± 0.007	34	2135 ± 70	[142]
			0.02	32.8	2150 ± 20	[146]
	BeO	PuO_2	Not determined	Not determined		
MgO-PuO_2	PuO_2	MgO	0.032 ± 0.006	40	2260 ± 30	[142]
	MgO	PuO_2	3.2 ± 1.5	43	2100	[150]
				57	1985 ± 35	[148]
Al_2O_3-PuO_2	PuO_2	Al_2O_3	0.28 ± 0.02	42	1910 ± 15	[142]
	Al_2O_3	PuO_2	0.14 ± 0.14			
$(Pu_{0.5}Th_{0.5})$ O_2-BeO	$(Pu_{0.5}Th_{0.5})O_2$	BeO	0.02			[147]
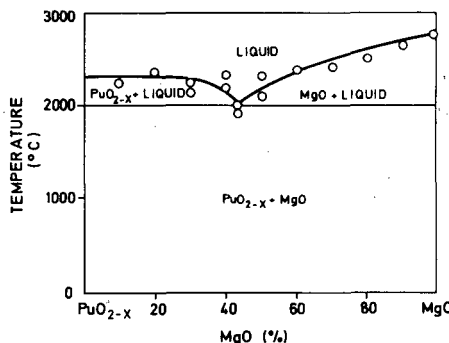
FIG. 22.   Proposed diagram for the system PuO_2-MgO.
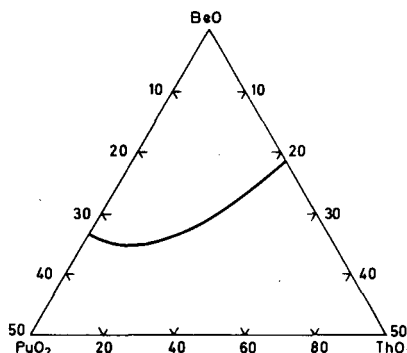
FIG. 23. PuO_2-BeO-ThO_2 system; position of eutectic valley.
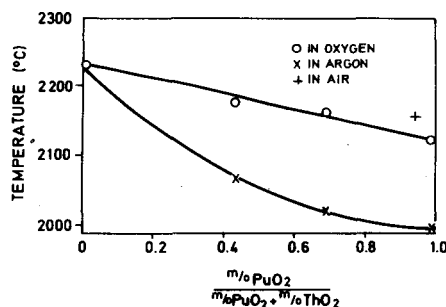
FIG. 24.   Melting points of PuO_2-BeO-ThO_2 specimens along the eutectic valley in oxygen and in argon.

position of the eutectic valley.   The experimental conditions used (oxy-acetylene flame melting) probably exclude the possibility of the loss of oxygen from the plutonia.

Figure 24   shows the difference in melting points along the eutectic valley between the specimens treated in an oxygen and argon atmosphere [142], and includes one melting point (in air) determined by Pardue et al. (reported in [147]).

1.2. Continuous solid solutions

1.2.1. CeO_2-PuO_2

Mulford and Ellinger [154] have published the lattice parameters for various compositions of CeO_2-PuO_2; Végard's Law is followed to within the accuracy of the measurements.

1.2.2. ZrO_2-PuO_2

The phase diagram was published by Carroll [156] (Fig. 25). A continuous range of fluorite-type solid solutions is evident from pure PuO_2 to 77 mole % ZrO_2. The region from 77 to 99.8 mole % ZrO_2 contains two phases in equilibrium at room temperature, monoclinic ZrO_2 and a face-centred cubic PuO_2-77 mole % ZrO_2 solid solution.

FIG. 25. The system PuO_2-ZrO_2.
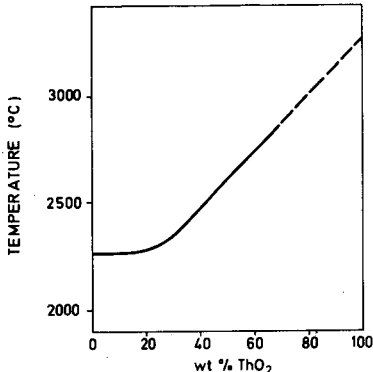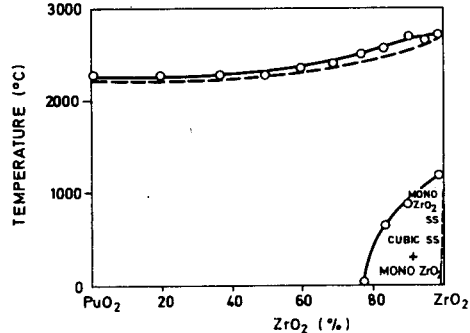
FIG. 26. The liquidus curve for the PuO_2-ThO_2 system.

In addition to this, 0.2 mole % PuO_2 dimensionally stabilizes monoclinic ZrO_2 and forms a special phase region [156]. However, all the specimens for this work were prepared by sintering in an inert gas at 1500 - 1550°C, so that the precise oxidation state of the plutonium is unknown. This will also be true for Carroll's determinations of the melting points [156].

TABLE XVI.   LATTICE PARAMETER OF THE $EuO_{1.5}$-PuO_2 SYSTEM

| PuO_2 (mole %)	Lattice parameter Å	Percentage of body-centred cubic phase present
100.0	5.3938 ± 0.0005	-
90.0	5.3935 ± 0.0005	-
85.0	5.3934 ± 0.0005	-
80.0	5.3974 ± 0.0005	-
70.0	5.4055 ± 0.0005	-
60.0	5.4138 ± 0.0005	-
55.0	5.417 ± 0.001	-
50.0	5.419 ± 0.002	-
40.0	5.420 ± 0.003	5
20.0	5.424 ± 0.005	20
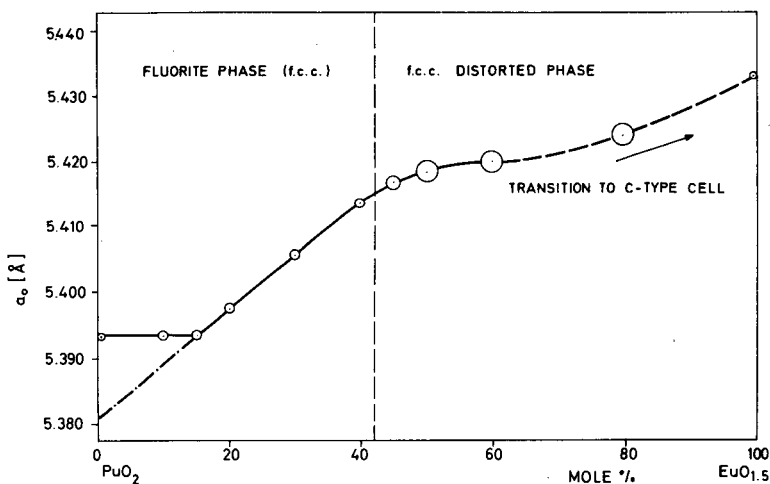
FIG. 27.   Lattice parameter versus mole % PuO_2 ($EuO_{1.5}$-PuO_2 system).

1.2.3. ThO_2-PuO_2

Mulford and Ellinger [154] have shown from lattice parameter measurements that a continuous range of solid solutions, obeying Végard's Law, is formed.   It seems likely that the materials prepared by Pardue et al.   in argon near 1700°C, which showed slight positive deviations from

TABLE XVII.   PHYSICO-CHEMICAL PROPERTIES OF THE TERNARY-QUATERNARY PLUTONIUM-METAL OXIDES

Formula valency state of metal ions	The condition of preparation and thermal stability					Structural data		References	Notes
	Temperature of crystal formation (°C)	atm.	Dwell time	Thermal stability limit[a] (°C)	Purity	Symmetry, space group, structure type	Unit cell dimensions (Å)		
$Li_4Pu^{VI}O_5$	400-500 (up to 900)	O_2	6 h	> 900 dec. $Li_3Pu^{V}O_4$	Pure	Tetragonal I4/m	a = 6.677 ± 0.002 c = 4.421 ± 0.003	[160] [161] [162]	
$Li_6Pu^{VI}O_6$	400-500	O_2		800 dec. $Li_3Pu^{V}O_4$	Pure	Hexagonal	a = 5.184 c = 14.59	[160] [161]	
$Li_3Pu^{V}O_4$	600	O_2	8 h	600 vacuum dec. $Li_7Pu^{V}O_6$ 1100 dec. PuO_2	Pure	Tetragonal	a = 4.464 ± 0.002 c = 8.367 ± 0.005	[162]	
$Li_7Pu^{V}O_6$	600	Vacuum Sealed bulb			Impure	? Li_7BiO_6 type		[162]	
α-Na$_4$Pu^{VI}O$_5$	400	O_2		500 trans. ß-Na$_4$Pu^{VI}O$_5$ 900 dec. Na$_3$Pu^{V}O$_4$	Pure	Cubic Fm3m	a = 4.718 ± 0.005	[161] [162]	

β-$Na_4Pu^{VI}O_5$	500	O_2	-	900 dec. $Na_3Pu^VO_4$ 1000	Pure	Tetragonal I 4/m	a = 7.449 ± 0.005 c = 4.590 ± 0.005	[161]	
$Na_6Pu^{VI}O_6$	500	O_2	-	750 dec. β-$Na_4Pu^{VI}O_5$	Pure	Hexagonal	a = 5.56 c = 15.9	[160] [161]	
$Na_3Pu^VO_4$	900	O_2	-	1000 dec. PuO_2	Pure	-	-	[160] [162]	1
$Ca_3Pu^{VI}O_6$	950-1050	O_2	-	> 1000 dec.	Impure	-	-	[141] [163]	
$Sr_3Pu^{VI}O_6$	900-1200	O_2	-	-	Pure	-	-	[141] [164]	
$SrPu^{VI}O_4$	900-1100	O_2	-	-	Pure	Rhombohedral $R\bar{3}m$, $SrUO_4$ type	a = 6.51 α = 35°41'	[141] [164]	
$SrPu^{IV}O_3$	1300	H_2	2 x 12 h	-	Impure-extract Ch_3OH	Cubic	a = 4.28 ± 0.03	[141] [151] [164]	
$Ba_3Pu^{VI}O_6$	800-1300	O_2	-	1400 dec.	Pure	Cubic $F\bar{4}3m$	a = 8.844 ± 0.006	[141] [164]	

TABLE XVII. (Cont.)

Formula valency state of metal ions	The condition of preparation and thermal stability					Structural data		References	Notes
	Temperature of crystal formation (°C)	atm.	Dwell time	Thermal stability limit (°C)	Purity	Symmetry, space group, structure type	Unit cell dimensions (Å)		
α-BaPu^{IV}O$_3$	1200	H$_2$	-	1300 ox.	Ethanol extract	Cubic Pm3m Perovskite	a = 4.39 a = 4.357 ± 0.007 a$_I$ = 4.322 ± 0.003 a$_{II}$ = 3.730 ± 0.003	[151] [164] [165]	 2, 3 2
β-BaPu^{IV}O$_3$	1600	H$_2$			Impure (?)	Orthorhombic (?)	a = 5.795 ± 0.004 b = 5.861 ± 0.004 c = 5.983 ± 0.004	[165]	
BaSr$_2$Pu^{VI}O$_6$	800-1300	O$_2$					a = 8.717 ± 0.008	[141] [164]	4
SrBa$_2$Pu^{VI}O$_6$	800-1300						a = 8.780 ± 0.002		
Pu^{III}AlO$_3$	1100-1500	H$_2$	2 h	m.p. 1810	Impure	Orthorhombic Amm 2 Perovskite	a = 3.750 b = 5.314 c = 5.350	[153]	
Pu^{III}VO$_3$	1100-1500	H$_2$	2 h		Pure	Orthorhombic Amm 2 Perovskite	a = 5.48 b = 5.61 c = 7.78	[151]	
Pu^{III}CrO$_3$	1100-1500	H$_2$	2 h		Pure	Orthorhombic Amm 2 Perovskite	a = 5.46 b = 5.51 c = 7.76	[151]	

$Pu^{III}MnO_3$	1100-1500	H_2	2 h		Impure	Pseudocubic Perovskite	a = 3.86	[151]	
$\alpha-Pu^{IV}GeO_4$	1100	O_2	2 x 12 h	1150° trans. $\beta-Pu^{IV}Ge O_4$	Pure	Tetragonal $I4_1/a$	a = 5.040 ± 0.002 c = 11.11 ± 0.01	[163] [141]	5
	230-240	H_2O	5-6 d	1150° trans. $\beta-Pu^{IV}Ge O_4$	Pure	Tetragonal $I4_1/a$ Scheelite	a = 5.043 ± 0.009 c = 11.13 ± 0.103		
$\beta-Pu^{IV}GeO_4$	1150	O_2	-			Tetragonal I4/amd Zircon	a = 7.073 ± 0.004 c = 6.499 ± 0.003	[141] [163]	6
$\alpha-Pu^{IV}SiO_4$	230-240	H_2O	5-6 d		Impure	Tetragonal I4/amd Zircon	a = 6.906 ± 0.006 c = 6.221 ± 0.006	[141] [163]	
$\beta-(U_{0.51}P_{0.5})(Si_{0.51}Ge_{0.5})O_4$	230-240	H_2	5-6 d			Tetragonal I4/amd Zircon	a = 6.995 ± 0.005 c = 6.364 ± 0.015	[141]	
$Pu^{III}Ta^VO_4$	1350	H_2	2 x 8 h		Pure	(?) $LaTaO_4$ type	-	[166]	
$Pu^{III}Nb^VO_4$	1200	Ar	2 x 12 h		Impure PuO_2 + $PuO_2 \cdot 2Nb_2O_5$	Monoclinic	a = 5.46 ± 0.002 b = 11.24 ± 0.02 c = 5.17 ± 0.02 = 94°35' ± 20'	[166]	
$PuO_2 \cdot 2Ta_2O_5$	1350-1450	O_2 air	● 10 h	1400° dec.		Tetragonal	a = 7.654 ± 0.005 c = 7.731 ± 0.005	[167]	

TABLE XVII.   (cont.)

Formula valency state of metal ions	The condition of preparation and thermal stability					Structural data		References	Notes
	Temperature of crystal formation (°C)	atm.	Dwell time	Thermal stability limit (°C)	Purity	Symmetry, space group, structure type	Unit cell dimensions (Å)		
$PuO_2 \cdot 2Nb_2O_5$	1200-1250	O_2 air	>10 h			Tetragonal	$a = 7.760 \pm 0.002$ $c = 7.792 \pm 0.006$	[167]	
$PuO_2 \cdot NbO$	1050-1150	O_2	Very short				Unknown structure	[167]	
$Ba_2 Pu^{III} Ta^V O_6$	1200-1300	H_2				Cubic Perovskite	$a = 8.59 \pm 0.07$	[167]	
$Pu^{III} Pa^V O_4$ $(Pu_{0.5} Pa_{0.5})O_{2+y}$	900	H_2				Cubic Fm3m Fluorite	$a = 5.443 \pm 0.002$	[163] [166]	7
$Ba_2 Pu^{III} Pa^V O_6$	1350-1400	H_2				Cubic Perovskite	$a = 8.748 \pm 0.006$	[164] [166]	8

[a] Thermal stability abbreviations:

ox.   = oxidation
trans.   = phase transition
m.p.   = melting point
dec.   = decomposition (product given)

Notes:

1. Possibly distorted NaCl structure.
2. a_I refers to a product prepared at 900°C, a_{II} to a product prepared at 1100°C.
3. Chackraburtty et al. [165] noted the possibility of the existence of $Ba_x Pu^{VI} O_3$, where x_1 is very small.
4. The lattice parameter is dependent upon the Ba/Sr ratio [164] and obeys Végard's Law up to 2.25 mole ratio of the Sr ion.
5. Preparation by annealing of corresponding oxides at 1100°C in flowing oxygen or by means of hydrothermal method.
6. This compound is formed during hydrothermal preparation of α-$PuGeO_4$.
7. The formula is limited by condition $0 < y < 0.5$.
8. The value of the lattice parameter shows that redox equilibrium $Ba_2 Pu^{III} Pa^V O_6 \rightleftharpoons Ba_2 Pu^{IV} Pa^{IV} O_6$ occurs.

Végard's Law, were slightly substoichiometric (reported in [143, 144]). The somewhat unexpected shape of the liquidus curve found by Freshley and Mattys [157] (Fig. 26) may also be due to reduction.

1.2.4. UO_2-PuO_2

This system is treated in detail in Section III of this report.

1.3. More complicated systems

1.3.1. Eu_2O_3-PuO_2

Haug and Weigel [158] have studied the lattice parameters of the $EuO_{1.5}$-PuO_2 binary system (Table XVI, Fig. 27). The complicated variation with concentration is very similar to that in the UO_2-rare earth oxide systems published by Rundle et al. [159]. There was some evidence that Pu(IV) was oxidized to a higher valency between 15 and 42% $EuO_{1.5}$, but this suggestion remains to be confirmed.

The fluorite-type lattice of the solution above 42 mole % $EuO_{1.5}$ appeared to be considerably distorted, while above 60 mole % $EuO_{1.5}$ transition to the body-centred cubic structure was indicated.

2. TERNARY AND QUATERNARY PLUTONIUM-METAL-OXIDES

The thermochemical properties of this group of the plutonium compounds have not been generally studied. In Table XVII the available basic physico-chemical properties are shown. It will be appreciated that many of these mixed oxides involve quinque- or sexavalent plutonium.

REFERENCES

[1] INTERNATIONAL ATOMIC ENERGY AGENCY, Thermodynamic and transport properties of uranium dioxide and related phases, IAEA, Vienna (1965).

[2] MOONEY, R.C.L., ZACHARIASEN, W.H., The Transuranium Elements, National Nuclear Energy Series, Div. IV-14B, McGraw Hill, New York (1949) 1442.

[3] ZACHARIASEN, W.H., Acta crystallogr. 2 (1949) 388.

[4] WESTRUM, E.F., Jr., The Transuranium Elements, National Nuclear Energy Series, Div. IV-14B, McGraw Hill, New York (1949) 936.

[5] HOLLEY, C.E., MULFORD, R.N.R., HUBER, E.J., HEAD, E.L., ELLINGER, F.H., BJORKLUND, C.W., Proc. 2nd UN Int. Conf. PUAE 6 (1958) 215.

[6] AKIMOTO, Y., Rpt UCRL-9093 (1960).

[7] SKAVDAHL, R.E., Rpt HW-75914 (1962).

[8] FORBES, R.L., FUHRMAN, N., ANDERSEN, J., TAYLOR, K., Rpt UNC-5144 (1966).

[9] DEAN, G., Proc. 3rd Int. Conf. on Plutonium, London, (1965).

[10] MULFORD, R.N.R., ELLINGER, F.H., JOHNSON, K.A., J. nucl. Mater. 17 (1965) 324.

[11] ANSELIN, F., DEAN, G., LORENZELLI, R., PASCARD, R., Carbides in Nuclear Energy, Macmillan, London (1964) 113.

[12] POTTER, P.E., private communication from A.E.R.E., Harwell.

[13] GARDNER, E.R., MARKIN, T.L., STREET, R.S., J. inorg. nucl. Chem. 27 (1965) 541.

[14] CHIKALLA, T.D., Rpt HW-71887 (1961).

[15] RUSSELL, L.E., BRETT, N.H., HARRISON, J.D.L., RILEY, B.F.J., in Plutonium 1960, Cleaver-Hume Press, London (1961) 489.

[16] ROBERTS, L.E.J., RUSSELL, L.E., ADWICK, A.G., WALTER, A.J., RAND, M.H., Proc. 2nd UN Int. Conf. PUAE 28 (1958) 215.

[17] SKAVDAHL, R.E., Rpt HW-76301 (1963).

[18] SKAVDAHL, R.E., CHIKALLA, T.D., Rpt HW-81601 (1964).

[19] Plutonium Recycle Program Annual Report, 1961, Rpt HW-70000 (1962).

[20] CHIKALLA, T.D., McNEILLY, C.E., SKAVDAHL, R.E., J. nucl. Mater. 12 (1964) 131.

[21] PASCARD, R., report to this panel.

[22] OHSE, R.W., report to this panel.

[23] SARI, C., BENEDICT, U., BLANK, H., report to this panel.

[24] DRUMMOND, J.L., WELCH, G.A., J. chem. Soc. (1957) 4781.

[25] WATERBURY, G.R., DOUGLASS, R.M., METZ, C.F., Analyt. Chem. 33 (1961) 1018.

[26] JACKSON, E.E., RAND, M.H., Rpt AERE-R-3636 (1963).

[27] BJORKLUND, C.W., STARITSKY, E., Rpt LA-1869 (1954).

[28] ANDERSON, H.J., Rpt HW-76303 (1963).

[29] BURNHAM, J.B., Rpt BNWL-91 (1965).

[30] Use of Plutonium as Fuel in Nuclear Reactors, Rpt EURAEC-790 (1963).

[31] DRUMMOND, J.L., WELCH, G.A., J. chem. Soc. (1956) 2565.

[32] FRANCIS, K.E., SOWDEN, R.G., Rpt AERE-R-2939 (1959).

[33] Correlation between the Methods of Precipitation of Plutonium Salts and Sintering their Oxides, Rpt EURAEC-705 (1963).

[34] Use of Plutonium as Fuel in Nuclear Reactors, Rpt EURAEC-176 (1961).

[35] Use of Plutonium as Fuel in Nuclear Reactors, Rpt EURAEC-408 (1962).

[36] Use of Plutonium as Fuel in Nuclear Reactors, Rpt EURAEC-1504 (1965).

[37] PUECHL, K.H., Rpt NUMEC-P-102 (1962).

[38] PUECHL, K.H., Rpt NUMEC-P-103 (1963).

[39] PUECHL, K.H., Rpt NUMEC-P-105 (1963).

[40] FACER, J.F., HARMON, K.M., Rpt HW-31186 (1954).

[41] HARMON, K.M., REAS, W.H., Rpt HW-49597A (1957).

[42] DAWSON, J.K., ELLIOTT, R.M., Rpt AERE-C/R-1207 (1957).

[43] RAO, G.S., SUBRAMANIAN, M.S., WELCH, G.A., J. inorg. nucl. Chem. $\underline{25}$ (1963) 1293.

[44] LEARY, J.A., MARAMAN, W.J., SCHONFELD, F.W., Rpt LA-(MS)-3107 (1964).

[45] JENKINS, I.L., WATERMAN, M.J., J. inorg. nucl. Chem. $\underline{26}$ (1964) 131.

[46] PUECHL, K.H., Rpt NUMEC-P-60 (1961).

[47] PUECHL, K.H., Rpt NUMEC-P-80 (1962).

[48] PUECHL, K.H., Rpt NUMEC-P-90 (1962).

[49] PUECHL, K.H., Rpt NUMEC-2389-2 (1964).

[50] LEARY, J.A., Rpt LA-1913 (1954).

[51] LEARY, J.A., MORGAN, A.N., MARAMAN, W.J., Ind. Engng Chem. ind. (int.) Edn $\underline{51}$ 27 (1959).

[52] MAINLAND, E.W., ORTH, D.A., FIELD, E.L., RADKE, J.H., Ind. Engng Chem. ind. (int.) Edn $\underline{53}$ 685 (1961).

[53] PUECHL, K.H., Rpt NUMEC-P-104 (1963).

[54] BENEDICT, G.E., HARMON, K.M., JANSEN, G., Jr., MUDGE, L.K., SCOTT, F.A., Rpt HW-SA-2915 (1963).

[55] BREWER, L., Chem. Rev. $\underline{52}$ (1953) 1.

[56] KATZ, J.J., GRUEN, D.M., J. Am. chem. Soc. $\underline{71}$, (1949) 2106.

[57] BAGNALL, K.W., LAIDLER, J.B., J. chem. Soc. (1964) 2693.

[58] TEMPLETON, D.H., DAUBEN, C.H., Rpt UCRL-1886 (1952).

[59] RAND, M.H., FOX, A.C., STREET, R.S., Nature, Lond. $\underline{195}$ (1962) 567.

[60] GRIFFEN, C.S. MENDELSSOHN, K., KING, E., LEE, J.A., RAND, M.H., STREET, R.S., "Self-irradiation damage in transuranic elements and compounds", Proc. 3rd International Conference on Plutonium, London, 1965.

[61] ATLAS, L.M., SCHLEMAN, G.J., READEY, D.W., J. Am. Ceram. Soc. $\underline{49}$ (1966) 624.

[62] MULFORD, R.N.R., LAMAR, L.E., "The volatility of plutonium oxide", Plutonium 1960, Cleaver-Hume Press, London (1961) 411.

[63] ACKERMANN, R.J., FAIRCLOTH, R.L., RAND, M.H., J. phys. Chem., Ithaca $\underline{70}$ (1966) 3698.

[64] LIVEY, D.T., FESCHOTTE, P., Atom. Energy Rev. $\underline{4}$, Special Issue 1 (1966) 53.

[65] RILEY, B.F.J., private communication from A.E.R.E., Harwell (1964).

[66] MARKIN, T.L., RAND, M.H., in Thermodynamics $\underline{I}$, IAEA, Vienna (1966) 145.

[67] McNEILLY, C.E., J. nucl. Mater. $\underline{11}$ (1964) 53.

[68] BRETT, N.H., RUSSELL, L.E., in Plutonium 1960, Cleaver-Hume Press, London (1961) 397.

[69] LE BLANC, J.M., ANDRIESSEN, H., Rpt EURAEC-434.

[70] RAND, M.H., Atom. Energy Rev. $\underline{4}$, Special Issue 1 (1966) 7.

[71] HYDE, B.G., BEVAN, D.J.M., EYRING, L., Phil. Trans R. Soc. A 259 (1966) 583.

[72] SAWYER, J.O., HYDE, B.G., EYRING, L., Bull. Soc. chim. Fr. $\underline{4}$ (1965) 1190.

[73] BEVAN, D.J.M., KORDIS, J., J. inorg. nucl. Chem. $\underline{26}$ (1964) 1509.

[74] BEVAN, D.J.M., J. inorg. nucl. Chem. $\underline{1}$ (1955) 49.

[75] CHAPIN, D.S., FINN, M.C., HONIG, J.M., Proc. 4th Conf. Rare Earth Research, Gordon & Breach, New York (1966) 607.

[76] RAND, M.H., in Thermodynamics $\underline{II}$, IAEA, Vienna (1966) 603.

[77] OETTING, F.L., J. inorg. nucl. Chem. $\underline{27}$ (1965) 2151.

[78] KINCHIN, L., PEASE, R., Rep. Prog. Phys. $\underline{18}$ (1955) 1.

[79] OLSEN, C.E., ELLIOT, R.O., SANDENAW, T.A., in Radiation Damage in Reactor Materials, IAEA, Vienna (1963) 35.

[80] SANDENAW, T.A., J. nucl. Mater. $\underline{10}$ (1963) 165.

[81] OSBORNE, D.W., WESTRUM, E.F., J. chem. Phys. $\underline{21}$ (1953) 1884.

[82] JONES, W.M., GORDON, J., LONG, E.A., J. chem. Phys. $\underline{20}$ (1952) 695.

[83] WESTRUM, E.F., HATCHER, J.B., OSBORNE, D.W., J. chem. Phys., $\underline{21}$ (1953) 419.

[84] NAGELS, P., private communication from Studvencentrum voor Kernenergie, Mol-Donk (1966).

[85] WILLIS, B.T.M., Proc. R. Soc. $\underline{A274}$ (1963) 134.

[86] ROOF, R.B., J. nucl. Mater. $\underline{2}$ (1960) 39.

[87] TAYLOR, J.C., LOASBY, R.G., DEAN, D.J., LINFORD, P.F., Proc. 3rd Int. Conf. on Plutonium, London, 1965.

[88] LEE, J.A., private communication from A.E.R.E., Harwell (1966).

[89] SPARKS, J.T., KOMOTO, T.T., Rpt UCRL-14360 (1965) 47.

[90] DAWSON, J.K., J. chem. Soc. (1952) 1882.

[91] WESTRUM, E.F., GRØNVOLD, F., in Thermodynamics of Nuclear Materials, IAEA, Vienna (1962) 3.

[92] Brussels EURAEC Report, Rpt EURAEC-307 (1960).

[93] KING, E.G., CHRISTENSEN, A.U., U.S. Bureau Mines Report Invest. No. 5789 (1961).

[94] PANKRATZ, L.B., KELLEY, K.K., U.S. Bureau Mines Report Invest. No. 6248 (1963).

[95] KUZNETSOV, R.A., REZUKHINA, T.N., Zh. fiz. khim. 34 (1960) 2467; ibid.
35 (1961) 956; Russ. J. phys. Chem. 34 (1960) 1164; ibid. 35 (1961) 470.

[96] KING, E.G., WELLER, W.W., PANKRATZ, L.B., U.S. Bureau Mines Report Invest. No. 5857 (1961).

[97] PANKRATZ, L.B., U.S. Bureau Mines Report Invest. No. 6781 (1966).

[98] PANKRATZ, L.B., KING, E.G., KELLEY, K.K., U.S. Bureau Mines Report Invest. No. 6033 (1962).

[99] PANKRATZ, L.B., KING, E.G., U.S. Bureau Mines Report Invest. No. 6175 (1963).

[100] POPOV, M.M., IVANOV, M.I., Atomn. Energ. 2 (1957) 360; Soviet. J. Atom. Energy 2
(1957) 439.

[101] HOLLEY, C.E., MULFORD, R.N.R., HUBER, E.J., HEAD, E.L., BJORKLUND, C.W., Proc.
2nd UN Int. Conf. PUAE 61 (1958) 215.

[102] MARKIN, T.L., BONES, R.J., GARDNER, E.R., private communication (see also Ref. [66]).

[103] ATLAS, L.M., SCHLEHMAN, G.J., in Thermodynamics II, IAEA, Vienna (1966) 407.

[104] BAIRIOT, H., VANHELLEMONT, G., private communication from BelgoNucléaire, Brussels.

[105] CHIKALLA, T.D., private communication from Battelle North-West, 1966.

[106] STULL, D.R., SINKE, G.C., Thermodynamic Properties of the Elements, American Chemical
Society, Washington, D.C. (1956).

[107] MULFORD, R.N.R., ELLINGER, F.H., JOHNSON, K.A., J. nucl. Mater. 17 (1965) 324.

[108] PHIPPS, T.E., SEARS, G.W., SIMPSON, O.C., J. chem. Phys. 18 (1950) 724.

[109] PARDUE, W.M., KELLER, D.L., J. Am. Ceram. Soc. 47 (1964) 610.

[110] PAPROCKI, S.J., KELLER, D.L., ALEXANDER, C.A., PARDUE, W.M., Rpt BMI-1591 (1962).

[111] OHSE, R.W., private communication.

[112] MULFORD, R.N.R., in Thermodynamics I, IAEA, Vienna (1966) 231.

[113] ACKERMANN, R.J., RAUH, E.G. THORN, R.J., CANNON, M.C., J. phys. Chem., Ithaca 67
(1961) 762.

[114] ACKERMANN, R.J., GILLES, P.W., THORN, R.J., J. chem. Phys. 25 (1956) 1089.

[115] DE MARIA, G., BURNS, R.P., DROWART, J., INGHRAM, M., J. chem. Phys. 32 (1960) 1373.

[116] ACKERMANN, R.J., RAUH, E.G., CHANDRASEKHARAIAH, M.S., Argonne National
Lab. Rpt ANL-7048 (1965).

[117] ACKERMANN, R.J., FAIRCLOTH, R.L., RAUH, E.G., THORN, R.J., J. inorg. nucl. Chem. 28
(1966) 111.

[118] ACKERMANN, R.J., THORN, R.J., in Thermodynamics I, Vienna (1966) 243.

[119] BLANK, H., BENEDICT, U., SARI, C., private communication from E.I.T., Karlsruhe.

[120] MARKIN, T.L., STREET, R.S., private communication from A.E.R.E., Harwell (1966).

[121] DEAN, G., PASCARD, R., report to this panel.

[122] MARKIN, T.L., McIVER, E.J., Proc. 3rd Int. Conf. on Plutonium, London, 1965.

[123] HENRION, R., DIELS, P., report to this panel.

[124] BRETT, N.H., FOX, A.C., J. inorg. nucl. Chem. 28 (1966) 1191.

[125] CHICALLA, T.D. in Plutonium 1960, Cleaver-Hume Press, London (1961) 455.

[126] BRETT, N.H., RUSSELL, L.E., Trans. Br. Ceram. Soc. 62 (1963) 97.

[127] MARKIN, T.L., STREET, R.S., IAEA panel paper (to be published in J. inorg. nucl. Chem.).

[128] CHIKALLA, T.D., Rpt HW-69832 (1961).

[129] PIJANOWSKI, S.W., DELUCA, L.S., Rpt KAPL-1957 (1960).

[130] LYON, W.L., BAILY, W.E., Trans. Am. nucl. Soc. 8 (1965) 376.

[131] LYON, W.L., BAILY, W.E., Rpt GEAP-4878 (1965).

[132] EPSTEIN, L.F., J. nucl. Mater. (to be published).

[133] GRØNVOLD, F., J. inorg. nucl. Chem. 1 (1955) 357.

[134] COHEN, I., BERMAN, R.M., J. nucl. Mater. 18 (1966) 77.

[135] MARKIN, T.L., ROBERTS, L.E.J., Thermodynamics of Nuclear Materials, IAEA, Vienna (1962) 693.

[136] MARKIN, T.L., ROBERTS, L.E.J., Thermodynamics of ceramic systems, (to be published in
Trans. Br. Ceram. Soc.).

[137] MARKIN, T.L., private communication from A.E.R.E., Harwell (1966).

[138] AITKEN, E.A., EDWARDS, J.A., JOSEPH, R.A., J. phys. Chem. 70 (1966) 1084.

[139] AITKEN, E.A., JOSEPH, R.A., J. phys. Chem. 70 (1966) 1090.

[140] RAND, M.H., private communication.

[141] KELLER, C., Kernforschungszentrum Rpt KFK-225 (1964).

[142] HOUGH, A., MARPLES, J.A.C., J. nucl. Mater. 15 (1965) 298.

[143] DAYTON, R.W., PAPROCKI, S.J., Rpt BMI-1707 (Del)(1964).

[144] DAYTON, R.W., PAPROCKI, S.J., Rpt BMI-1721 (Del) (1965).

[145] DAYTON, R.W., PAPROCKI, S.J., Rpt BMI-1723 (Del) (1965).

[146] DAYTON, R.W., PAPROCKI, S.J., Rpt BMI-1727 (Del) (1965).

[147] DAYTON, R.W., PAPROCKI, S.J., Rpt BMI-1733 (Del) (1965).

[148] CARROLL, D.F., J. Am. Ceram. Soc. 47 (1964) 650.

[149] CARROLL, D.F., Rpt HW-81601, 21.

[150] CARROLL, D.F., Rpt HW-76303 (1963) 21.

[151] RUSSELL, L.E., HARRISON, J.D.L., BRETT, N.H., J. nucl. Mater. 2 (1960) 310.

[152] McEWEN, L.H., Ed., Rpt HW-65078 (1960).

[153] RUNNALLS, O.J.C., Proc. 3rd Int. Conf. on Plutonium, London, 1965.

[154] MULFORD, R.N.R., ELLINGER, F.H., J. phys. Chem., Ithaca 62 (1958) 1466.

[155] CARROLL, D.F., J. Am. Ceram. Soc. 46 (1963) 194.

[156] CARROLL, D.F., Rpt HW-69305 (1961).

[157] FRESHLEY, M.D., MATTYS, H.M., Rpt HW-76300 (1962) 26.

[158] HAUG, H. WEIGEL, F., J. nucl. Mater. 9 (1963) 360.

[159] RUNDLE, R.E., BAENZINGER, N.C., WILSON, A.S., McDONALD, R.A., J. Am. Chem. Soc. 70 (1948) 99.

[160] KOCH, L., Dissertation, Technische Hochschule, Karlsruhe (1963), Rpt KFK-196 (1964).

[161] KELLER, C., KOCH, L., WALTER, K.H., J. inorg. nucl. Chem. 27 (1965) 1205.

[162] KELLER, C., KOCH, L., WALTER, K.H., J. inorg. nucl. Chem. 27 (1965) 1225.

[163] KELLER, C., Nukleonik 5 (1963) 41.

[164] KELLER, C., Nukleonik 4 (1962) 271.

[165] CHACKRABURTTY, D.M., JAYADEVA, U.C., SIVARAMAKRISHNAN, C.K., Acta Crystallogr. 16 (1958) 1060.

[166] KELLER, C., WALTER, K.H., J. inorg. nucl. Chem. 27 (1965) 1253.

[167] KELLER, C., J. inorg. nucl. Chem. 27 (1965) 1233.

LIST OF PARTICIPANTS

The members attending the Panel Meeting, held on 24-28 October, 1966, at the Headquarters of the International Atomic Energy Agency in Vienna to assess the thermodynamic properties of the plutonium-oxygen and uranium-plutonium-oxygen systems, were:

RAND, M. H. (Chairman)	Atomic Energy Research Establishment, Harwell, Didcot, Berks., United Kingdom
ACHACHINSKY, V. V.	State Committee for the Utilization of Atomic Energy, USSR
ACKERMANN, R. J.	Argonne National Laboratory, Argonne, Ill., United States of America
BAIRIOT, H.	BelgoNucléaire, Brussels, Belgium
BLANK, H.	Euratom, Karlsruhe, Federal Republic of Germany
HOLLEY, C. E., Jr.	University of California, Los Alamos Scientific Laboratory, Los Alamos, N.Mex., United States of America
JAKEŠ, D.	The Nuclear Research Institute of the Czechoslovak Academy of Sciences, Řež, Czechoslovakia
KOIZUMI, M.	Atomic Fuels Corporation, Tokai-mura, Japan
KOLAR, D.	Jožef Stefan Nuclear Institute, Ljubljana, Yugoslavia
LAPAGE, R.	Atomic Energy Establishment, Aldermaston, Berks., United Kingdom
MARKIN, T. L.	Atomic Energy Research Establishment, Harwell, Didcot, Berks., United Kingdom

MULFORD, R. N. R.   University of California,
                          Los Alamos Scientific Laboratory,
                          Los Alamos, N. Mex., United States
                          of America

NAGELS, P.   Centre d'étude de l'énergie nucléaire,
                          Mol-Donk, Belgium

OHSE, R. W.   Euratom,
                          Karlsruhe, Federal Republic of Germany

PASCARD, R.   Centre d'études nucléaires de
                            Fontenay-aux-Roses,
                          Seine, France

RAMANIAH, M. V.   Atomic Energy Establishment Trombay,
                          India

STOLL, W.   ALKEM,
                          Leopoldshafen, Federal Republic
                          of Germany

SECRETARIAT

Scientific Secretary   HARA, R.
                          Division of Research and Laboratories

Editor   FREEMAN, S. M.
                          Division of Scientific and
                            Technical Information

REPORTS SUBMITTED TO THE PANEL

The following reports were submitted to the Panel, and the assessment contained in this publication is based on these reports and discussions held among the Panel members:

ACKERMANN, R. J.   A critical thermodynamic appraisal
                                 of the vaporization behaviour of the
                                 PuO_{2-x} phase

BAIRIOT, H.   Report on work carried out by
                                 P. Henrion and P. Wiels on mixed
                                 (U, Pu) oxides

JAKEŠ, D.   The binary system of plutonium
                                 dioxide and ternary and quarternary
                                 plutonium-metal oxides

HARIHARAN, A. V., and   Preparation of plutonium oxides:
RAMANIAH, M. V.   a literature survey

KOIZUMI, M., KANEKO, H.,   Formation of $\alpha\, Pu_2O_3$ from PuO_2-UO_2
and AKUTSU, H.   solid solution during sintering in H_2
                                 gas atmosphere

MARKIN, T. L.   1. The Pu-O phase diagram;
                                 2. Thermodynamic data for plutonium
                                    oxides;
                                 3. The U-Pu-O phase diagram;
                                 4. Thermodynamic data for (U, Pu)
                                    oxides

MULFORD, R. N. R., and   Thermodynamic properties of
HOLLEY, C. E., Jr.   plutonium oxides

NAGELS, P.   Heat capacities of the actinide
                                 dioxides

OHSE, R. W.   Preliminary report on vapour
                                 pressure studies of plutonium oxide
                                 with special consideration of the
                                 hypostoichiometric range

85

PASCARD, R.

1. On the ternary diagram uranium-plutonium-oxygen;
2. Vapour pressure of PuO_2;
3. Vapour pressure of plutonium and uranium mixed oxides

SARI, C., BENEDICT, U., and BLANK, H.

Preliminary results of an investigation on phase relations in the U-Pu-O diagram

IAEA SALES AGENTS

Orders for Agency publications can be placed with your bookseller or any of our sales agents listed below:

ARGENTINA
Comisión Nacional de
Energía Atómica
Avenida del Libertador
General San Martin 8250
Buenos Aires - Suc. 29

AUSTRALIA
Hunter Publications,
23 McKillop Street
Melbourne, C.1

AUSTRIA
Georg Fromme & Co.
Spengergasse 39
A-1050, Vienna V

BELGIUM
Office international de librairie
30, avenue Marnix
Brussels 5

BRAZIL
Livraria Kosmos Editora
Rua do Rosario, 135-137
Rio de Janeiro

Agencia Expoente Oscar M. Silva
Rua Xavier de Toledo, 140-1° Andar
(Caixa Postal No. 5.614)
São Paulo

BYELORUSSIAN SOVIET SOCIALIST
REPUBLIC
See under USSR

CANADA
The Queen's Printer
Ottawa, Ontario

CHINA (Taiwan)
Books and Scientific Supplies
Service, Ltd.,
P.O. Box 83
Taipei

CZECHOSLOVAK SOCIALIST REPUBLIC
S.N.T.L.
Spolena 51
Nové Město
Prague 1

DENMARK
Ejnar Munksgaard Ltd.
6 Nörregade
Copenhagen K

FINLAND
Akateeminen Kirjakauppa
Keskuskatu 2
Helsinki

FRANCE
Office international de
documentation et librairie
48, rue Gay-Lussac
F-75, Paris 5ᵉ

GERMANY, Federal Republic of
R. Oldenbourg
Rosenheimer Strasse 145
8 Munich 8

HUNGARY
Kultura
Hungarian Trading Co. for Books
and Newspapers
P.O.B. 149
Budapest 62

ISRAEL
Heiliger and Co.
3 Nathan Strauss Street
Jerusalem

ITALY
Agenzia Editoriale Internazionale
Organizzazioni Universali (A.E.I.O.U.)
Via Meravigli 16
Milan

JAPAN
Maruzen Company Ltd.
6, Tori Nichome
Nihonbashi
(P.O. Box 605)
Tokyo Central

MEXICO
Librería Internacional
Av. Sonora 206
Mexico 11, D.F.

NETHERLANDS
N.V. Martinus Nijhoff
Lange Voorhout 9
The Hague

NEW ZEALAND
Whitcombe & Tombs, Ltd.
G.P.O. Box 1894
Wellington, C.1

NORWAY
Johan Grundt Tanum
Karl Johans gate 43
Oslo

PAKISTAN
Karachi Education Society
Haroon Chambers
South Napier Road
(P.O. Box No. 4866)
Karachi 2

POLAND
Ośrodek Rozpowszechniana
Wydawnictw Naukowych
Polska Akademia Nauk
Pałac Kultury i Nauki
Warsaw

ROMANIA
Cartimex
Rue A. Briand 14-18
Bucarest

SOUTH AFRICA
Van Schaik's Bookstore (Pty) Ltd.
Libri Building
Church Street
(P.O. Box 724)
Pretoria

SPAIN
Librería Bosch
Ronda de la Universidad 11
Barcelona

SWEDEN
C.E. Fritzes Kungl. Hovbokhandel
Fredsgatan 2
Stockholm 16

SWITZERLAND
Librairie Payot
Rue Grenus 6
1211 Geneva 11

TURKEY
Librairie Hachette
469, Istiklâl Caddesi
Beyoğlu, Istanbul

UKRAINIAN SOVIET SOCIALIST
REPUBLIC
See under USSR

UNION OF SOVIET SOCIALIST
REPUBLICS
Mezhdunarodnaya Kniga
Smolenskaya-Sennaya 32-34
Moscow G-200

UNITED KINGDOM OF GREAT
BRITAIN AND NORTHERN IRELAND
Her Majesty's Stationery Office
P.O. Box 569
London, S.E.1

UNITED STATES OF AMERICA
National Agency for
International Publications, Inc.
317 East 34th Street
New York, N.Y. 10016

VENEZUELA
Sr. Braulio Gabriel Chacares
Gobernador a Candilito 37
Santa Rosalia
(Apartado Postal 8092)
Caracas D.F.

YUGOSLAVIA
Jugoslovenska Knjiga
Terazije 27
Belgrade

IAEA publications can also be purchased retail at the United Nations Bookshop at United Nations Headquarters, New York, at the news-stand at the Agency's Head-quarters, Vienna, and at most conferences, symposia and seminars organized by the Agency.

In order to facilitate the distribution of its publications, the Agency is prepared to accept payment in UNESCO coupons or in local currencies.

Orders and inquiries from countries where sales agents have not yet been appointed may be sent to:

Distribution and Sales Group, International Atomic Energy Agency,
Kärntner Ring 11, A-1010, Vienna I, Austria